National University of Lesotho

The Potential Impact of Climate Change on Wind Speed and Solar Radiation in Lesotho

Taelo Tsolele (201603673)

A dissertation submitted in partial fulfillment of
the requirements for the degree of

Master of Science in Sustainable Energy

Offered by the

Energy Research Centre
Faculty of Science & Technology

August 2024

Acknowledgement

I would like to express my deepest gratitude to my supervisor, Moeketsi Mpholo for his unwavering support, invaluable guidance, and patience during the course of my research. His experience and knowledge have inspired me to see to the completion of this paper. I am also thankful to the Energy Research Center for providing me with all the resources for this dissertation, as well as giving me an opportunity to undertake this exciting program. Moreover, I thank my family and friends who stood by me during the course of my studies, providing all the necessary support. Lastly, I would like to give special thanks to my colleagues. I dedicate this dissertation to my late father, John Tsolele, whom from my early age imparted the wisdom of eduction in me. Continue to Rest in Peace, Mokoena

Abstract

In this study, a Jupyter Notebook software was utilized to study the potential impact of climate change on wind speed and solar radiation in Lesotho using a CORDEX-Africa regional climate model to simulate the past, present, and future climate conditions under different scenarios at 10 m above ground level. Historical climate data from 1950 to 2005 showed a consistent average wind speed of 1.50 - 3.0 m/s and solar radiation of 200 - 225 W/m^2, except in the north-east of the country where the Butha-Buthe and Mokhotlong districts are located, solar radiation of 175 - 200 W/m^2 was averaged. The RCP4.5 scenario projected a stable average wind speed ranging from 1.50 - 2.75 m/s except for the peak of 3.00 m/s in 2030. The projected solar radiation had a minimum average solar radiation of 150 W/m^2 and a maximum average solar radiation of 275 W/m^2, reaching up to 340 W/m^2 by 2045. The RCP8.5 scenario projected a similar wind speed trend, exceeding 3.00 m/s from 2042 to 2045, and a peak solar radiation of 370 W/m^2 in 2043. These projections imply that Lesotho's solar and wind energy generation will not be negatively impacted, thus offering significant opportunities for sustainable energy development. The findings support investments in wind and solar infrastructure throughout the country, extending to places such as Butha Buthe, Quthing, and Mokhotlong with the newly acquired renewable energy resources due to climate change.

Table of Contents

1 Introduction

1.1 Background

For centuries, global economies have relied heavily on fossil fuels such as coal, natural gas and oil as the primary energy resources but in recent years, the impact of these energy resources on the environment has become an issue around the world due to the greenhouse gas (GHG) emissions released during energy production. The emissions are linked to climate change [1, 2]. In 2022, the total amount of GHGs related to energy increased by 1% reaching a record of 41.5 gigatonnes (Gt) of carbon dioxide (CO_2) equivalent [3]. As a result, renewable energy resources (RER) have become the ideal choice of energy production due to their minimal impact on the environment. Since 2007, a paradigm shift in energy production occurred due to a significant decline in the cost of renewable energy systems, particularly solar and wind [4], from a global levelized cost of electricity (LCOE) for utility-scale of more than 1 MW capacity of $0.417/kWh in 2010 to $0.048/kWh in 2021 for solar PV, while onshore wind LCOE decreased from $0.102/kWh to $0.033/kWh in the same period [5].

Lesotho is a country in the Sub-Saharan Africa region. It is entirely landlocked within South Africa. It has an area of about 30,455 km^2 with a population of about 2.1 million of which about 70% resides in the rural area as of 2022 [6,7]. The utility-grid connection in rural areas is considered uneconomical and expensive due to the small electricity demand as compared to the cost of connecting the areas [8]. The country achieved an electrification rate of about 52% in 2022 as reported by the The Reporter, (2022) [9]. According to LEWA [Lesotho Electricity and Water Authority], (2021) Lesotho had a peak demand of 203.48 MW in 2021/22 while the installed electricity generation within the country was at 74.7 MW, mainly through the 'Muela Hydropower station which generates 72 MW [10]. The rest is generated through small hydropower plants. This implies that 128.78 MW, which translates to 63% energy deficit, was imported from South Africa and Mozambique through the Southern African Power Pool (SAPP) [10].

The national Department of Energy has proposed a plan to generate electricity locally and has identified renewable sources of energy as the priority to play a significant role in electrifying the country especially because Lesotho has no fossil fuels [11]. Lesotho Energy Policy 2015-2025 was developed to address the current energy shortage in the country as well as plan for

future energy demand. The vision for the policy is that energy shall be universally accessible and affordable in a sustainable manner, with a minimal negative impact on the environment, hence the government will ensure the security of electricity supply within the country.

Lesotho has an ongoing 70 MW capacity solar power plant at Ha-Ramarothole in Mafeteng, the first phase of 30 MW capacity which was commissioned in 2023 while the second stage of 40 MW capacity is expected to be completed in 2024 [12]. In another project, the EUfunded Electrification Financing Initiative and the UK-funded Renewable Energy Performance Platform (REPP) have each made an investment of USD 4.9-million into a project-finance vehicle led by OnePower (1PWR) to establish 11 mini-grids in Lesotho [13]. 1PWR also received grant financing from the African Development Bank (AfDB) to develop a 20 MW grid-connected power plant at Ha-Ramarothole in the district of Mafeteng [14]. The government of Lesotho plans to increase the existing 'Muela Hydropower Station energy generation by 40% from Phase 2 of the Lesotho Highlands Water Project (LHWP) and establish the Oxbow Hydropower Plant which will generate about 80 MW capacity. The hydropower component completion will be in 2029 with the expectation that phase 2 of the project will be completed in 2028 [15].

Taele et al. (2012) state that Lesotho has a daily average solar irradiation that ranges from 5.5 - 7.2 kWh/m^2 and about 3,200 – 4,000 sunshine hours per year [16]. It has a considerable potential for photovoltaics, with values ranging from approximately 1600 - 1750 kWh/kWp, maximum values in the highlands [17]. The abundant solar radiation can be optimized to meet the energy deficit in the country by establishing solar mini-grids for the remote areas and for the grid-connected systems. For wind energy, the wind resource assessments done at Masitise, Sani and Letseng-la-Terae indicate the mean wind speeds of 5.97 m/s, 4.93 m/s, and 5.5 m/s at 10 m above ground level, respectively [16,17]. Lesotho possesses abundant renewable energy resources that can be harnessed to meet its energy demands. The country has an untapped wind energy potential of 758 MW, a 70 MW solar energy capacity at Ha Ramarothole, a 1,334 MW pumped storage potential at Monontsa, and 361 MW of hydroelectric resources [20].

Currently Lesotho does not generate wind energy but Hirundo Energy is developing two wind farms in the country. One is located in the Mohale's Hoek district. It comprises 12 wind turbines with each turbine having a capacity of 3 – 6 MW. Another wind farm of 8 wind turbines with the same capacity range is located at Masite Nek (Ha 'Majane) in the Maseru

district [21]. Both wind farms are expected to generate approximately 25% of the country's local electricity consumption.

1.2 Problem Statement

In the coming years, the climate change effects with increased temperatures, reduced rainfall and varying wind speeds are projected [22]. The generation of intermittent renewable energy depends on climate conditions. This study analyses the potential impact of climate change on intermittent renewable energy resources (IRER) in Lesotho. Due to their dependency on the climate, the IRER may be susceptible to future climate conditions. David E.H. et al. (2021) indicate that the impact of wind energy and hydropower are uncertain due to the decline in some regions and an improvement in others while the impact on solar energy is minor [23].

1.3 Research Question and Objectives

The following is the research question for this project: What is the potential impact of climate change on renewable energy generation in Lesotho?

To address this question, the following objectives will be addressed:

- To determine the trend of how climate change is expected to affect the climate conditions responsible for solar and wind energy production.
- To identify the effects of climate change on solar radiation and wind speed resource up to 2045.

1.4 Justification

The research study will help energy stakeholders (policy-makers, renewable energy developers and funding institutions) to make informed decisions on implementing solar and wind energy projects. The findings will not only be useful in the energy field but also be a resource for meteorologists to appreciate future climate trends, while economists will be able to analyze the financial implications due to climate change. Furthermore, the study will contribute to the Sustainable Development Goal 7 initiative which aims to provide affordable and clean energy while tackling climate change and preserving oceans and forests [24].

1.5 Dissertation Structure

The dissertation is structured in five chapters. The first chapter is the introduction which gives a brief description of the problem that this research study addresses. The second chapter is the literature review which outlines the Climate Change Theory and climate modelling. The third chapter presents the methodology. It explains the steps taken to obtain the study results. The fourth chapter presents and discusses the study results. The final chapter, Chapter Five, is the conclusion that summarises the reseach findings.

2 Literature Review

2.1 Overview of Climate Change

The term “climate change” was first widely discussed in public from the 1980s to the early 1990s and frequently appeared alongside the term “global warming” [25]. Since then, it has been adopted as an important issue on the international political agenda. During this period, the leading scientists and governments around the world became increasingly aware of the warming of the planet due to a large and growing evidence that supports this claim and the United Nations Inter-governmental Panel on Climate Change (IPCC) which released its First Assessment Report in 2007. The report concluded that the warming of the climate system is unequivocal and a settled fact [26]. It is now evident from the observations of the rising global sea levels from the melting snow and ice as well as the average air and ocean temperatures that, according to the IPCC, future climate conditions are expected to take a similar pattern as in the past [27].

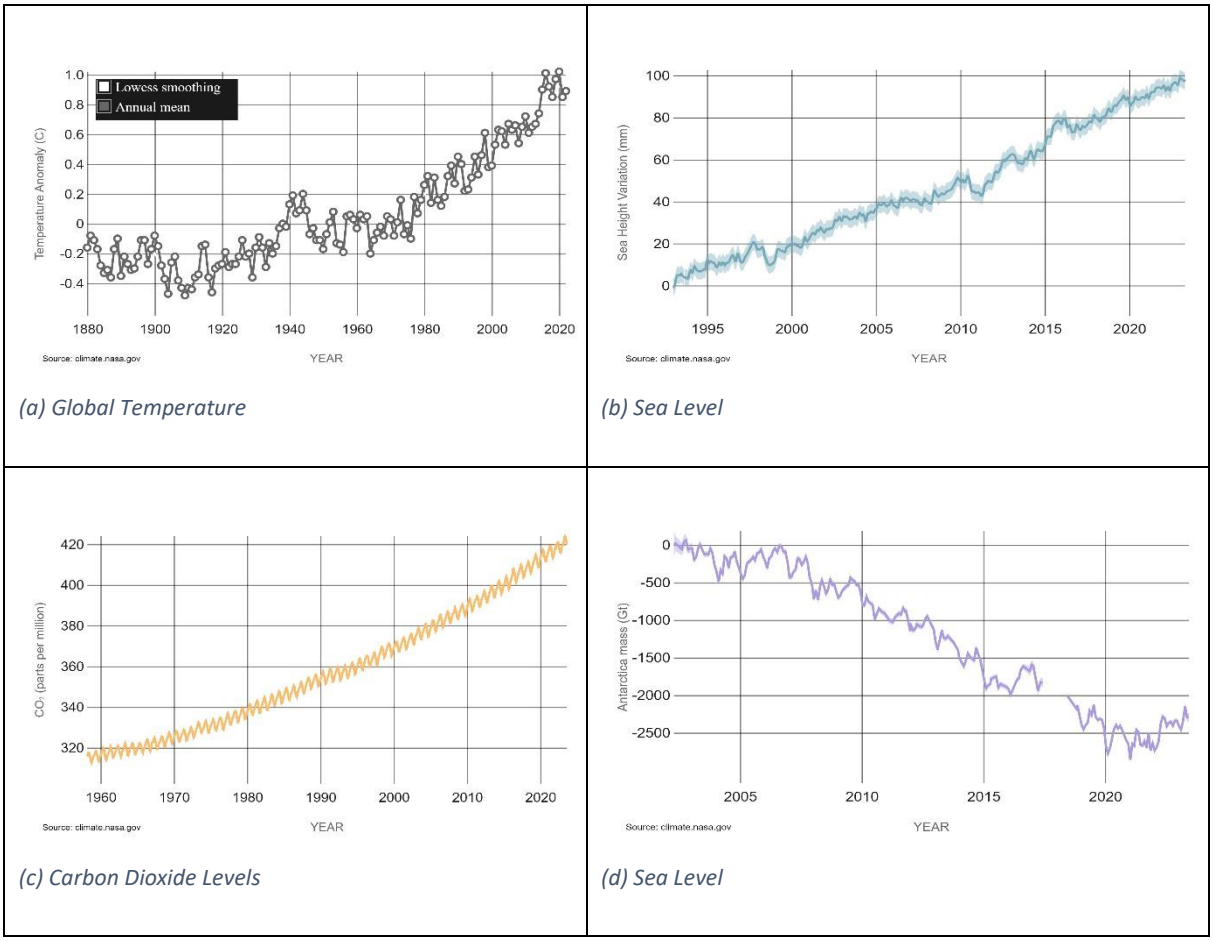

Figure 1: Indicates (a) Global Temperature, (b) Sea Level, (c) Carbon Dioxide Levels, and (d) Antarctica Ice Sheets Mass [28]

As shown in Figure 1(a), the global average surface temperatures increased from -0.16 ℃ in 1880 to 0.9 ℃ in 2020. Since the records started in 1880, the global surface temperature change from 1951 to 1980 is plotted against the long-term average in Figure 1. As observed through the satellite, the sea level increased by 98 millimeters since the records started in 1993 to 2022 as shown in Figure 1(b) [28]. The sea rises as a result of two factors related to global warming;

the expansion of seawater as the earth warms and added water from the melting of the ice sheets and glaciers. Since 2002, the satellite shows that the ice sheets in
Antarctica have been losing mass as shown in Figure 1(d), the rate of change decreased by 146.0 billion metric tons per year from the period 2002-2023 [28]. NASA's GRACE mission started in 2002 and ended in 2017, it began collecting the data again in 2018.

The IPCC defines climate change as changes in the condition of the climate that last for a long time, usually decades or more, and can be detected by variations in the mean and/or variability of its properties. Global warming refers to an average increase in the Earth's temperature that leads to the changes in the climate [29]. There are possible causes of climate change, including internal or external natural processes or long-lasting anthropogenic modifications to the atmosphere composition or land usage. Over the past decades, there has been a global debate in the scientific community about the role of human activities in the warming of the planet. The debate divided the scientists into two groups; climate change deniers vs climate change advocates, to date there are scientists who still believe that the current climate conditions are due to the natural factors rather than the human factors. The percentage of climate scientists who agreed that the current available scientific evidence that supports the warming of the planet increased from 41% in 1991 to 74% in 2007.

2.2 The Greenhouse Effect

Human activities are believed to be responsible for the high levels of greenhouse gases released into the atmosphere, such gases include carbon dioxide (CO_2), methane (CH_4), nitrous oxide (N_2O), water vapor (H_2O) and ozone (O_3). These gases can absorb and emit infrared energy [30]. They constitute a small fraction of the atmospheric composition but have large negative impacts on the atmosphere, while two gases that dominate the atmosphere (nitrogen and oxygen) has no impact on climate change. In 2019, the amount of CO_2 in the atmosphere at 410 parts per million (ppm) was more than it had been in at least 2 million years and the concentration of CH_4 was at 1866 parts per billion (ppb) and N_2O was at 332 ppb. Both respective concentrations were more than they had been in at least 800,000 years. Shown in Figure 2 is the increased concentration of the main GHGs contributors in the atmosphere from 1850-2019.

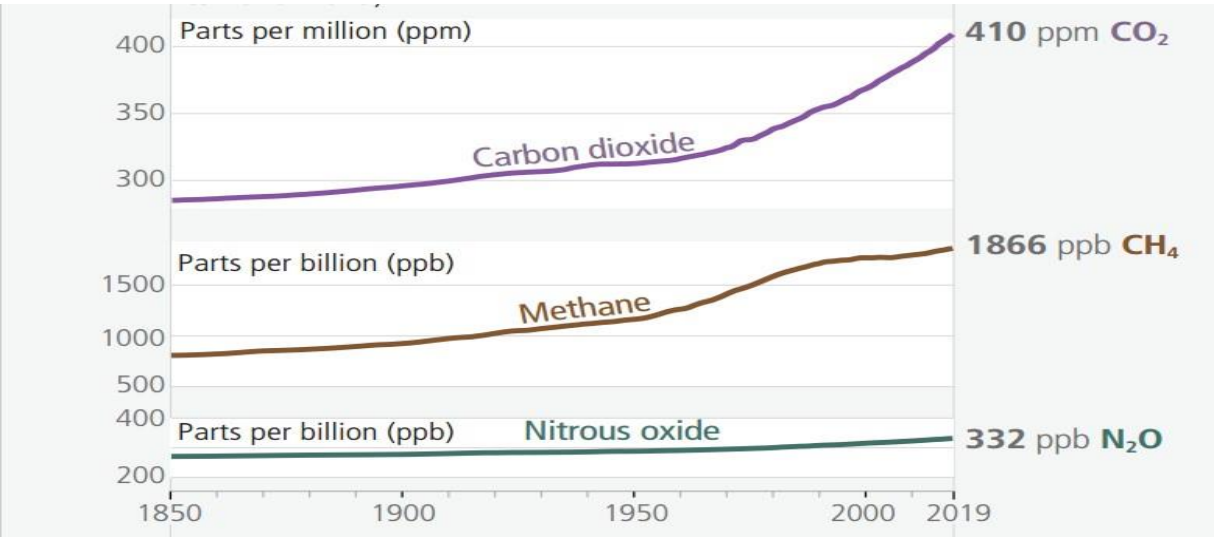

Figure 2: Concentration of GHGs in the Atmosphere Since 1850 [31]

The ability of GHGs to absorb energy in the atmosphere and emit it to the surface to warm Earth is known as the greenhouse effect. This phenomenon occurs naturally in the atmosphere and it is important to sustain life on Earth because it prevents some of the heat from the planet from escaping into space through the atmosphere. Without it, the average temperatures on Earth would be around -19℃ [32]. Scientists are concerned that high levels of GHGs released into the atmosphere by the burning of fossil fuels for energy will result in energy imbalance and change the climate on Earth [30], thus endangering the ecosystem, human health, infrastructure and the economy.

2.3 Components of Climate System

The climate system is complex. It consists of 5 major components which are the atmosphere (the gaseous envelope around the Earth), the hydrosphere (the water in liquid form on Earth), the biosphere (all the living organisms), the cryosphere (water in solid form on Earth) and the lithosphere (the land surface), influenced by various external mechanisms such as the sun [33], as shown in Figure 3. Over time, the climate system changes due to a combination of internal dynamics and external factors such as solar variations, volcanic eruptions, and anthropogenic changes such as the altered atmospheric composition and land use [34].

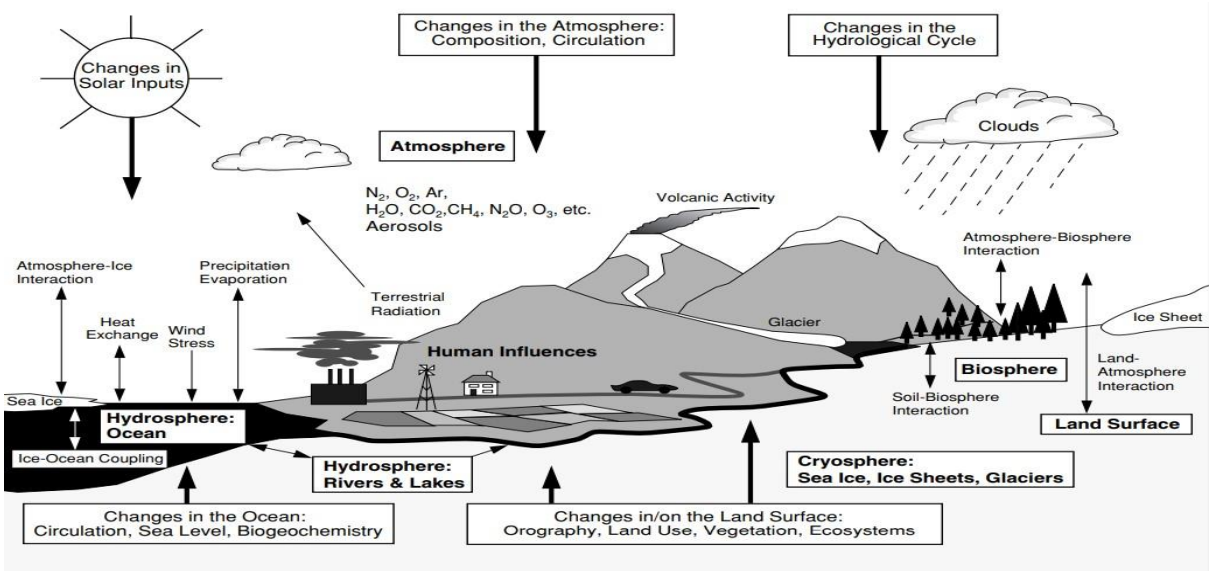

Figure 3: Components of the Climate System [33].

2.4 Human Activities and Climate Change

Scientists have concluded that the human activities such as cultivating crops, burning fossil fuels for energy, clearing forests and raising livestock are mainly responsible for the rapid climate change that has occurred since the 1950s. These activities release GHGs into the atmosphere. When only the natural climate variabilities are considered, it is difficult to address the changes in global temperatures and, as shown in Figure 4, the average global temperatures would be significantly lower compared to today's temperatures. However, when considering human activities, the change in global warming can be traced to these activities dating back to the 1880s. The scientific observations indicate that the increase in average global temperature is directly proportional to the human activities. It is therefore, imperative to reduce the pollution released to the environment to save the planet.

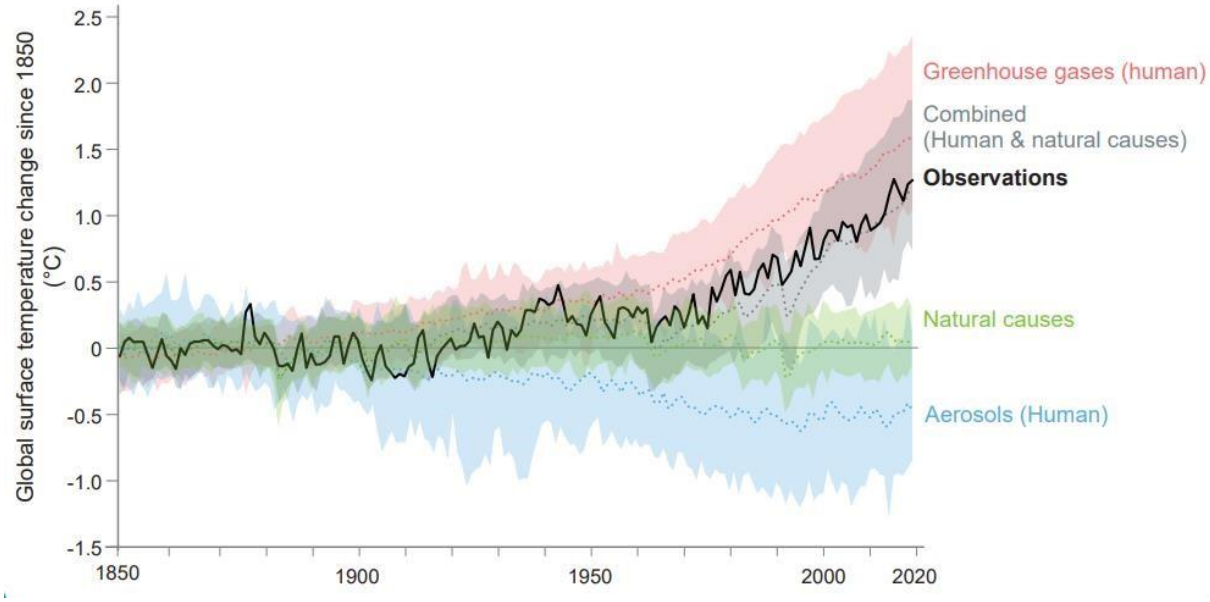

Figure 4: Human Influence on the Climate Change [35]

2.5 Global Current Status and Trends of Climate Change

Global average surface temperature (GTS) increased from 1.09[0.95 to 1.20] °C between 2011 and 2020 compared to 1850–1900 [31]. The terrestrial area had the most increase, from 1.59[1.34 to 1.83] °C, while the ocean experienced the least increase, from 0.88[0.68 to 1.01] °C. In the first two decades of the 21st century 2001-2020, the global surface temperature was (0.99[0.84 to 1.10] °C) higher than from 1850 to 1900, as shown in Figure 5. It increased at a more rapid rate from 1970 than in the 50 year period in the last decades. The cause of the increase was likely to be the human activities. The IPCC 2023 reports that the main driving factor of the increase in global surface temperature from 0.8°C in the period1850-1900 to 1.3°C in 2010-2019 is the human activities [31].

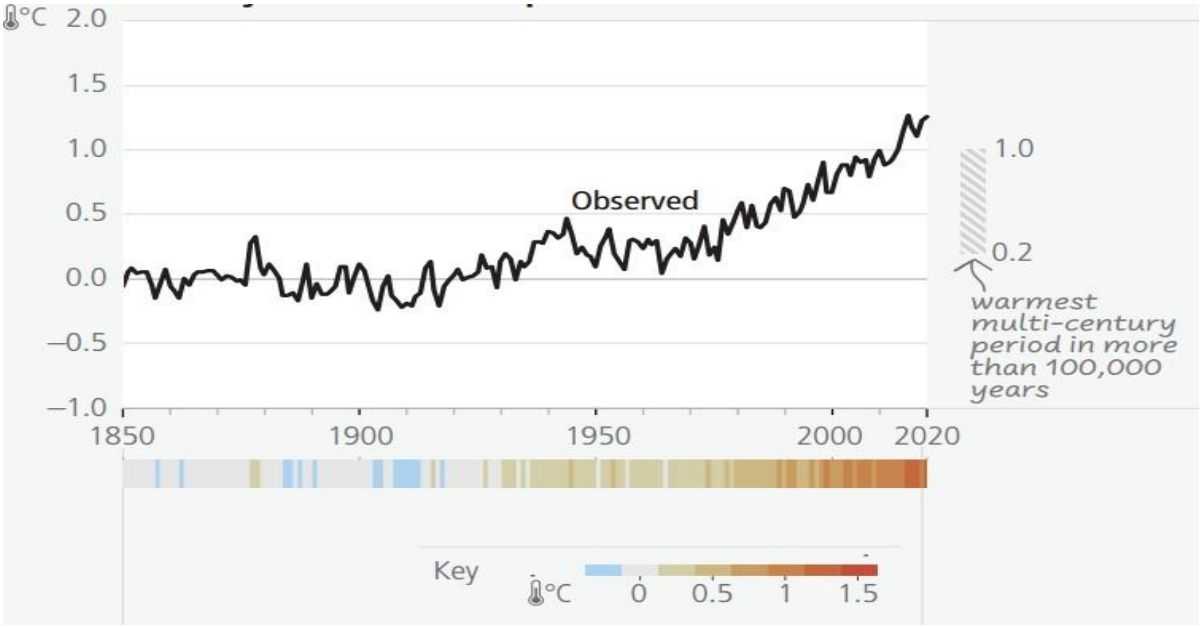

Figure 5: Global Surface Temperature [31]

The greenhouse emissions are likely to be the main contributors to the warming of 1.0℃ to 2.0℃. Other factors such as the aerosols may have contributed to the cooling of 0.0℃ to 0.8℃ while the natural forces such as solar variation and volcanic activity changed the GST from -0.1℃ to +0.1, as shown in Figure 6. The anthropogenic aerosols have a net cooling effect that peaked in the late 20th century. The highest average annual GHGs were recorded in the decade 2010-2019 with a growth rate of 1.3% per year. The combined sectors of energy, industry, transportation and building accounted for 79% of global GHGs in 2019, while agriculture, forestry and other land use accounted for 22%. Since around 1750, there have been observed increases in well-mixed GHG concentrations which are, undoubtedly, due to GHG emissions from these sectors as a result of economic development.

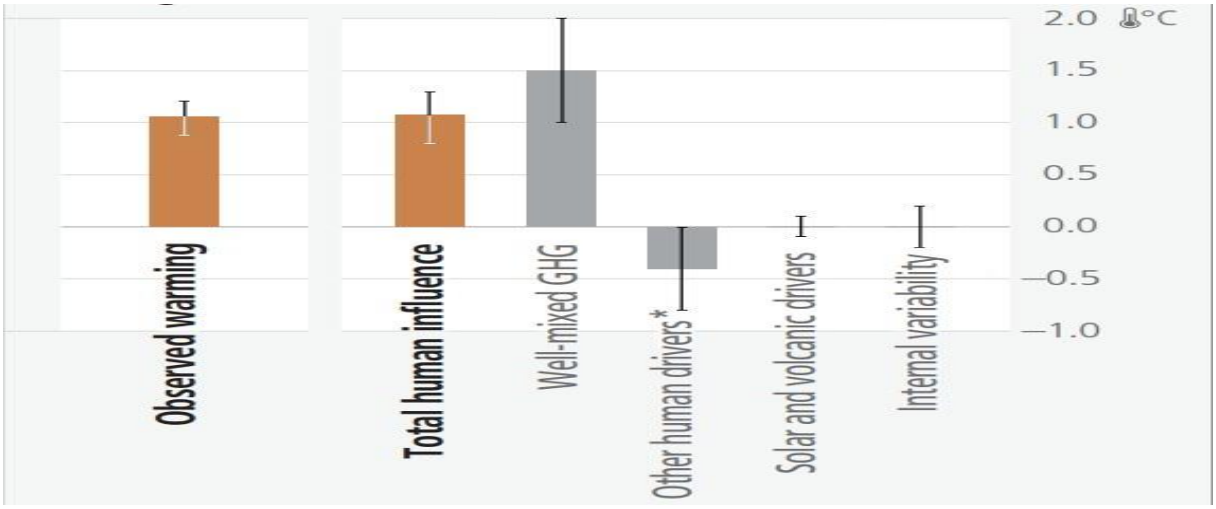

Figure 6: The observed Impact of Emissions from Human Activities [31]

2.6 Observed Impacts of Climate Change

Climate change has caused significant and increasingly permanent losses to terrestrial, freshwater, cryosphere, coastal and open ocean ecosystems [36]. It has resulted in some species becoming extinct over the centuries. However, human activities have accelerated the extinction process to such an extent that an estimated 10% of the species in the last 10,000 years have gone extinct [37]. This is about 1,000 times the natural rate of extinction. Unless immediate steps are taken to increase the resilience of natural regions through preservation, connection and restoration, many more species will become extinct as a result of climate change [38].

United Nations sustainable development goal 2 (SDG 2) includes achieving zero hunger by 2030. Despite an overall increase in agricultural production, climate change has reduced food and water security [39], thus hindering other SDG achievements. The Food and Agriculture Organization (FAO) of the United Nations further claims that food and water-borne diseases linked to climate change have become more common and so has the incidence of diseases carried by the vectors [40]. The increase in temperature, as a result of climate change, has also resulted in reduced economic development in climate-exposed sectors such as energy, tourism, fishery, forestry, and agriculture. For instance, the devastation of houses and infrastructure, the loss of assets and income, health and food security and the negative consequences on gender and social fairness have all had an impact on individual livelihoods [41, 42]

2.7 Future Climate Change

The IPCC 2023 has projected that global warming will continue to increase in the future due to continued GHG emissions to the environment and that under higher emissions scenarios, the global average temperature is estimated to exceed 1.5°C and 2°C, relative to 1850-1900 mean temperatures in the 21st century unless precautions are taken to reduce CO_2 and other greenhouse gases [31]. About 1.5°C is projected in the near term (2021-2040) through considered scenarios and modeled pathways, the implication is that every degree of global warming will increase the number of simultaneous threats on the planet [43]. In most of Africa, Asia, North America and Europe, heavy precipitation and related flooding are expected to worsen and become more frequent with 1.5°C global warming. In addition, the increase in meteorological drought is predicted in a few places. More frequent and/or severe agricultural and ecological drought is predicted in a few regions throughout all the inhabited continents except Asia, compared to 1850–1900 [31].

2.8 Shared Socioeconomic Pathways and the Future Emissions of CO_2

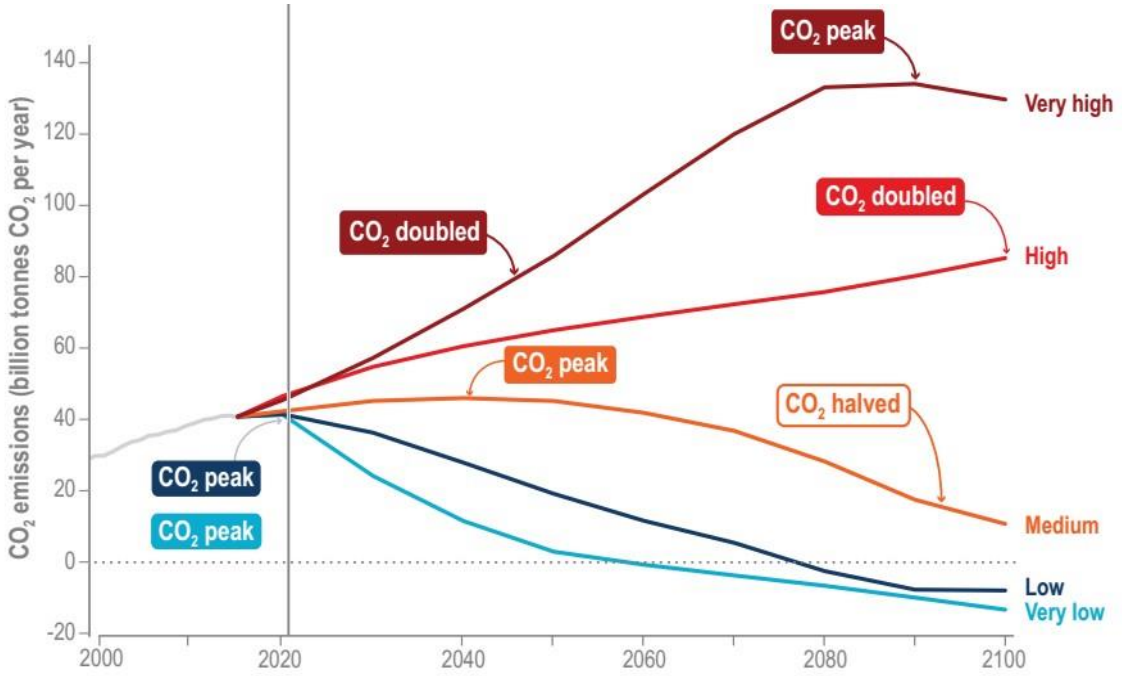

Figure 7: Future Annual Greenhouse Emissions [44]

The shared socioeconomic pathways (SSPs) are used in climate science to describe future greenhouse gas emission scenarios and their potential impact on the global society and the environment. They are useful to policymakers in understanding the potential outcomes of different climate pathways, the socioeconomic factors and the development of strategies for climate change mitigation. The total past and future GHG emissions that are projected in the 2015-2100 period to accelerate the impact of climate change are shown in Figure 7, and the highlight of the figure is CO_2 which is the main cause of global warming.

The SSP5-8.5 scenario projects a high level of greenhouse emissions and their impact on the environment [45]. It depicts the consequences of the future where mitigations are not taken to address the prevailing climate change. The emissions of CO_2 from all the sectors are projected to reach a high of about 130 gigatons of CO_2 per year ($GtCO_2/yr$) from the SSP58.5 scenario, the SSP3-7.0 scenario projects a future with high economic growth and inequality in the society. This shows a high reliance on fossil fuels as energy sources and limited attention to the environmental impact [43,44]. The SSP3-7.0 shows a projected amount of 80 gigatons of CO_2 per year ($GtCO_2/yr$) at the end of the 21st century which is double the amount which was observed in 2015. The SSP2-4.5 represents a scenario with intermediate greenhouse emissions. It also indicates a future where efforts are made to limit these emissions [47]. With this scenario, CO_2 levels are expected to slow down after 2050. SSP1-1.9 and SSP1-2.6 indicate a future where significant steps are taken to mitigate climate change and limit the impact of global warming [45,46]. Both scenarios show a significant drop of GHG emissions in the short term to amount below zero of gigatons of CO_2 per year.

2.9 The Effects of Climate Change on Renewable Energy Resources

Renewable energy resources depend on climate conditions. For example, direct climate change parameters, such as higher ambient temperature, can negatively affect the efficiency of solar cells. Higher wind speeds may result in increased wind power generation and harsh weather conditions such as storms and hurricanes which can pose a risk to wind turbines and, hence, negatively impact their operations [23]. The effects of climate change on renewable energy are essential to understand and to address in order to ensure the sustainability, resilience and effectiveness of renewable energy technologies to adapt to the changing climate [23]. Energy planners, stakeholders, and policymakers can make informed decisions by incorporating

climate change into energy planning and can prepare or mitigate the impacts on renewable energy supply.

2.10 Global Surface Temperature Projections as a Result of CO_2 Emissions

In 2015, the UN Climate Change Conference adopted an international legally binding treaty on climate change which would later be known as the "Paris Climate Agreement" [50]. The aim of this agreement is to mitigate global warming to the levels below 2.0℃ and try to limit it to 1.5℃ above pre-industrial levels [45, 51]. The IPCC, 2023 has indicated varying emissions as shown in Figure 8, depending on socio-economic assumptions, the degree of climate change mitigation, air pollution for aerosols and non-methane ozone precursors [31].

The global surface temperature is projected as high as 5.5℃ and 4.5℃, using the scenarios of SSP5-8.5 and SSP3-7.0 respectively. Global surface temperatures are projected below 2.0℃ when using SSP1-1.9 but are projected to be between 2.0℃ and 3.0℃ when using the SSP12.6 scenario.

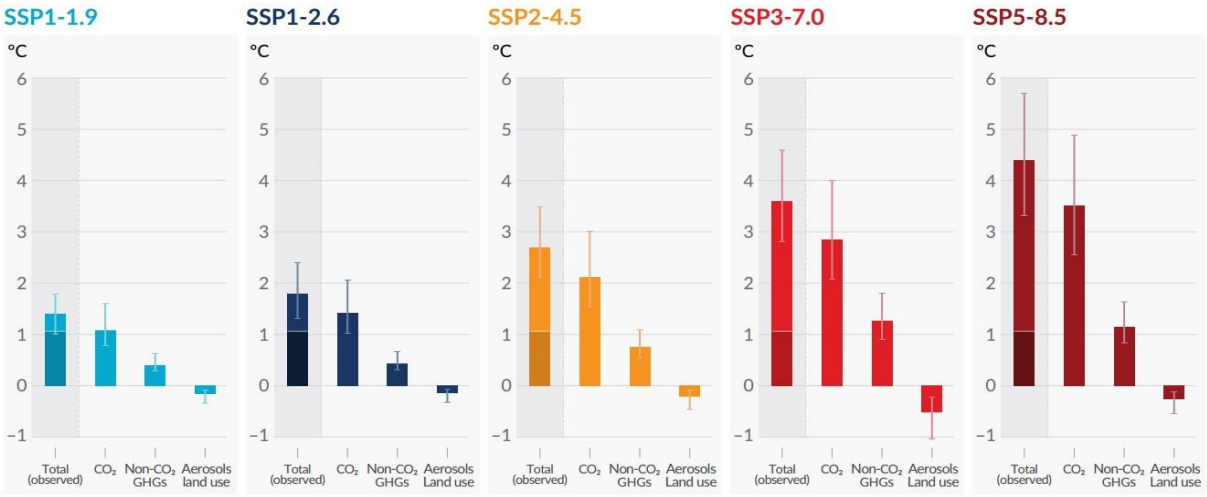

Figure 8: Global Surface Temperature Projections as a Result of CO_2 Emissions

2.11 Climate Change Politics and Policies

Meckling (2023) urges that politics should not be considered as a barrier to achieving climate change but rather be considered as a target of intervention to advance environmental solutions

[52], this is because attempts to address environmental problems such as climate change are linked to the politics approach in order to help the policymakers to develop the strategies that fill the gaps such as the ambition gap, the implementation gap and the international action gap which are critical to the effectiveness policies [52, 53]. The political will, a well-aligned multilevel governance, institutional frameworks, legislation, policies, strategies as well as improved access to funding and technology are all necessary for effective climate action which is facilitated by inclusive governance systems, cooperation across many policy areas and clear goals [54].

Regulatory and economic tools may support significant reductions in the emissions if they are expanded and implemented broadly [31, 55]. When well-implemented, carbon pricing tools have encouraged low-cost emissions reduction strategies but have not been as successful in encouraging higher-cost strategies that are required for additional reductions when used on their own [56]. Strategies such as carbon taxes are implemented as part of emission reduction to generate revenue which will, in turn, support the low-income households. Eliminating fossil fuel subsidies may lower the emissions and result in the benefits such as increased public revenue, macroeconomic stability and sustainability performance [57]. However, eliminating the subsidies may have unfavorable distributional effects, particularly on the most economically vulnerable groups and depending on the economic situation. This can be mitigated by redistributing the saved revenue [58, 59].

2.12 Mitigation and Adaptation Strategies across Energy Systems

The energy sector is one of the major contributors of global warming. Though the sector is dependent on the effects of climate change as part of the obligations under the Paris Agreement, the majority of Nationally Determined Contributions (NDCs) submitted by the Parties to the United Nations Framework Convention on Climate Change (UNFCCC) contained the energy sector emission reduction components [60]. The major transformation of global energy systems and deep reduction in GHG emissions is required for climate change mitigation [61]. Breyer et al. (2020) state that in order to limit the anthropogenic temperature increase to 1.5℃ - 2.0℃ above pre-industrial levels, zero GHG emission energy systems are needed by the mid-21st century and major GHG emissions removal technologies have to be implemented in the early

2030s. They will have to be scaled up between the 2040s and the 2050s [62]. Adaption strategies can reduce the risks associated with climate change on the energy systems [63].

Energy systems that emit net zero emissions comprise reduction in the use of unabated fossil fuel, the use of carbon capture and storage in the remaining fossil fuel systems [64]. Electricity generation systems, such as renewable energy generators that emit no CO_2 need to be adopted and to be coupled with widespread electrification on both rural and urban areas. A combination of energy conservation and efficiency systems strategies can result in a more sustainable and energy-efficient future, benefitting both the environment and the economy. Significant emissions reductions at costs below USD 20 per ton of carbon dioxide equivalent are achieved through the adoption of solar and wind energy, enhancements in energy efficiency and the reduction of methane emissions in the sectors such as coal mining, oil and gas and waste management [63].

Diversifying energy generation through the sources such as wind, solar and small-scale hydropower, along with managing the demand through the measures such as storage and energy efficiency improvements, can enhance energy reliability and decrease susceptibility to climate change impacts. Implementing climate-responsive energy markets, updating design standards for energy assets based on the current and future climate projections, adopting smart-grid technologies, reinforcing transmission systems and enhancing the capacity to address supply shortages are highly feasible strategies in the medium to long term, thus offering additional benefits in terms of climate mitigation [65, 66].

Reducing greenhouse gas (GHG) emissions in industries requires a coordinated action across the value chains. The strategies include optimising the demand, improving energy efficiency, implementing circular material flows, adopting abatement technologies and making transformative changes in the production processes. In transportation, mitigating the CO_2 emissions involves sustainable biofuels, low-emission hydrogen and derivatives. However, the cost reductions and the production process improvements are essential for their effectiveness [67].

When charged with low-greenhouse gas emissions electricity, Electric vehicles have the significant potential to decrease greenhouse gas emissions from land-based transportation throughout their life cycle [68]. Progress in battery technologies can enable the electrification of heavy-duty trucks and to enhance traditional electric rail systems. In order to mitigate the environmental impact of battery production and to address the concerns about critical minerals,

strategies such as diversifying the materials and supply sources, improving the energy and material efficiency and implementing circular material flows can be employed [69].

2.13 Climate Change at Regional Scales

Historical GHG emissions in Africa (compared to other regions) are shown in Figure 9. As it can be observed, Asia had the highest GHG emissions in the world. The figure increased from about 10 Gt CO_2eq in 1990 to more than 25 Gt CO_2eq, during this period, GHG emissions in Africa were less than 5 Gt CO_2eq. Transition to renewable energy sources presents a strategic solution to diminish dependence on wood fuel and charcoal, particularly in urban areas. The transition offers a multitude of advantages such as reduced deforestation, mitigation of desertification, decreased fire risks and improved indoor air quality [70]. Additionally, adapting renewable energy technology encourages local development and improves agricultural yields. The transition to renewable energy also reduces the emissions to the atmosphere, saving the planet and improving the health of the society.

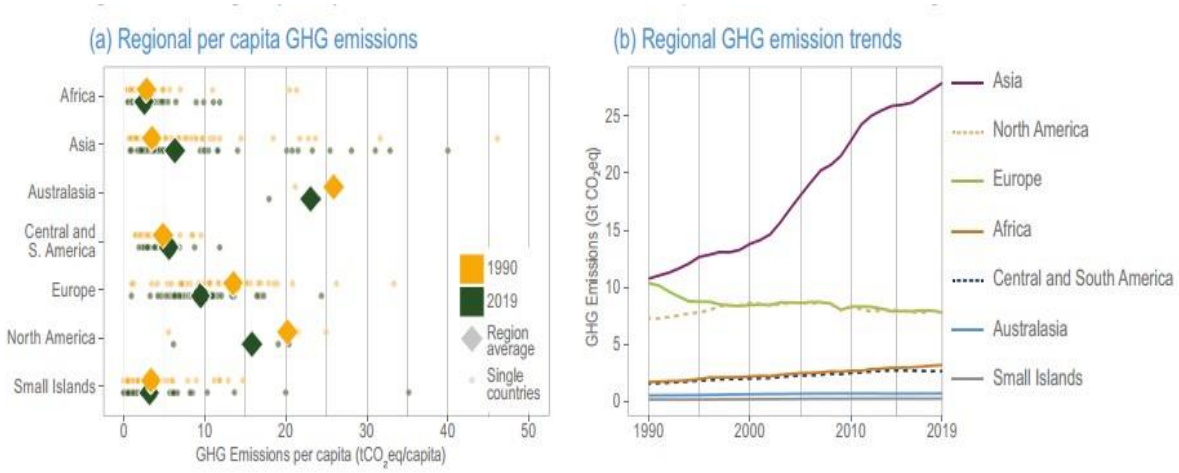

Figure 9: Greenhouse Gas in Africa compared to other World Regions from 1990-2019 [37]

The SSA region is recognized as highly susceptible to the impact of climate change due to its limited ability to adapt to or mitigate the effects of environmental shifts. Despite Africa being a minor contributor to greenhouse gas emissions that are linked to climate change, the continent has witnessed significant losses and damages in the key development sectors [37].

The repercussions, attributed to human-induced climate change encompass biodiversity decline, water shortages, reduced food production, loss of human lives and hindered economic growth. These negative impacts are expected to become widespread and severe with global warming levels between 1.5°C and 2°C [71]. Assuming localized and incremental adaptation measures, restricting global warming to 1.5°C is projected to significantly mitigate damages to African economies, agriculture, human health and ecosystems when compared to higher global warming levels [37, 72, 73].

In the Southern African region, the mean annual temperature in the region has increased by a range of 1.04°C to 1.44°C from 1961 to 2015, depending on the specific observational dataset employed [44]. Over the past four decades, there has been a notable escalation in the annual count of hot days in Southern Africa. Furthermore, there is a growing body of evidence suggesting an increased occurrence of heat stress with detrimental effects on both agriculture and human health [74]. At the same time, there has been a reduction in the frequency of cold extremes, including days with frost and with global warming levels reaching 1.5°C, 2°C, and 3°C above the pre-industrial levels, the anticipated mean annual temperatures in Southern Africa are expected to be, on average, 1.2°C, 2.3°C, and 3.3°C higher than the baseline average of 1994–2005, respectively. Meanwhile, the summer rainfall in the region is expected to decline in mean annual rainfall by 10–20% [75], coupled with an increase in the frequency of consecutive dry days throughout the rainy season.

2.14 Adaptation and Indigenous Knowledge

The adaptation capacity to climate conditions remains low in Africa and recent studies have directed their focus towards indigenous knowledge (IK) to support the development of sustainable and effective strategies of climate change. According to the IPCC, the term indigenous knowledge refers to the understanding, skills and philosophies developed by societies with the long histories of interaction with their natural surrounding [34].

IK has proven valuable in shaping diverse climate change adaptation strategies, spanning areas such as management practices, early warning systems risk and disaster management [76]. The significance lies in fostering knowledge co-production, and contributing to the creation of

resilient adaptation measures. A crucial importance for the integration of IK and scientific knowledge is in weather and climate services, enhancing the reliability and acceptability of forecasts within the local communities [77]. However, the decline of IK is evident due to the factors such as modernisation, rural-urban migration, alterations in landscapes and shifts in religious beliefs.

2.15 Climate Change in Lesotho

Lesotho is a country that is highly vulnerable to the impact of climate change due to its topography and socio-economic conditions and it has presented a Nationally Determined Contribution to strengthen the global efforts of both mitigation and adaptation according to the Paris Agreement, this is despite the country having a relatively low carbon emissions as compared to other developing and developed countries. In 2021, Lesotho's GHG emissions were estimated at 6.04 million tonnes while South Africa and Nigeria were the highest GHG emitting countries on the continent with 552.89 million tonnes and 444.50 million tonnes respectively as shown in Figure 10. Lesotho has adopted plans to further address and reduce the emissions by capitalizing on the available opportunities presented by the low-carbon development pathways and green economy in the sectors such as energy, transport, agriculture, forestry, waste management, land use and land use change [78].

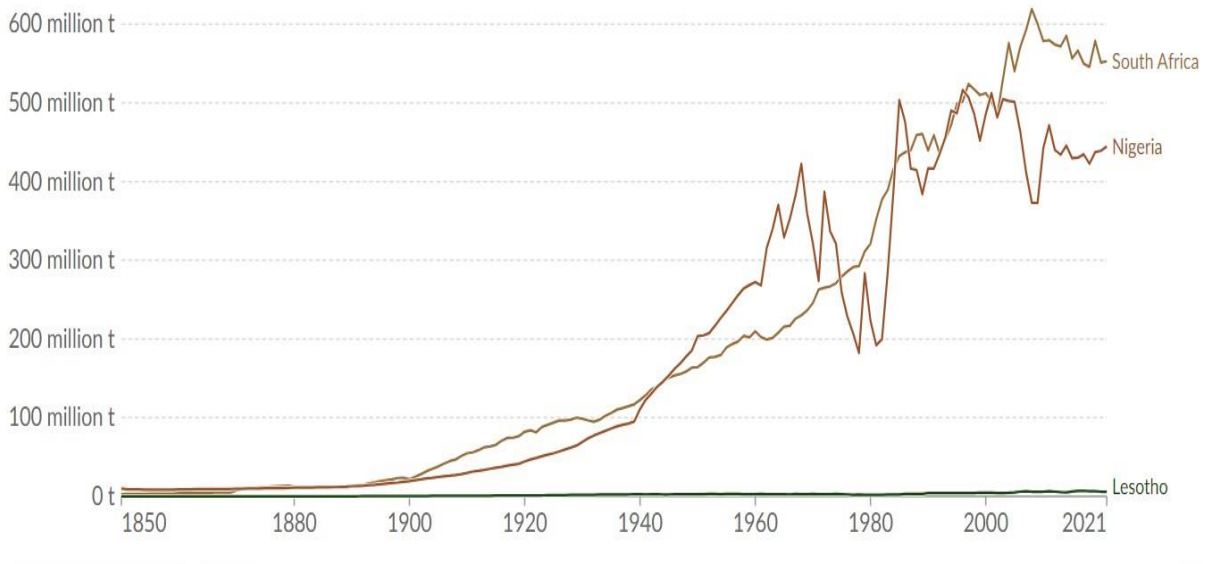

Figure 10: Lesotho's GHG Emission Compared to Other African High Emitting Countries [79]

In accordance with its Nationally Determined Contributions (NDC), Lesotho has aggressively pursued a number of policies aimed at advancing a low-carbon growth trajectory customized to its unique national circumstances. In addition to the significant expenditures in afforestation and rural electrification projects, these programmes also aim to harness the power of hydro, solar and wind power [78]. Nevertheless, in order for Lesotho to fully unlock its capacity to significantly contribute to global mitigation strategies, substantial assistance from the international community is required. The 2017-2027 Lesotho National Climate Change Policy under the Ministry of Energy and Meteorology was developed with a vision to build climate change resilience and low-carbon pathways including a prosperous economy and environment in the country [80], the policy was developed with the guiding principles of the Paris Agreement, Sustainable Development Goals, the African Union Agenda 2063, the United Nations Framework Convention on Climate Change (UNFCCC), and the National Strategic Development Plan.

Recent patterns in climate change and future projections consistently provide compelling evidence of climate variations, underscoring Lesotho's susceptibility to such changes. The country has witnessed a frequency of natural disasters, particularly drought and floods in recent years. Notably, critical water resources, including perennial springs, robust rivers and numerous dams, have significantly diminished. Agricultural activities as the sources of living in the rural areas are steadily diminishing, thus worsening the challenges faced by the population. Concurrently, the escalation of soil loss and land degradation has been accelerated by the compounding pressures of agricultural and livestock practices (such as over-cultivation and overgrazing), urbanization and deforestation [81]. The estimated annual loss of 40 million tons of soil through erosion compounds these environmental challenges.
The country's National Strategic Development Plan (NDSP) has outlined a plan to reverse environmental degradation and adapt to climate change as the main objective.

2.16 Overview of Climate Modelling

McGuffie and Henderson-Seller (2014) explain climate modeling in terms of parameterisation and define it as the process of representing a physical process mathematically by establishing a link between the key process parameters without explicitly modeling every step of the process

[82]. Climate models are computer simulations that represent the interactions of the Earth's atmosphere, the oceans, land surface and other components. They are used to understand and predict climate patterns and changes.

Types of Climate Models [82]:

- Energy Balance Models (EBM)
- Radiative Convective and Single Column Models
- Dimensionally Constrained Models (Statistical dynamical, Earth system models of Intermediate Complexity)
- General Circulation Models (GCM)

2.16.1 Energy Balance Models (EBM)

Energy balance models (EBMs) are mathematical representations used to understand and study the distribution and flow of energy inside the system. According to Robert Colman & Sergei Soldatenko (2020), it is also used in Coupled Model Intercomparison Project Phase 5 (CMIP5) to investigate climate variability and sensitivity [83]. The EBMs are used in various scientific fields such as climatology, ecology and physics to examine the energy exchange between different system components using the fundamental concept that energy can neither be created nor destroyed but can be changed from one form to another or can be transferred between different parts of the system. In climate modeling, the energy balance models are essential for understanding the interactions between incoming solar radiation and the outgoing terrestrial radiation, the energy absorbed and the energy absorbed and re-radiated by the atmosphere and surface [84, 85].

2.16.2 Radiative Convective and Single-Column Models

Single-column models (SCMs) and radiative convective models (RCMs) are basic tools that help in understanding the complex interactions that occur within the Earth's atmosphere in atmospheric and climate research. RCMs are designed to study the interaction between radiation and convection in the atmosphere with respect to the radiative component of the RCMs. This includes the phenomena such as greenhouse gas absorption and solar radiation

reflection by the Earth's surface and atmospheric gases that they absorb or re-emit. The process includes the absorption of heat from sunlight and the reflection back to the space. The convective component simulates the phenomena such as cloud formation and precipitation by concentrating on the upward movement of air masses by linking the radiative and convective processes.

The SCMs simplify the modeling domain to a single vertical column of the atmosphere, allowing a detailed investigation into the vertical processes without large computational costs associated with bigger models. This vertical column usually runs from the surface up to the top of the atmosphere and within this defined column. The SCMs contain parameterizations for several physical processes such as radiation, convection, turbulence, and surface fluxes.

2.16.3 Dimensionally Constrained Models

Scientific research uses dimensionally restricted models, such as Statistical Dynamical Models (SDMs) and Earth System Models of Intermediate Complexity (EMICs) which provide a compromise between the computational efficiency and the ability to capture the essential dynamics. The SDMs are one type of model that combines statistical aspects with the dynamical principles. Statistical properties are represented by these models while incorporating the main dynamical processes. The SDM simulations can run efficiently in many cases because they are sometimes limited by dimensionality, unlike the more complex types of models. In the SDMs, statistical relationships are established on the basis of observational data. These relationships are then used to simulate the behaviour of the system in some areas such as climate science and weather prediction as they allow for significant dynamic features to be captured without becoming computationally impractical.

The EMICs are another class of dimensionally restricted models which simulate the interactions among the different components of the Earth system such as the atmosphere, oceans, land surface and ice at an intermediate level of complexity that lies between the simple models and comprehensive Earth System Models (ESMs). The EMICs reduce some processes and the parameterisations, thereby making them computationally more efficient than the higher resolution ESMs. Nevertheless, these simplifications enable them to capture substantive feedback and interactions across the components for the researchers who study the various

scenarios including the long-term behaviour of the Earth System. Such models prove to be ideal for investigating the large-scale climate phenomena, understanding human impacts on the environment as well as exploring the possible climatic projections. They strike a balance between realism and computational efficiency hence they can be employed by the scientists who address the diverse scientific issues.

2.16.4 General Circulation Models/Global Climate Models (GCM)

The General circulation models (GCMs), also known as global climate models, are the numerical tools used in atmospheric science for simulating the Earth's climate system. These mathematical models encompass the physical processes that govern atmospheric behaviour, the ocean, the land surface and the sea ice. The GCMs play a vital role in explaining and forecasting climatic patterns including the changes in temperature, rainfall and other such variables [86]. The representation of the atmospheric dynamics is one of the important features of GCMs and their structure breaks the atmosphere into a three-dimensional grid, using the equations that are based on the fundamental laws of physics such as fluid dynamics or thermodynamics to make it possible for them to calculate air masses movement, heat transfer and other types of atmospheric processes. Besides their ability to simulate these movements within the ocean depths, the contribution of the GCMs to this process also includes oceanographic simulations which take into account the factors such as the ocean currents as well as the heat exchange and the sea surface temperatures. Additionally, the GCMs have components that attempt to reproduce land surface processes such as the vegetation dynamics and the land-atmosphere interaction in order to accurately depict how the changes in land cover can alter the climatic patterns which result from deforestation or urbanization. The representation of the sea ice dynamics is crucial for capturing the interactions between the atmosphere and the polar regions, especially in the context of climate change.

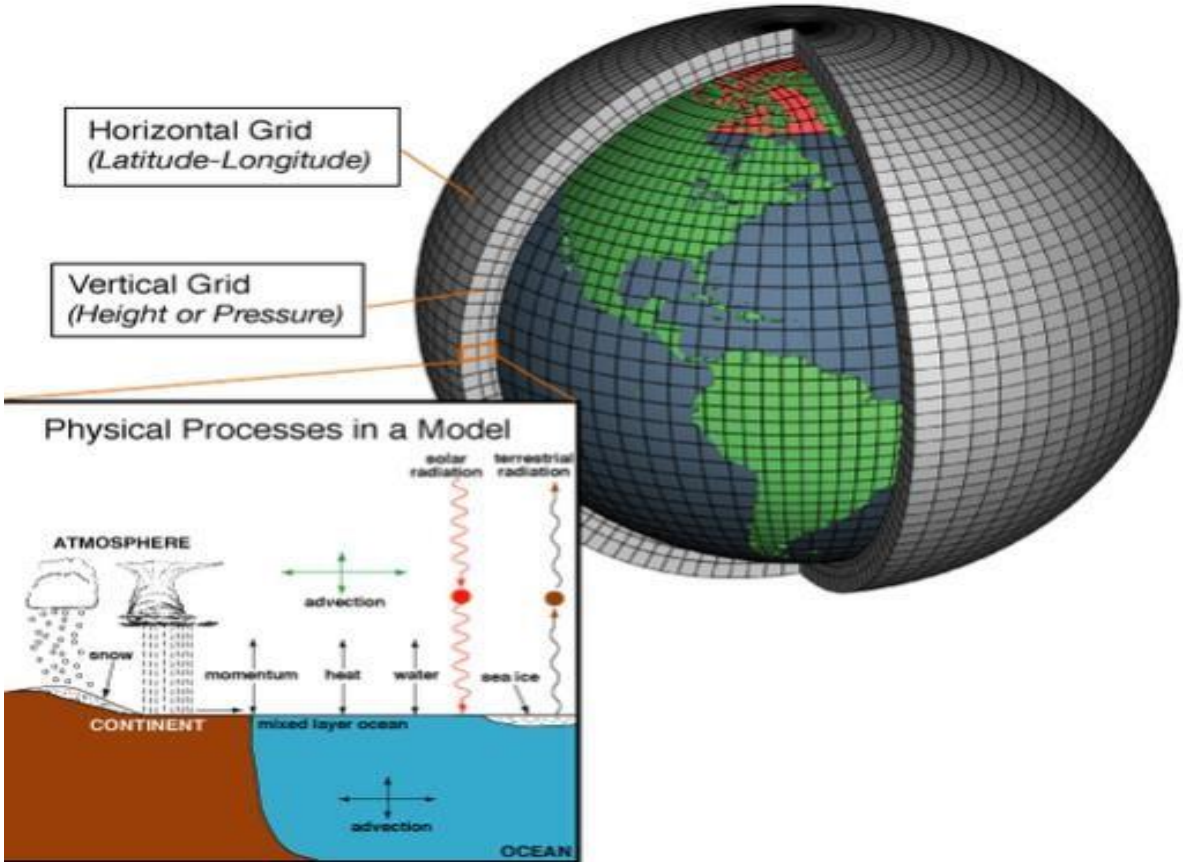

Figure 11: Typical Global Climate Model [87]

The GCMs models are the best tools available for scientistific investigation on how the Earth climate system may evolve over time in response to the different kinds of conditions. They divide the planet into a three-dimensional grid (with four-dimensional time added for a good measure) and then perform the calculations for each part of the grid, inside which certain physical laws (obtained from basic principles of physics, chemistry, and mathematics) are supposed to govern the climate system behaviour, as shown in Figure 11. The key assumption is that the laws which govern the climate system at any given moment in time and at any given place on the planet will also govern its behaviour in the future and in response to the hypothetical what-if scenarios.

2.17 Climate Models Simulation

The IPCC representative concentration pathway scenario or future greenhouse gas concentration trajectories are outlined, incorporating the terrain and land-use data sets such as

the atmospheric composition, precipitation, wind speed, and solar radiation. The GCMs provide the RCMs with the boundary conditions such as the atmospheric conditions and large-scale atmospheric circulation patterns to RCMs [88]. The schematic of this scenario is shown in Figure 12. The RCMs use the boundaries to make regional climate simulations with the focus on smaller spatial scales and the fine details that GCMs cannot adequately capture. The resolution for the GCMs can range between 100 and 200km, making it difficult to observe the finer details and the local variations, while the RCMs can reproduce the climate of a finer spatial resolution that ranges between 1 and 20km [89, 90], with greater accuracy of regional climate phenomena, including land-sea interactions, topographic effects and smallscale atmospheric circulations.

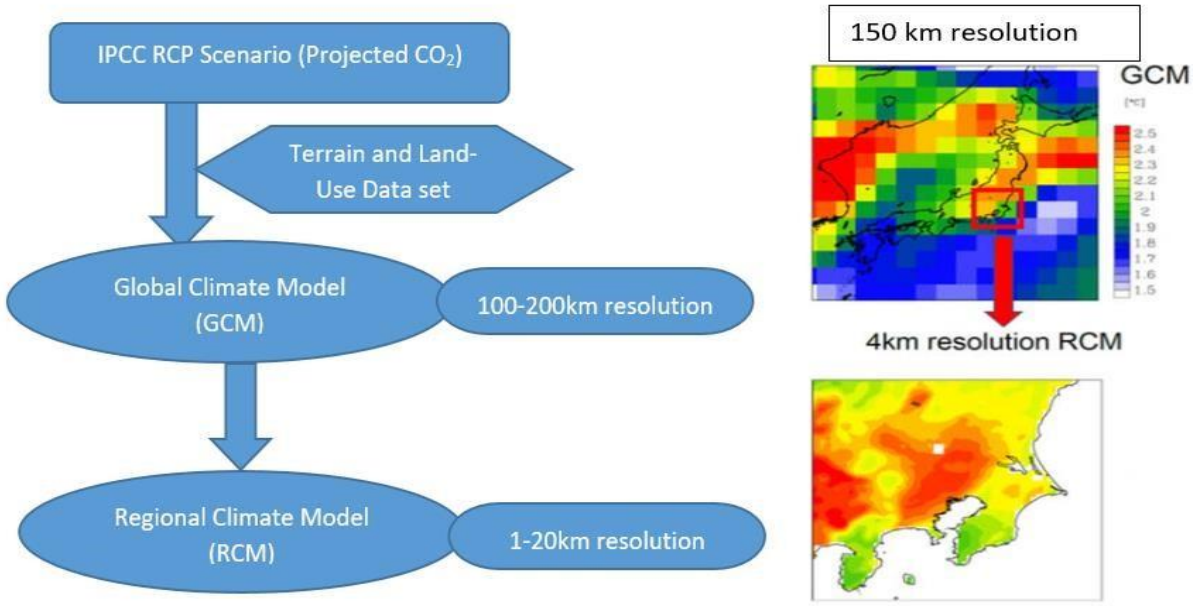

Figure 12: Climate Model Simulation [91]

The collaboration between the GCMs and RCMs facilitates a comprehensive understanding of climate dynamics across various spatial scales. The GCMs provide the broader context of global climate change and its drivers, while the RCMs offer a detailed perspective into regional climate patterns, variability and extremes [92]. This integrated approach can be optimized to assess the potential impact of climate change on different regions and for developing the targeted adaptation and mitigation strategies to address the regional vulnerabilities.

2.18 Downscaling

The term "downscaling" refers to the process of generating local- and region-specific highresolution climate information from global climate model outputs at a relatively coarse spatial resolution. It handles the spatial discontinuity that exists between the GCMs whose typical resolution span is of order 100–200 kilometers. The finer-scale information needed to do regional climate assessments whose requirements may be 1–20 kilometers or even smaller.

The downscaling process can be achieved through two main approaches:

2.18.1 Dynamic Downscaling

Regional Climate Models (RCMs) (RCMs) constitute the advanced weather models that have higher resolutions and spatial settings used to simulate the climate processes in the regions of interest. They use boundary conditions from the GCMs to drive the simulations but operate at a finer scale. However, they allow for the representation of the local climate features at a higher resolution than the GCMs.

Nested Grids: The RCMs do not stagger the grids like rectangular grid configurations, but they use a circular configuration where a fine grid is at the center and coarser resolutions become less detailed around it [93]. The coarser outer domain gives a preliminary environment, whereas the inner domain where the climate processes on a small scale occur is used as a boundary condition [94].

Physics-Based Modeling: RCMs use the same physical equations as those used in GCMs except for specific changes made to reflect the characteristics of the land, including the topography and land use. It is those small-scale climate events on a local scale that happen regularly.

2.18.2 Statistical Downscaling

Empirical-statistical methods: these statistical downscaling techniques are based on the statistical relationship between the large-scale atmospheric variables from GCMs and the local climate observed in the weather stations or other areas. The calculated relationships are then used to produce downscaled climate projections for specific areas from the GCM outputs. The

regression models are the most widely used techniques for statistical downscaling. Multiple regression models and machine learning methods derive statistical links between predictor variables and predictors using historical observations.

There are advantages and disadvantages for both dynamic and statistical downscaling approaches. Dynamic downscaling, through the use of the RCMs, offers theoretically sound estimations of regional climate processes although the requirement for substantial computing skills and resources may be a limiting factor. Statistical downscaling is less computationally expensive and can be more easily applied to various GCM types although it may lack some of the finer scale processes, typically resolved by RCMs.

2.19 Model Error and Uncertainty

In climate modeling, a model error is the difference between the predictions of a model and the actual field measurements, it is the extent to which the dynamics and basic physical processes of the climate system are accurately represented by the model. Inaccurate representations of atmospheric processes, land surface interactions, ocean dynamics and other elements of the Earth's climate system can lead to model mistakes in climate models. The model error indicates the degree to which the model's assumptions and equations diverge from the actual physical processes. Uncertainty in climate modeling is the lack of accuracy or confidence in the model's predictions. It originates from a variety of the sources of different aspects of the modeling process.

Sources of uncertainty in climate modeling comprise:

- Internal variability (Natural variability in the climate system, such as El Niño and La Niña events) can lead to short-term fluctuations)
- Emission Scenario Uncertainty (different possible future emissions introduce uncertainty in projecting future climate conditions)
- Model uncertainty (Climate models are simplifications of the real world, and the choices (such as omissions) made in model structure can impact results.)
- Downscaling uncertainty (some important features operate in a coarse scale and may not capture the local features)

Uncertainty represents a comprehensive concept, acknowledging a spectrum of the factors that contribute to imprecision in climate model predictions. Both model error and uncertainty are critical considerations in improving the reliability and usefulness of climate models.

2.19.1 Strategies for Dealing with Uncertainty in Climate Modeling

Addressing uncertainties in climate modeling involves strategies such as quantifying and identifying sources of uncertainty, running multiple simulations, conducting sensitivity analyses, planning for various scenarios, calibrating and validating models, transparently communicating uncertainties, investing in research and model enhancement and promoting international collaboration for data sharing and expertise [95, 96]. These approaches contribute to the improvement of climate predictions, enhancing accuracy and informing the decision-making processes effectively.

2.20 The Coordinated Regional Downscaling Experiment (CORDEX)-Africa

CORDEX is a regional climate model developed by the World Climate Research Programme (WCRP) to improve regional climate scenarios through downscaling of the global climate models (GCMs) [97]. CORDEX provides a platform for generating high-resolution climate projections to study and understand climate variability at regional scale [98]. The CORDEXAfrica focuses specifically on improving climate models and projections for the African continent. The main objective is to address the challenges facing African's diverse climate zones, and the continent's vulnerability to the impacts of climate change. CORDEX-Africa uses RCMs to downscale the GCM results, providing results of high-resolution around 50 km or less [99]. The downscaled results are capture fine-scale climate process that were not visible on the GCM.

CORDEX Africa data and projections are used in various sectors, such as agriculture, energy, disaster risk management, infrastructure planning, and water resource. The projections are important for planning as well as developing adaptation and mitigation strategies in response to the climate change. More scientists and researchers are relying on CORDEX due to its ability to produce results of high-resolution and reliabla climate projections

2.21 Previous Climate Modelling Studies

Several studies have been conducted on climate modelling in different regions of the world. This section will take a look at some of the work that has been done in this area of study. Pieter de Jong et al. (2019) estimated the impact of climate change on wind and solar energy by 2030s and the 2080s in Brazil using a South American regional climate model from three downscaled global models [22]. The results of that study showed a slight increase of solar energy at solar power plants in the north-east of the country. Furthermore, wind potential was also projected to increase by more than 40% at some of the existing wind power plants. Waleed Abbas et al. (2020) conducted a study on the impact of climate change on renewable energy resources in the Arab World using the climate data obtained from the web-based WorldClim and the global climate model (ECHAM5-MPIOM) downscaled by the RegCM and CORDEX regional climate models [100]. The impact of climate change on renewable energy resources in the Caribbean region conducted by Angeles et al. (2010) used a parallel climate model (PCM) coupled with a numerical model regional atmospheric modeling system (RAMS) to simulate solar and wind energy in the island of Puerto Rico.

Another study on the impact of climate change on wind and photovoltaic energy resources in the Canary Islands and adjacent regions was conducted by Gutirrez et al. (2021) using a set of climate simulations obtained from the MENA-CORDEX to simulate the present and future climate conditions in two scenarios [2]. Most studies used climate models to project future climate conditions and to power production equations. However, power production equations result in large variations for long-term climate change scenarios which make it less attractive in the scientific community [101].

2.22 Climate Change Scenarios

Climate change scenarios serve as speculative representations of the forthcoming climates, relying on diverse assumptions regarding the future greenhouse gas emissions, the socioeconomic trends and related variables. These scenarios help the scientists, the

policymakers and interested parties to examine the various potential outcomes and to evaluate the impact of climate change across different scenarios. The key aspects of the climate change scenarios used by CMIP5 for the IPCC for the Fifth Assessment Report (AR5) are the Representative Concentration Pathways (RCPs). These include a set of greenhouse gas concentration trajectories in the atmosphere over time, different RCP defined by the radiative forcing levels by the year 2100 (as compared to pre-industrial levels) [102].
They are also used in this report to make climate change projections. There are four different RCPs;

RCP2.6: An optimistic scenario that assumes strong mitigation pathways, large-scale reductions in emissions and increasing rates of renewable energy deployment, affirming progress towards a low-carbon world. Radiative forcing is maximal at approximately 3 W/m² by the time plateaus in and then fades out during the course of the 21st century.

Implication: This outcome aligns with the aspirational goal of the Paris Agreement and is consistent with achieving a rise in global temperatures of well below 2°C above the preindustrial levels.

RCP4.5: This scenario is a moderate GHG emission one and it anticipates some mitigation such as the policies to reduce the emissions (changing energy sources), radiative forcing peaks at approximately 4.5 W/m² before reverting to the new equilibrium without overshooting.

Implications: This scenario implies a future where global warming is limited but still exceeds 2°C above the pre-industrial levels. Substantial efforts are required to adapt to the impact of climate change.

RCP6.0: The Medium-high GHG emissions scenario assumes a continued increase in emissions and some modest mitigation effort but is less ambitious than the RCP2. 6 and RCP4. 5. The Radiative forcing peaks at approximately 6 W/m^2 by 2100 remain constant afterwards.

Implications: This situation relates to a world warmed by more than 2.0 degrees C above the pre-industrial levels which come with major climate change effects. It stresses the need for mitigation and adaptation measures to deal with these impacts.

RCP8.5: The highest emission scenario (high GHG emissions)- starts from the assumption that people will continue to use large volumes of fossil fuels and are not interested in changing their efforts to mitigate the effects. The values of radiative forcing keep growing until the end of the century up to approximately 8.5 W/m² in 2100

Implications: This scenario corresponds to a future where global warming exceeds 4°C above the pre-industrial levels, resulting in severe and widespread impact on the ecosystems, societies and economies. It underscores the urgent need for ambitious mitigation actions to avoid the most catastrophic consequences of climate change.

2.23 Solar and Wind Energy Global Trends

In 2022, a renewable power capacity with a total of 348 GW was added to the global energy mix, this was a 13% increase from the 306 GW added in 2021. However, the International Energy Agency (IEA) has stated that in order to be on track with the IEA net zero scenarios by 2030, renewable power additions need to increase by 2.5 times the current additions [103]. Wind and solar energy dominated the renewable power addition with 92% of the total renewable additions (22% wind and 70% solar). The annual renewable power capacity additions shown in Figure 13 indicate increasing trends in global renewable power addition from 2017-2022 and it is expected to continue to increase in the future.

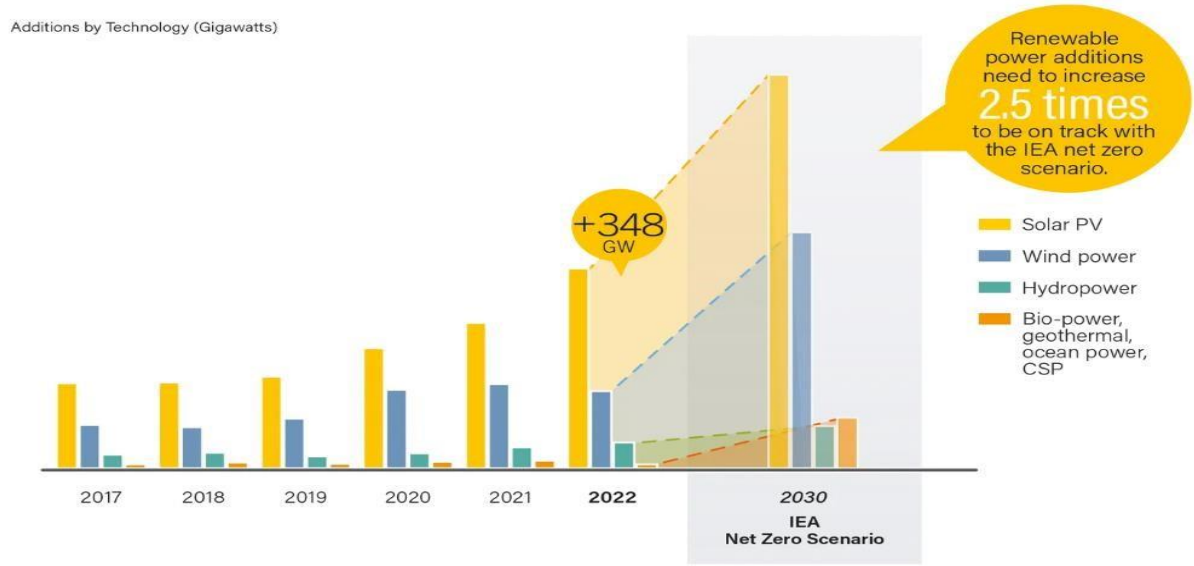

Figure 13: Annual Renewable Power Capacity Additions, 2017-2022, vs the total Installation Required to Reach IEA Net Zero Scenario in 2030 [103]

The IEA has outlined the following factors as the main reason of increasing the wind and solar power supply;

Policies: promoting the growth of the solar photovoltaic (PV) and wind energy has inceased consistently, with over 140 countries currently endorsing such measures. Simultaneously, the major markets including China, the European Union, India, Japan, and the United States, have significantly elevated their policy ambitions and the corresponding support for the expansion of these renewable energy sources.

Cost of Electricity: From 2010 to 2022, the cost of generating electricity, measured as the levelized cost, witnessed substantial declines—approximately 90% for solar photovoltaic (PV), 70% for onshore wind and 60% for offshore wind. Although recent years have seen some cost increases, notably impacting the wind power in advanced economies, these cost reductions align with the projected learning rates associated with the expanded deployment and technological advancements in the renewable energy sector. Overall, a symbiotic relationship has emerged between the policy support and cost reductions, establishing a positive feedback loop; heightened policy backing has spurred increased deployment, resulting in cost reductions which, in turn, have facilitated further deployment.

Manufacturing capacity and industrial policies: IEA forecasts now systematically consider advancements in the supply chains of clean energy, surpassing the actual deployment in certain instances and presenting a prospect for accelerated growth, particularly in solar photovoltaic (PV).

Financing conditions: The significance of the cost of capital for solar photovoltaic (PV) and wind power is particularly noteworthy, given that most of their lifetime expenses stem from upfront capital costs. Established and proven policy and regulatory structures have played a crucial role in diminishing financing expenses by offering operators high revenue certainty, typically through extended contractual agreements. In the current context, the elevated borrowing costs raise apprehension as they pose some challenges to project the economics, potentially shifting the cost considerations back toward the technologies with the lower initial expenses, often associated with pollution but entailing long-term expenditures for fuel

These factors have generally had a favourable impact on the expansion of wind power and solar photovoltaic (PV), contributing to consistent year-on-year growth in forecasted deployment. However, the projected increase in wind and solar PV generation to reach the net zero emission scenario in 2030 falls significantly short of the necessary level to restrict global warming to 1.5 °C. Therefore urgent measures and solutions are required to reach this goal.

2.23.1 Levelized Cost of Electricity for Wind and Solar Energy

Renewable energy equipment prices and commodity as well as project delays affect renewable energy project costs. The global weighted average levelised cost of electricity (LCOE) which decreased in 2021 for solar PV as well as for onshore and offshore wind power. However, the global capacity additions of these technologies did not show any sign of decreasing [103, 104]. In 2021, the global weighted average LCOE for th newly commissioned utility-scale solar PV plants decreased from USD 0.055/kWh in 2020 to USD 0.048/kWh while the global weighted average LCOE of the newly commissioned onshore wind projects decreased from USD 0.039/kWh in 2020 to USD 0.033/kWh in 2021 [104]. The newly commissioned utility-scale solar PV projects LCOE decreased by 88% from 2010 to 2021.

In 2021, a significant number of projects were affected by the increasing solar PV module costs at the end of 2020. The impact was, however, limited as outlined by the IRENA Outlook 2023, which states that only three out of the top 25 markets of new installations experienced an increase in their country-level total weighted average installed costs in 2021 [104]. Many countries experienced an increase in the average cost of electricity from onshore wind and solar PV in 2022 due to the supply chain constraints that started in 2020 and the general commodity cost inflation that began in 2022. These increases were larger for onshore wind than for solar PV. The increase in commodity and renewable energy equipment costs has a delayed impact on the project costs due to the time difference between a financial investment decision and when a project is commissioned [105, 106].

2.24 Synthesis of Literature

Climate change, as defined by the IPCC, refers to long-term changes in climate conditions, often spanning decades and detected through variations in the average and variability of climate properties. Global warming specifically denotes the increase in the Earth's average temperature, which subsequently alters climate patterns. The causes of climate change include the natural processes and human activities such as altering the atmosphere composition and land use. Since 1880, global surface temperatures have risen from -0.16℃ to 0.9℃ by 2020. Satellite observations indicate that sea levels have risen by 98 millimeters from 1993 to 2022, due to

thermal expansion of seawater and melting ice sheets and glaciers. The IPCC 2023 report projects continued to increase global warming, potentially exceeding
1.5℃ and 2℃ relative to pre-industrial levels in the 21st century, unless significant reductions in greenhouse gas emissions are made.

Renewable energy sources, such as solar and wind, are influenced by climate conditions. For instance, higher temperatures can reduce solar cell efficiency, while increased wind speeds can enhance wind power generation. However, extreme weather events can damage wind turbines. Lesotho is particularly vulnerable to climate change impacts due to its geography and socio-economic status. Despite its low carbon emissions, it has committed to global mitigation and adaptation efforts under the Paris Agreement. Climate models simulate interactions within the Earth's system to predict climate patterns and changes, using the various scenarios based on future emissions and socio-economic trends to explore the potential outcomes.

The energy balance model (EBM) uses a simplified approach in climate science to understand the energy balance entering and exiting the Earth’s climate system. However, the main disadvantage of its simplicity is the reduced accuracy and details for the applications that require a high spatial resolution. Radiative-convection models (RCMs) combine both radiative transfer and convective processes, making them suitable for studying the interaction between the two important atmospheric processes. Their main disadvantage for this study is their ability to exclude complex atmospheric dynamics such as wind patterns and interactions between different atmospheric columns. Single-column models (SMCs) are useful for analysing various atmospheric phenomena because they can incorporate a wide range of physical processes, including radiation, convection and cloud formation. However, they are limited in their ability to describe horizontal interactions between different regions.

Dimensionally Constrained Models offer the advantage of resource efficiency, reduced complexity and interpretation. Their disadvantages include potential loss of detail risk of introducing biases and reduced flexibility. General Circulation Models (GCMs) are capable of simulating the entire climate system, including interactions between the atmosphere, land, ocean and ice. The main disadvantage of the GCMs is that they require a lot of computational resources due to their complexity in simulating multiple interaction components of the
Earth’s climate system. The GCMs are also used to predict future climate conditions and to make long-term climate projections which are important for understanding the potential

longterm effects of climate change. As a result, the GCMs were chosen as the suitable model for this study.

From 2017 to 2022, wind and solar energy dominated global renewable power additions, making up 92% of the total. The cost of solar and wind energy has decreased significantly, with the levelized cost of electricity (LCOE) for solar PV plants dropping from $0.055/kWh in 2020 to $0.048/kWh and the onshore wind projects decreasing from $0.039/kWh to $0.033/kWh. This trend is expected to continue, further advancing renewable energy adoption.

3 Methodology

The objective of this study was to analyze the potential impact of climate change on wind speed and solar radiation in Lesotho. The CORDEX-Africa regional climate model was used to simulate the past, present and future climate conditions under different scenarios. This approach is used widely for long-term climate change scenarios because of the small deviations in the results. It is also recommended by the IPCC to interpret the climate change findings easily. The Jupiter Notebook software was used to extract climate data and to model the historical and projected climate change. The projections are more critical for planning and policy development for meteorological and energy sectors hence this study is conducted in collaboration with the Lesotho Meteorological Services (LMS). Lesotho lies between the following GPS coordinates: Latitude; -29º 30’ 10.7’’ S, Longitude; 28º 12’ 56.5’’ E in the Southern African region as shown in Figure 14.

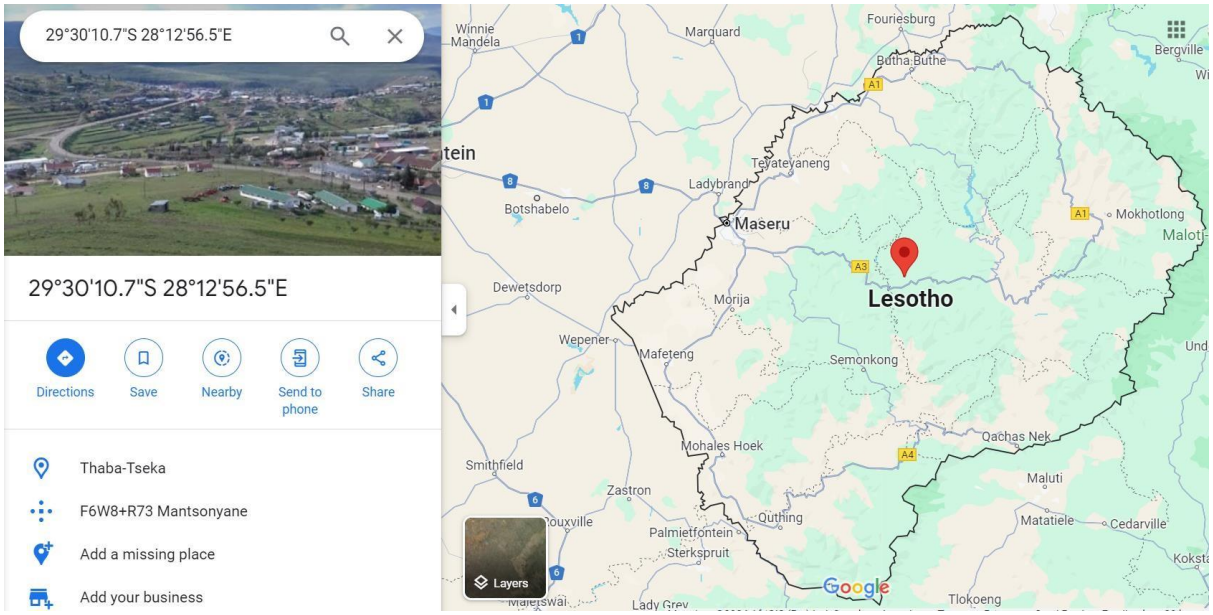

Figure 14: An Aerial Satellite View of Lesotho Surrounded by South Africa. Source[Google Maps]

3.1 Data Extraction Process

3.1.1 The Coordinated Regional Downscaling Experiment (CORDEX) Africa

The downscaled climate change data projections from the Coupled Model Intercomparison Project Phase 5 (CMIP5) global climate model were obtained for the African region from CLMcom, which is the institute responsible for data generation. The CMIP5 climate model produces reliable climate information [107]. The monthly variables of near-the-surface wind speed (wind speed) and surface downwelling shortwave radiation (solar radiation) of CORDEX experiments were scaled down to 50 km resolution over the Africa region (acronym: AFR-44) based on the CCLM4-8-17 regional climate model [108].

The regional climate model is driven by the CNRM-CERFACS-CNRM-CM5, which is the climate model developed by the French National Center for Meteorological Research (CNRM) jointly with the European Center for Research and Advanced Training in Scientific Computation (CERFACS). The CNRM-CM5 represents the fifth version of their climate model and it is used to simulate the Earth's climate system to study the past, the present and the future climate scenarios [109].

The geographic envelope describing the dataset spatial coverage is as follows: Longitude: -24.64, 60.28, Latitude: 42.240002, -45.759998. An example of the full 'metadata' derived from the CORDEX regional climate model is shown in Figure 15. It shows the variable name near-the-surface wind speed (acronym: sfcWind). The experimental raw data (history, RCP4.5 and RCP8.5) were modeled on the CORDEX-Africa website using the CCLM4-8-17 regional climate model and extracted as the NetCDF4 file for variables of solar radiation and wind speed in the African region. The NetCDF4 files were further modeled with the Jupiter Notebook software to display solar radiation and wind speed on the African continent and Lesotho.

id = cordex.output.AFR-44.CLMcom.CNRM-CERFACS-CNRM-CM5.rcp85.r1i1p1.CCLM4-8-17.v1.mon.sfcWind.v20140401|esgf1.dkrz.de
version = 20140401
_timestamp = 2016-11-25T16:24:19.163Z
access = HTTPServer, GridFTP, OPENDAP, Globus
cf_standard_name = wind_speed
data_node = esgf1.dkrz.de
dataset_id_template_ = cordex.%(product)s.%(domain)s.%(institute)s.%(driving_model)s.%(experiment)s.%(ensemble)s.%(rcm_name)s.%(rcm_version)s.%(time_frequency)s.%(variable)s
datetime_start = 2006-01-16T12:00:00Z
datetime_stop = 2100-12-16T12:00:00Z
domain = AFR-44
driving_model = CNRM-CERFACS-CNRM-CM5
east_degrees = 60.28
ensemble = r1i1p1
experiment = rcp85
experiment_familys = All, RCP
geo = ENVELOPE(-24.64, 60.28, 42.240002, -45.759998)
index_node = esgf-data.dkrz.de
instance_id = cordex.output.AFR-44.CLMcom.CNRM-CERFACS-CNRM-CM5.rcp85.r1i1p1.CCLM4-8-17.v1.mon.sfcWind.v20140401
institute = CLMcom
master_id = cordex.output.AFR-44.CLMcom.CNRM-CERFACS-CNRM-CM5.rcp85.r1i1p1.CCLM4-8-17.v1.mon.sfcWind
metadata_format = THREDDS
north_degrees = 42.24
number_of_aggregations = 1
number_of_files = 10
product = output
project = CORDEX
rcm_name = CCLM4-8-17
rcm_version = v1
size = 131210904
south_degrees = -45.76
time_frequency = mon
variable = sfcWind
variable_long_name = Near-Surface Wind Speed
variable_units = m s-1
west_degrees = -24.64

Figure 15: Metadata Derived from CORDEX Regional Climate Model

3.1.2 Jupyter Notebook Software

The Jupyter Notebook is an open-source web application that lets users compose and share documents that contain real code, equations, plots and narrative text. Many of the Jupyter Notebook authors are scientific experts in their fields. As a result, it has become the most preferably used notebook to produce scientific results due to its compatibility with multiple programming languages such as Python, R and Julia [110]. A typically executed Jupyter Notebook written by J.F Pimentel et al. (2021) containing two Markdown cells and two code cells is shown in Figure 16 [111]. It dislays the process of using the Jupyter Notebook from the input to the output.

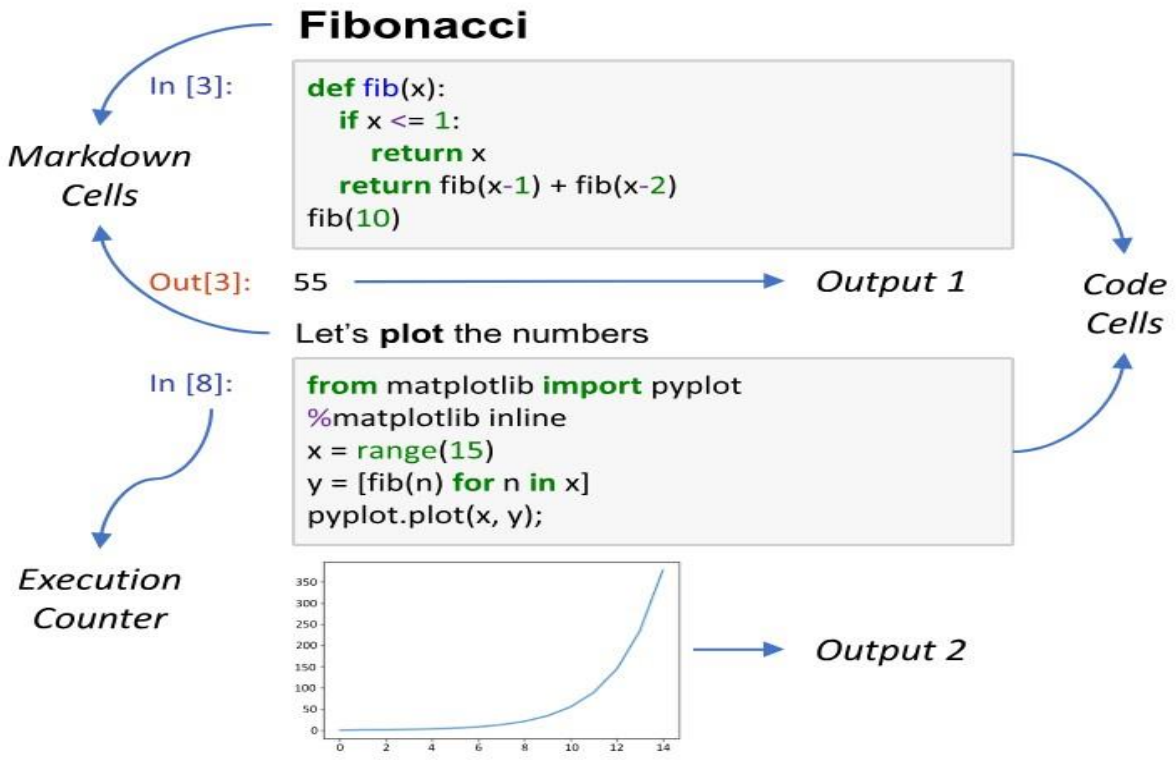

Figure 16: An Executed Jupyter Notebook [111]

The fundamental structure is the notebook, which is divided into cells that can be code cells, runnable units of code in real-time, or Markdown cells that are used to write notes and docstrings explanations [112].

The following commands need to be Pre-installed for data processing;

3.1.2.1 Pip install netCDF4

The command "pip install netCDF4", as shown in Figure 17, is used to install the ‘netCDF4’ Python package from the Python Package Index (PyPI). “pip” is a package manager for Python; It is used to install and to manage additional packages that are not part of the python standard library. After installing the user can command, the netCDF4 package in the Python code to read and write the data in the Network Common Data Form (NetCDF) format — a file format that is widely used for scientific data endeavours.

```
import netCDF4

# Open the NetCDF file
with netCDF4.Dataset('file.nc', mode='r') as ncfile:
    # Print the variable names in the file
    print(ncfile.variables.keys())

    # Read a variable from the file
    variable = ncfile.variables['variable_name']
    data = variable[:]

    # Print the data
    print(data)
```

Figure 17: Example of Importing NetCDF4 Dataset

3.1.2.2 Pip install cartopy

The command ‘pip install cartopy’, as shown in Figure 18, installs the “cartopy” Python package using the “pip” package manager. Cartopy is a Python package designed to make it easier to draw maps and to analyse the geospatial data on them. It offers advanced mapping capabilities with extensive support for several map projections and the data formats. It also implements the most efficient matplotlib algorithms. “Cartopy” has some dependencies that need to be installed first; They include ‘numpy’, ‘scipy’, ‘shapely’, ‘pyshp’, ‘six’, and ‘geos’. These dependencies can be installed using ‘pip’ or other package managers such as ‘apt-get’ (Linux) and brew (macOS).

```
import cartopy.crs as ccrs
import matplotlib.pyplot as plt

# Create a figure and a map projection
fig = plt.figure(figsize=(8, 6))
proj = ccrs.PlateCarree()

# Create a map
ax = fig.add_subplot(111, projection=proj)

# Add coastlines and a grid
ax.coastlines()
ax.gridlines()

# Show the plot
plt.show()
```

Figure 18: Installing Cartopy

3.1.2.3 Pip install netCDF4 matplotlib

The command 'pip install netCDF4 matplotlib,' as shown in Figure 19, is used to install the 'netCDF4' and 'matplotlib' Python packages using the 'pip' package manager. The 'netCDF4' is a Python package for reading and writing data in the Network Common Data Form (NetCDF) format, a popular scientific data format. It provides a high-level interface for working with NetCDF files, including support for reading and writing the data, querying the metadata and manipulating the data arrays. The 'matplotlib' is a popular Python package for creating static, animated and interactive visualizations in Python. It provides a wide range of plotting functionality, including support for 2D and 3D plotting, contour plots, histograms, scatter plots and more.

```python
import netCDF4
import matplotlib.pyplot as plt

# Open the NetCDF file
with netCDF4.Dataset('file.nc', mode='r') as ncfile:
    # Read a variable from the file
    variable = ncfile.variables['variable_name']
    data = variable[:]

# Create a plot
plt.plot(data)

# Add a title and labels
plt.title('My Plot')
plt.xlabel('X-axis')
plt.ylabel('Y-axis')

# Show the plot
plt.show()
```

Figure 19: NetCDF4 Matplotlib

3.1.2.4 Pip install xarray

The ‘xarray’ command epicted in Figure 20 is a library for working with the labeled multidimensional arrays; it provides a convenient and flexible way to manipulate and analyze large and complex datasets.

```python
import xarray as xr
import matplotlib.pyplot as plt

# Open a NetCDF file
ds = xr.open_dataset('file.nc')

# Plot the data
ds['variable_name'].plot()
plt.show()
```

Figure 20: Xarray Command

3.1.2.5 Extracting Wind Speed Data using Jupyter Notebook

An example of a Python script for this study that uses the 'matplotlib', 'xarray', and 'cartopy' libraries to plot the wind speed data from a NetCDF file called 'Hismerged_wind_speed.nc' is shown in Figure 21. This is what the script does: The resulting plot shows the wind speed data for the selected time step overlaid on a map of the world using a PlateCarree projection. The coastlines and country boundaries are also shown, and a colorbar is added to indicate the wind speed values. The label for Lesotho is also added to the plot.

The code imports the necessary libraries, opens a NetCDF file containing wind speed data, extracts the 'sfcWind' variable, selects a single time step, creates a figure and axes with a 'PlateCarree' projection, adds coastlines and country boundaries to the plot, sets the x-axis ticks, plots the 'sfcWind' variable using 'contourf', adds a colorbar with a label, sets the title of the plot, adds a label for Lesotho, and displays the plot using 'plt.show()'. The same steps are taken to plot solar radiation data using CORDEX Africa.

```python
import matplotlib.pyplot as plt
import xarray as xr
import cartopy.crs as ccrs
import cartopy.feature as cfeature

# Open the merged dataset
Hismerged_ds = xr.open_dataset("Hismerged_wind_speed.nc")

# Extract the sfcWind variable
sfcWind = Hismerged_ds.sfcWind

# Select a single time step
sfcWind_time = sfcWind.isel(time=0)

# Create a figure and axes with a PlateCarree projection
plt.figure(figsize=(10,5))
ax = plt.axes(projection=ccrs.PlateCarree())

# Add coastlines to the plot
ax.coastlines()

# Add country boundaries to the plot
ax.add_feature(cfeature.BORDERS.with_scale('10m'))

# Set the x-axis ticks
ax.set_xticks(range(-180,181,60), crs=ccrs.PlateCarree())

# Plot the sfcWind variable
cf = ax.contourf(sfcWind_time.lon, sfcWind_time.lat, sfcWind_time, transform=ccrs.PlateCarree())

# Add a colorbar to the plot
cbar = plt.colorbar(cf, ax=ax, shrink=0.5, aspect=5)
cbar.set_label('Wind Speed')

# Set the title of the plot
plt.title('Wind Speed from 1950 to 2005'.format(sfcWind_time.time.values))

# Add the label for Lesotho
lesotho = cfeature.NaturalEarthFeature('cultural', 'admin_0_countries', '10m',
                                       facecolor='none', edgecolor='black')
ax.add_feature(lesotho)
ax.text(29.5, -29.5, 'Lesotho', transform=ccrs.PlateCarree(), color='red',fontsize=10)

# Show the plot
plt.show()
```

Figure 21: Typical Example of Extracting CORDEX Africa Data using Jupyter Notebook

3.2 Methodology Reliability

The CORDEX Africa software model has been used widely according to Alesandro Dosio et al. (2021). Regional Climate Models have been utilized to dynamically downscale the results from an ensemble of CMIP5 Global Climate Models (GCMs), producing high-resolution (0.44°, approximately 50 km) historical and future climate projections for Africa [113]. A

study conducted in West Africa showed that using the ensemble mean to project rainfall in the region reduce the uncertainty in the climate model forecasting [114], the spatial distribution of the correlation coefficient between the observational data and the RCMs indicates that all models, except HIRHAM, exhibit positive values across the most parts of the African continent [115].

Several studies on wind and solar energy resources have been conducted in Lesotho, according to Yengane et al. Lesotho has solar radiation of 5.5-7.2 kWh/m^2 on average [116]. At the same time, the wind speed observed in the country ranks amongst the top 15 best countries with the highest potential for wind power generation in Africa [20]. The solar radiation and wind speed observed in the country have a good potential for solar PV power plants and wind plants respectively. The solar radiation and wind speed observed using the CORDEX Africa data are slightly different from the data observed. The observed solar radiation in Lesotho for the period 1950-2005 was 200-225 W/m^2 except in the north-east part of the country where Butha-Buthe and Mokhotlong districts are located, while from the literature annual solar radiation range between 5.5-7.2 kWh/m^2 on average.

Furthermore, the average wind speed observed using the CORDEX Africa data ranged from 1.5-3.0 m/s while LMS has a reported monthly mean speed that ranges from 1.4 m/s - 8 m/s which are generally westerly varying between south-westerly and north-westerly of the country. The discrepancy in the observed average wind speed and solar radiation might have been brought about by model error and uncertainty associated with the model as discussed.

4 Results and Discussion

In this study, the Jupyter Notebook software was utilized to study the potential impact of climate change on wind speed and solar radiation resources in Lesotho using a CORDEXAfrica regional climate model to simulate th past, present and future climate conditions under different scenarios. The study was conducted under the RCP4.5 and RCP8.5 climate scenarios. The findings were compared to the baseline study.

4.1 Baseline Period

The selection of a baseline period is crucial as it affects the evaluation of changes in climate variables. Various baseline periods may be employed for different objectives such as analyzing historical climate changes, making future projections and comparing different datasets. The historical climate changes were selected as the preferred baseline period to compare the historical climate conditions to the current and projected conditions. The historical average wind speed and average solar radiation from 1950 - 2005 were selected and studied across the African region, with Lesotho as the main study focus.

4.1.1 Wind Speed

The historical average wind speed in the African region at 10 m a.g.l shows a great deal of both terrestrial and marine variation amongst the countries, from 1950 - 2005, as shown in Figure 22. The average wind speed (AWS) ranges between 7.5 - 12.0 m/s in the South region of the continent on the South Atlantic and the South Indian Oceans, the AWS is the highest on this location but 7.5 - 9.0 m/s was the occurring AWS near terrestrial. The South Atlantic Ocean has a varying AWS that ranges from between 4.5 - 7.5 m/s but near terrestrial 7.5 - 9.0 m/s is the occurring AWS. However, the predominant AWS on the Indian Ocean ranges between 4.5 - 7.5 m/s and the near terrestrial, 6.0 - 7.5 m/s was the occurring AWS .

On the North Atlantic Ocean, the average terrestrial wind was found to be in the range of 6.0 - 7.5 m/s on the coastline of West Africa from Mauritania to Liberia and 7.5 - 9.0 m/s from Western Sahara to Morocco. The average wind speed on the western-central African coastline was at 3.0 - 4.5 m/s while on the eastern-central African coastline ranged between

6.0 - 10.5 m/s. The predominant AWS was 6.0 - 7.5 m/s from the coastline of Mozambique to South Somalia, while 7.5 - 10.5 m/s AWS dominated the rest of the coastline of Somalia. On the Northern Africa coastline, along the Mediterranean sea, the AWS varies between 4.5 - 7.5 m/s with 4.5 - 6.0 m/s being the predominately AWS. This also extends to along the Red Sea coastline where 4.5 - 6.0 m/s AWS was also observed.

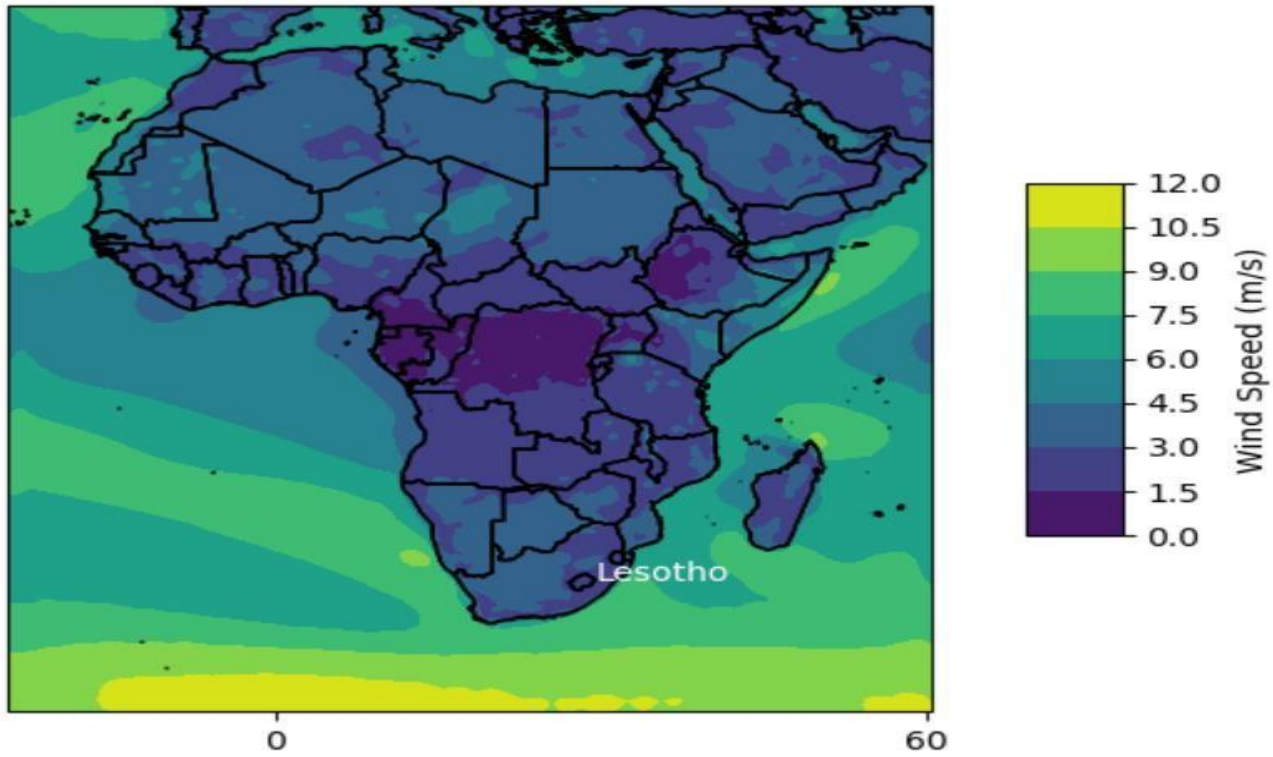

Figure 22: Observed Average Wind Speed in Africa from 1950-2005 at 10 m a.g.l

On land in the north, the predominant AWS from west to east Africa was observed to be 1.5 - 6.0 m/s with Chad recording a relatively high AWS of about 4.5 - 6.0 m/s. The AWS in Central Africa ranged between 0.0 - 3.0 m/s with the countries such as Gabon and Cameroon having AWS of fewer than 1.5 m/s, the region has the lowest AWS on the continent. The Southern African Development Community (SADC) has an AWS that ranges between 0.0 - 4.5 m/s. Only the Democratic Republic of Congo (DRC) has the least AWS of less than 1.5 m/s predominantly in the northern region. The rest of the region had an AWS of 1.5 - 3.0 m/s but the countries such as South Africa, Botswana, and Namibia showed strong AWS of 1.5 - 4.5 m/s.

The average wind speed observed in Lesotho from 1950 - 2005 at 10 m a.g.l is shown in Figure 23. During this period, the country had an evenly distributed AWS of 1.5 - 3.0 m/s across the

districts. The country is landlocked witthin South Africa and the same AWS can be observed along the borders. , the observed AWS implies that Lesotho can be able to generate wind energy from the wind resource since most of the cut-in-speed of wind turbines is around 2.5 m/s.

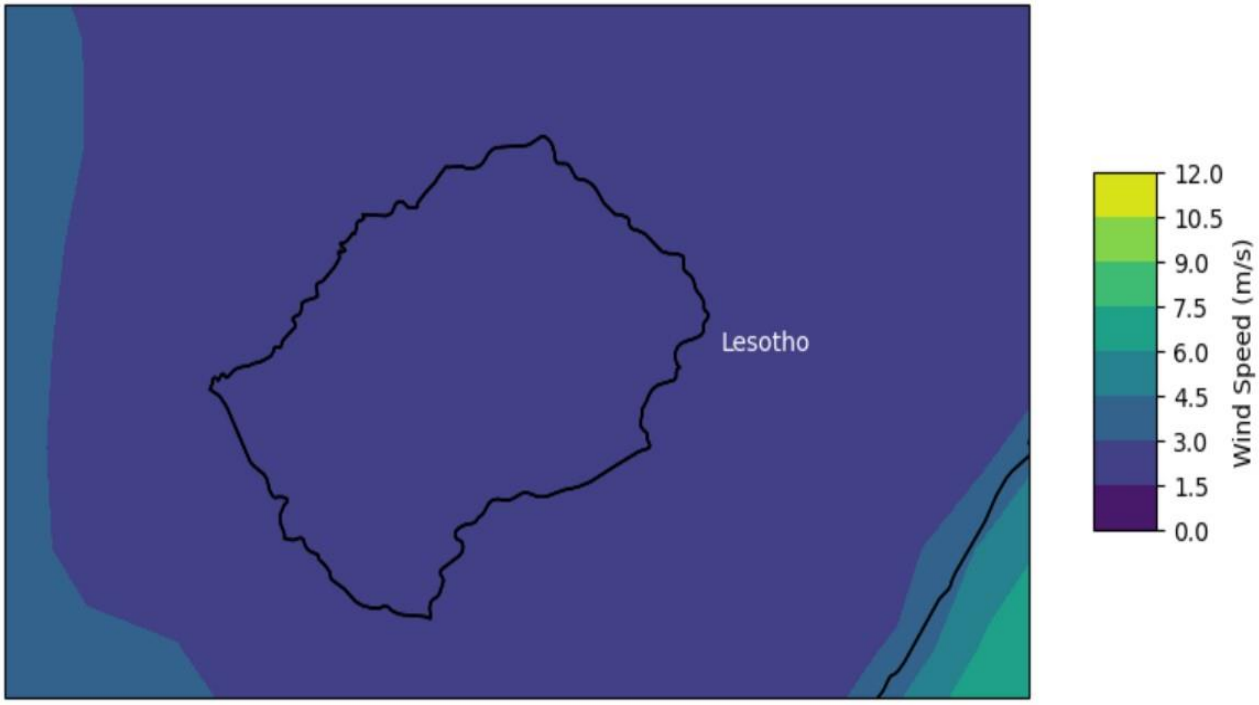

Figure 23: Observed Average Wind Speed in Lesotho from 1950-2005 at 10 m a.g.l

4.1.1.1 Observed Wind Speed Trend in Lesotho

The historical observed wind speed trend against time in Lesotho from 1950 to 2005 is shown in Figure 24. The trend indicates an average wind speed of about 2.60 m/s, reaching more than 3.00 m/s in some years. The AWS remained constant during this period with a minimum value of about 1.50 m/s and a maximum AWS of more than 3.00 m/s. Only in 1956, 1975, 1957, 2003 and 2005 did the average wind speed exceed 3.00 m/s.

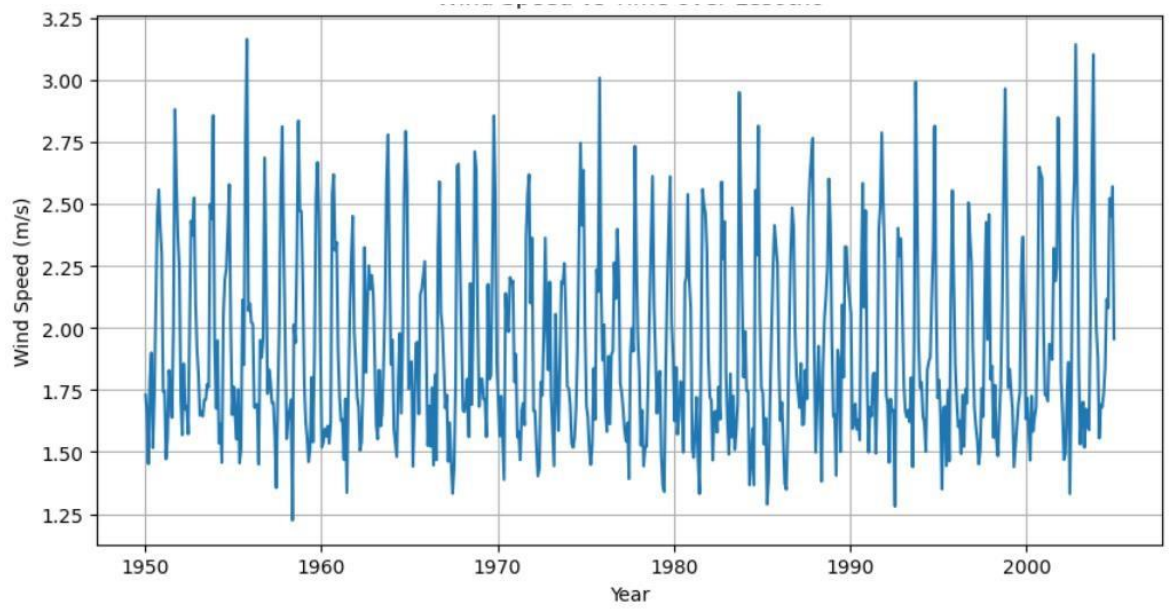

Figure 24: Historical Wind Speed in Lesotho

4.1.2 Solar Radiation

The African continent had the best average solar radiation (ASR) especially in the northern and southern parts of the region indicting a significant potential to generate solar energy, as shown in Figure 25, where the observed solar radiation from 1950 - 2005 at 10 m a.g.l is shown. The ASR in the western countries ranged from 150 - 275 W/m^2 with Mauritania and the western Sahara having the best ASR of 225 - 275 W/m^2 Meanwhile, Nigeria, Benin,

Ghana, Cote D'Ivoire and Togo had the lowest ASR of 150 - 200 W/m^2 in the western region. In the central African region, the ASR was ranked the lowest on the continent. It was observed to range between 125 and 250 W/m^2 with Chad having the highest ASR of 175 - 250 W/m^2 while DRC had the lowest ASR in the region of 125 - 175 W/m^2. The eastern African region had an ASR ranging from 125 - 275 W/m^2, with Sudan having the highest ASR up to 275 W/m^2 in southern Sudan while Uganda had the lowest ASR in the region as low as 100 - 125 W/m^2.

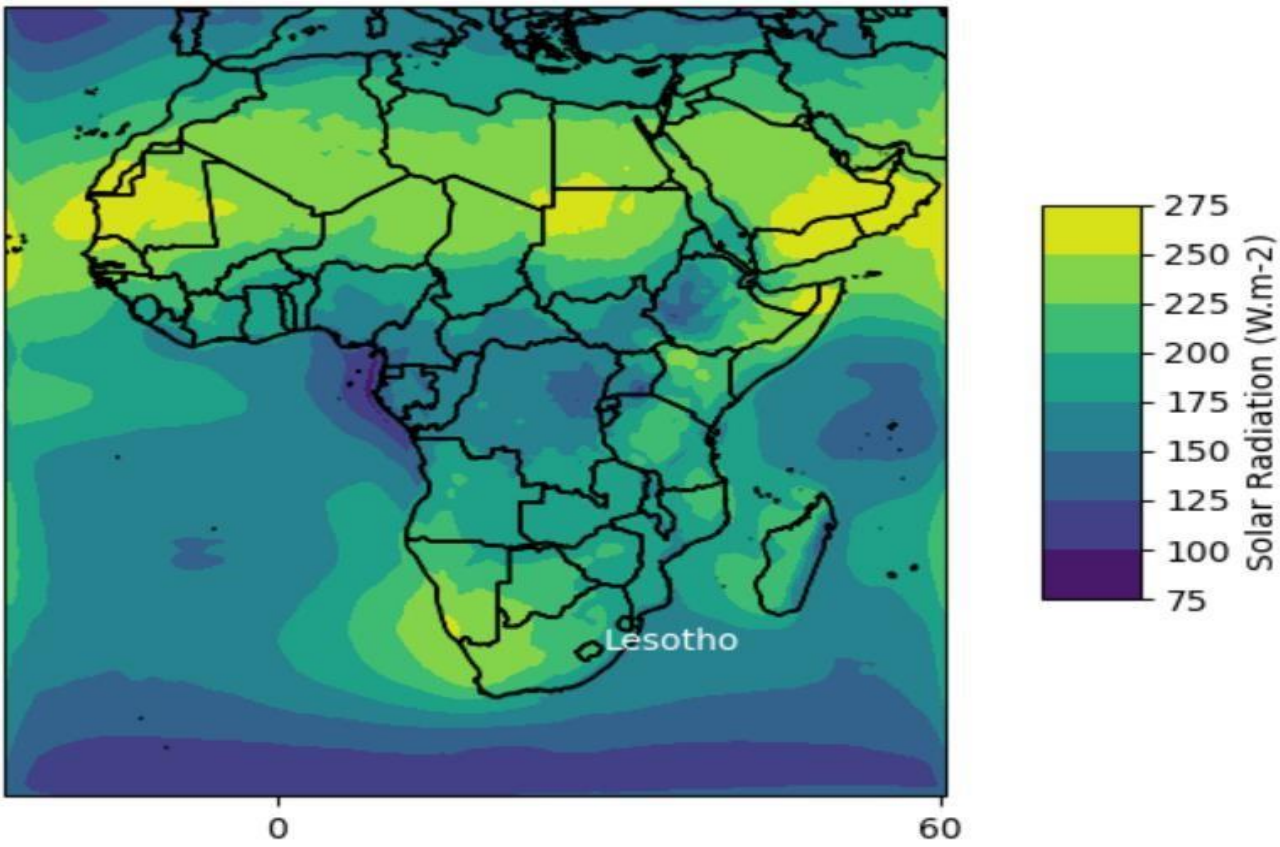

Figure 25: Observed Average Solar Radiation in Africa from 1950-2005 at 10 m a.g.l

The Northern African countries had one of the highest average solar radiation levels on the continent. The ASR ranged between 150 and 275 W/m^2, with the western Sahara having the highest ASR of between 225 - 275 W/m^2 while South Sudan had the lowest ASR of 150-200 W/m^2. The Southern African region had an ASR ranging from 175 - 250 W/m^2 which was the second highest on the continent. Namibia and South Africa had an ASR in the region of about 225 - 250 W/m^2 while Zambia had a relatively lower ASR in the region of 175 - 200 W/m^2.

The average solar radiation observed in Lesotho from 1950 - 2005 at 10 m a.g.l is shown in Figure 26, during this period, the country had an evenly distributed ASR of 200 - 225 W/m^2 except in the north-east part of the country where Butha-Buthe and Mokhotlong districts are located. A lower ASR of 175 - 200 W/m^2 was observed in these parts of Lesotho and the same ASR was observed along the Quthing district border with South Africa. The observed ASR implies that the country can have solar energy resources to generate renewable energy.
The rest of the borderline with South Africa had an observed ASR of 200 - 225 W/m^2.

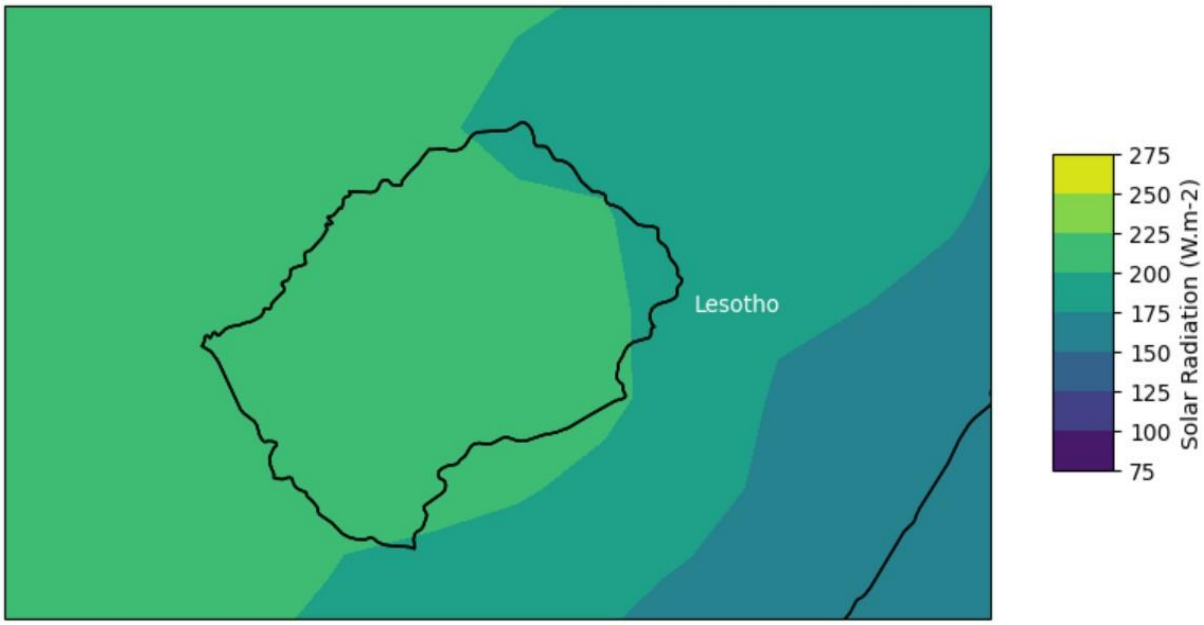

Figure 26: Observed Solar Radiation in Lesotho

4.1.2.1 Observed Solar Radiation Trend in Lesotho

The historical observed solar radiation trend against time in Lesotho from 1950 to 2005 is shown in Figure 27. The country indicated an average solar radiation of about 275 W/m^2 extending to more than 300 W/m^2 in some years. This remained constant for the 1950 to 2005 period. Since the beginning of the record in 1950, the results showed a minimum ASR of about 140 W/m^2 and a maximum ASR exceeding 300 W/m.^{2} From 2001 to 2005, the observed data maintained an ASR of more than 300 W/m^2 signifying an increase in ASR.

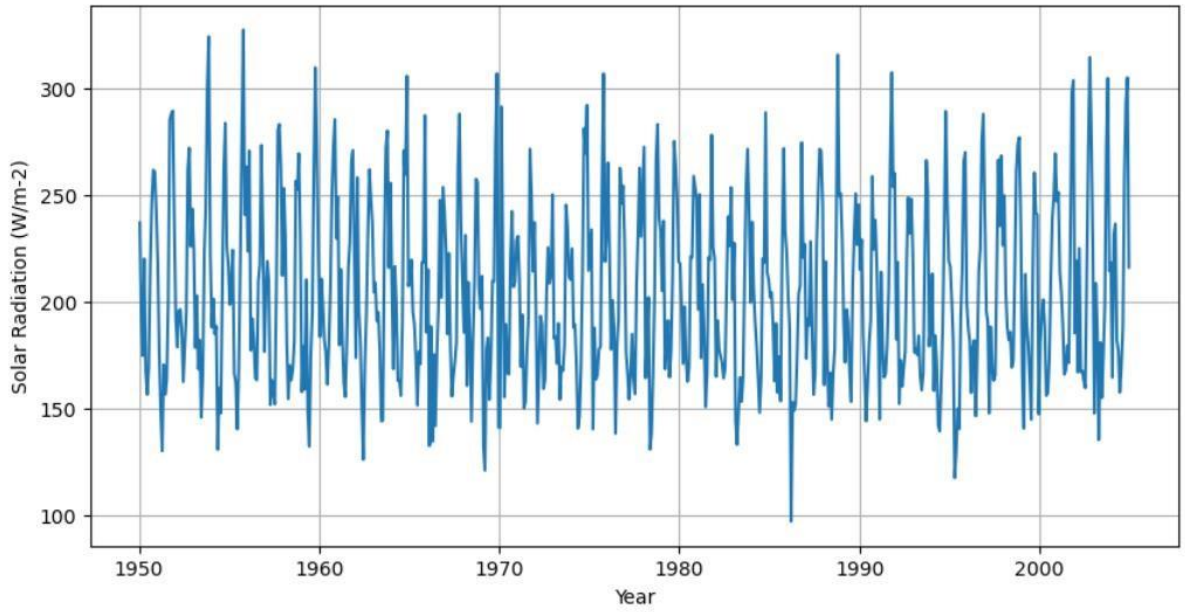

Figure 27: Historical Solar Radiation in Lesotho

4.2 Projected Period

4.2.1 Representative Concentration Pathway 4.5

Wind Speed

The projected average wind speed (AWS) from 2024-2045 under RCP4.5 against the observed average wind speed from 1950 to 2005 on the African continent at 10 m above ground level (a.g.l) is shown in Figure 28. On close observation, the AWS data shows a difference from the baseline analysis. At 10 m a.g.l, the AWS in the western African coastline is projected to be in the range of 3.0 - 7.5 m/s. The Mauritania coastline is projected to have the best AWS of 6.0 - 7.5 m/s while the Sierre Leone and Liberia coastline has the least AWS of 3.0 - 4.5 m/s. In central Africa, the AWS was projected to be in the range of 0.0 - 6.0 m/s which is the lowest among the regions on the continent. Chad was projected to have the best AWS of 3.0 - 6.0 m/s in the area while DRC was dominated by the least AWS of 0.0 - 1.5 m/s.

Eastern Africa had an AWS ranging from 0.0 - 6.0 m/s with Somalia having the best AWS in the region of 4.5 - 6.0 m/s while Ethiopia had the least AWS of 0.0 - 3.0 m/s, along the coastline. The Eastern African region had a relatively higher AWS of 6.0 - 10.5 m/s than other regions.

In North Africa, the AWS was determined to be in the range of 1.5 - 6.0 m/s. Western Sahara had the best AWS of 4.5 - 6.0 m/s on land while on the coastline an AWS of 9.0 - 10.5 m/s was observed. South Sudan had the least AWS of 1.5 - 3.0 m/s in the region. The AWS along the Mediterranean Sea coastline ranged from 4.5 to 7.5 m/s extending to the Red Sea. The AWS in Southern Africa was determined to be in the range of 1.5 - 4.5 m/s which was one of the lowest on the continent. South Africa, Botswana and Namibia had the best AWS of 3.0 - 4.5 m/s while Angola and Zambia had the worst AWS of 1.5 - 3.0 m/s in the region.

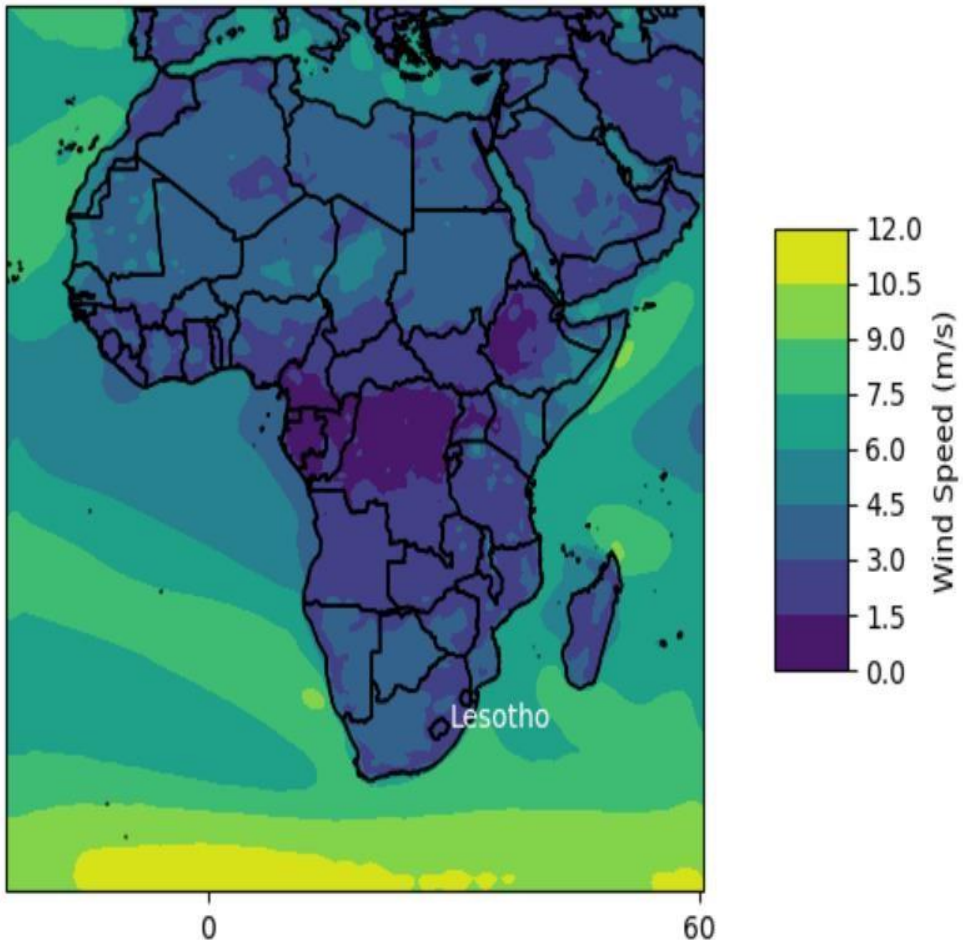

(a) Observed Wind Speed (1950 - 2005)

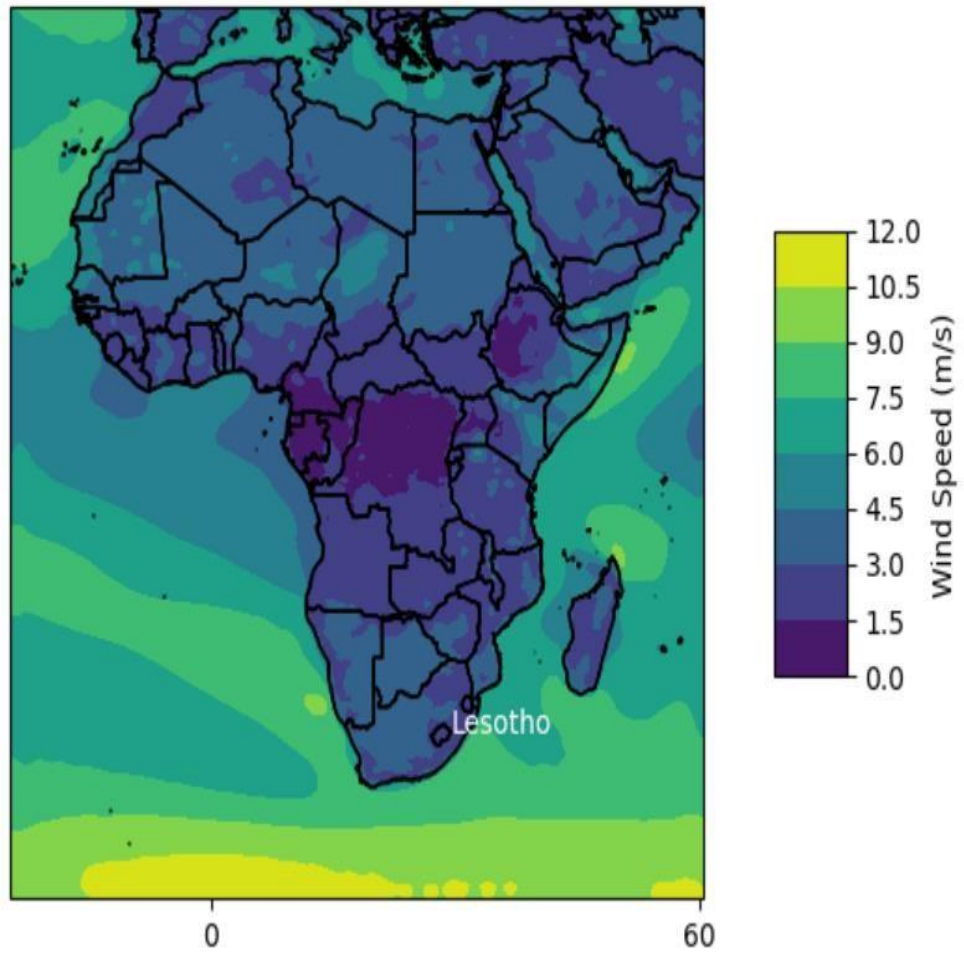

(b) Projected Average Wind Speed (2024 - 2045)

Figure 28: Average Wind Speed in Africa at 10 m a.g.l

The noticeable wind speed changes in the African continent under the RCP4.5 scenario are summarized in Table 1.

Table 1: Notable Wind Speed Changes in Africa under RCP4.5

Country/Region	**Baseline Wind Speed (m/s)**	**Projected Wind Speed (m/s)**
Central Africa	**0.0 - 3.0**	**0.0 - 6.0**
Chad	1.5 - 6.0	3.0 - 6.0
DRC	0.0 - 3.0	0.0 - 1.5
North Africa	**1.5 - 4.5**	**1.5 - 6.0**
Western Sahara	4.5 - 6.0	4.5 - 6.0
South Sudan	1.5 - 3.0	1.5 - 3.0
Southern Africa	**1.5 - 4.5**	**1.5 - 4.5**
Namibia, Botswana and South Africa	1.5 - 4.5	3.0 - 4.5
Angola, and Zambia	1.5 - 3.0	1.5 - 3.0
West Africa	**1.5 - 6.0**	**3.0 - 7.5**
Mauritania	3.0 - 6.0	6.0 - 7.5
Sierra Leone, Liberia	1.5 - 3.0	3.0 - 4.5
East Africa	**0.0 - 6.0**	**0.0 - 6.0**
Somalia	3.0 - 6.0	4.5 - 6.0
Ethiopia	0.0 - 3.0	0.0 - 3.0

The projected average wind speed in Lesotho from 2024 to 2045 under the RCP4.5 against the observed average wind speed from 1950 - 2045 at 10 m a.g.l is shown in Figure 29, demonstrating an evenly distributed AWS of 1.5 - 3.0 m/s throughout the country. The projected AWS was also the same along the country's borders with South Africa indicating a slight potential to generate wind energy in the country and along the borders. The projected AWS was similar to that observed in the baseline period under this scenario while other countries in the African region experienced a change.

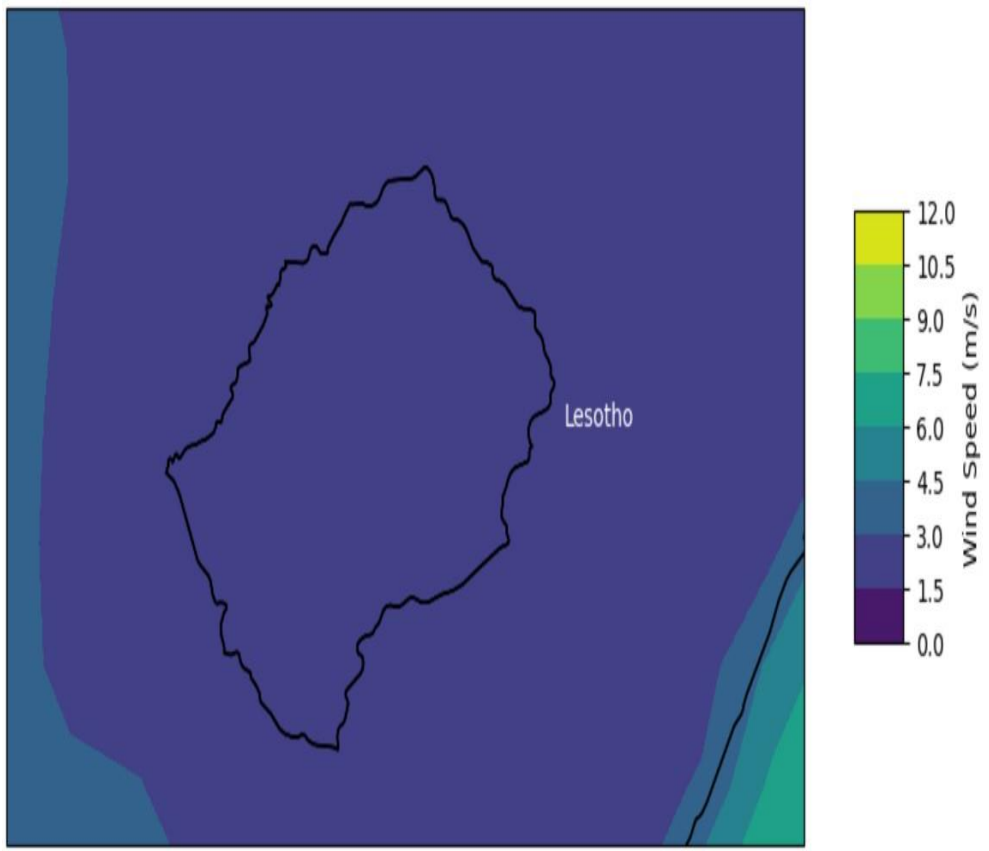

(a) Observed Wind Speed (1950 - 2005)

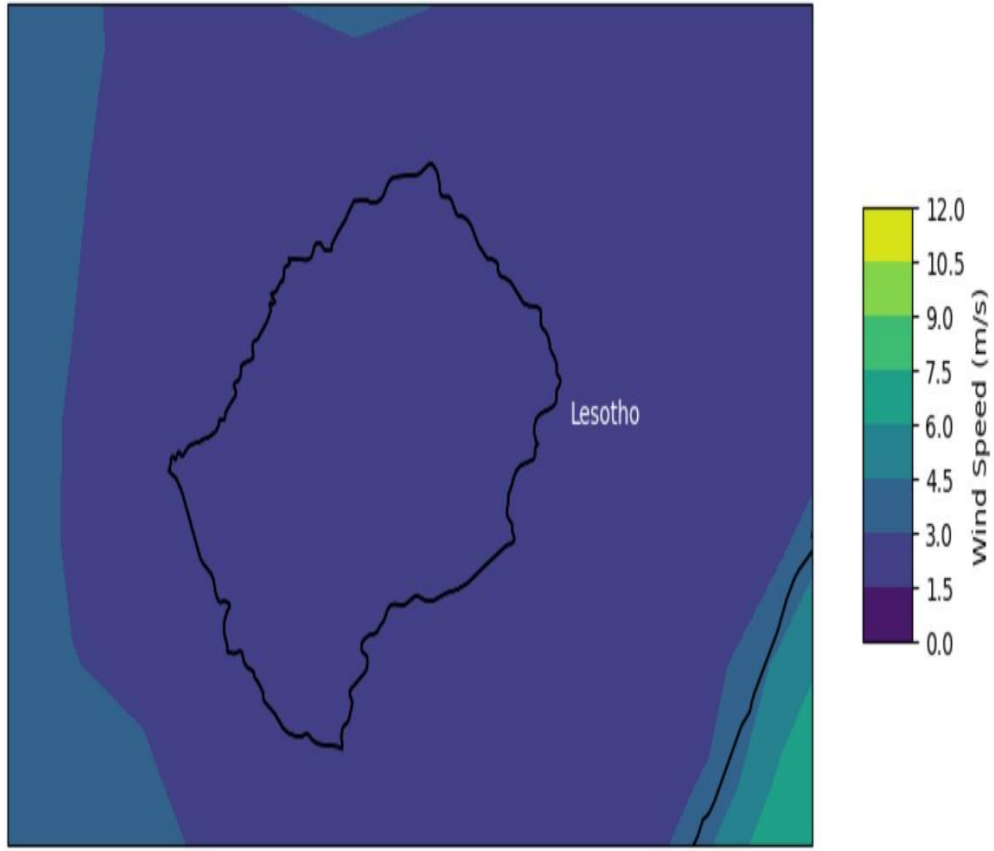

(b) Projected Wind Speed (2024 - 2045)

Figure 29: Average Wind Speed in Lesotho from at 10 m a.g.l

Projected Wind Speed Trend in Lesotho

The projected average wind speed trend simulated against time from 2024 to 2045 under RCP4.5 is shown in Figure 30. Overall, from 2024 to 2045 the average wind speed projected under the RCP4.5 scenario is 2.15 m/s at 10 m a.g.l. The results showed a minimum average wind speed of 1.50 m/s and a maximum average wind speed of 2.75 m/s, while LMS has reported monthly mean speed that ranges from 1.4 m/s - 8 m/s which are generally westerly varying between south-westerly and north-westerly [117]. The projected AWS trend increased from 2024 to 2031, the simulation show a steady AWS of 2.75 m/s or more with the maximum record of AWS of 3.00 m/s in 2030. The projected AWS trend from 2031 to 2045 shows a drop of an AWS slightly on or below 2.75 m/s with 2038 being an exception with a record of projected AWS of more than 3.00 m/s. The lowest projected average wind speed recorded was in 2031 with a minimum AWS of 1.55 m/s and a maximum AWS of approximately 2.50 m/s.

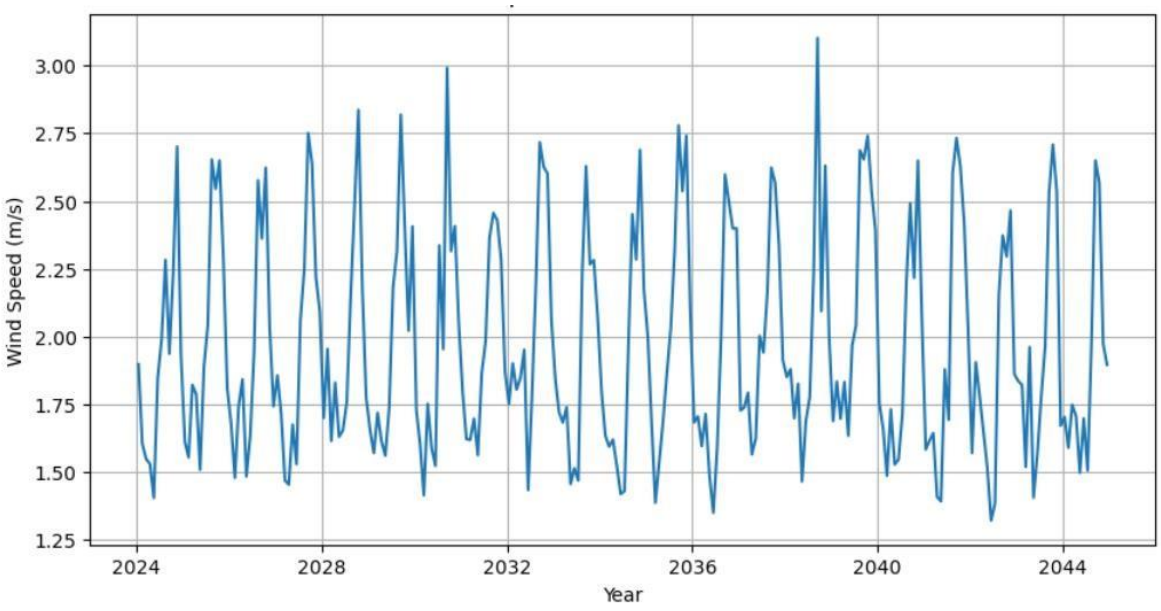

Figure 30: Projected Maximum Wind Speed Trend in Lesotho at 10 m a.g.l under RCP4.5 Scenario

The annual variations in wind speed and direction can be influenced by atmospheric pressure difference; wind is generated by atmospheric pressure as it moves from an area of high pressure to an area of low pressure. These pressures can vary over time during the year due to the variation of meteorological conditions [118]. Topography and terrain (physical landscape

such as mountains, valleys and urban areas) can also influence wind speed by blockage on mountains or funnelling through the valleys.

Solar Radiation

The projected average solar radiation (ASR) from 2024 - 2045 under RCP4.5 against the observed average solar radiation from 1950 - 2005 on the African continent including the coastlines is shown in Figure 31, the projected ASR shows a variation from the baseline data observed from 1950 to 2005. The projected ASR is expected to significantly decrease across the continent under the RCP4.5 scenario indicating an impact on solar energy resources in the region. In West Africa, the projected ASR was expected to be in the range 175 - 275 W/m^2 which is the highest on the continent, Mauritania had the best terrestrial and along the coastline ASR of 250 - 275 W/m^2. The projected ASR arial coverage was similar to the ASR observed from 1950 - 2005. Sierra Leone, Cote D'Ivore, Ghana, and Nigeria had the lowest ASR of 150-200 W/m^2 while Nigeria had the lowest ASR of 125 - 150 W/m^2 in the region along its coastline.

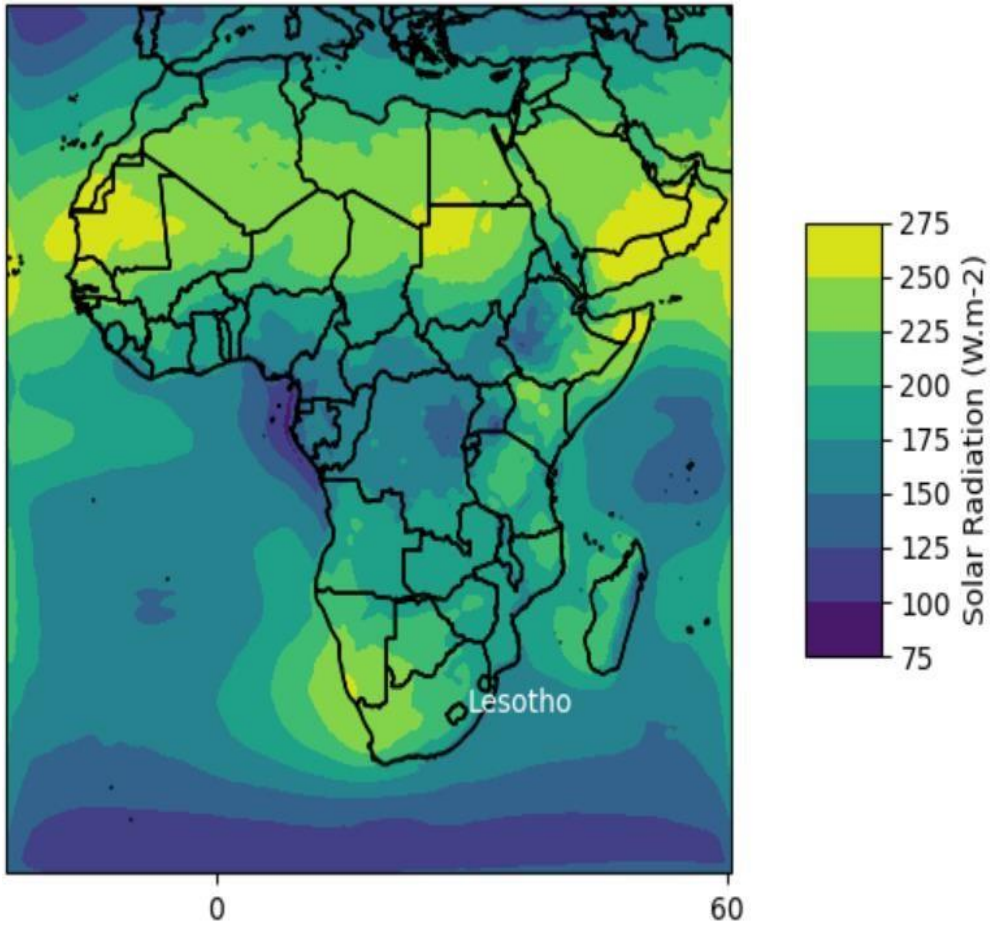

(a) Observed Solar Radiation (1950 - 2005)

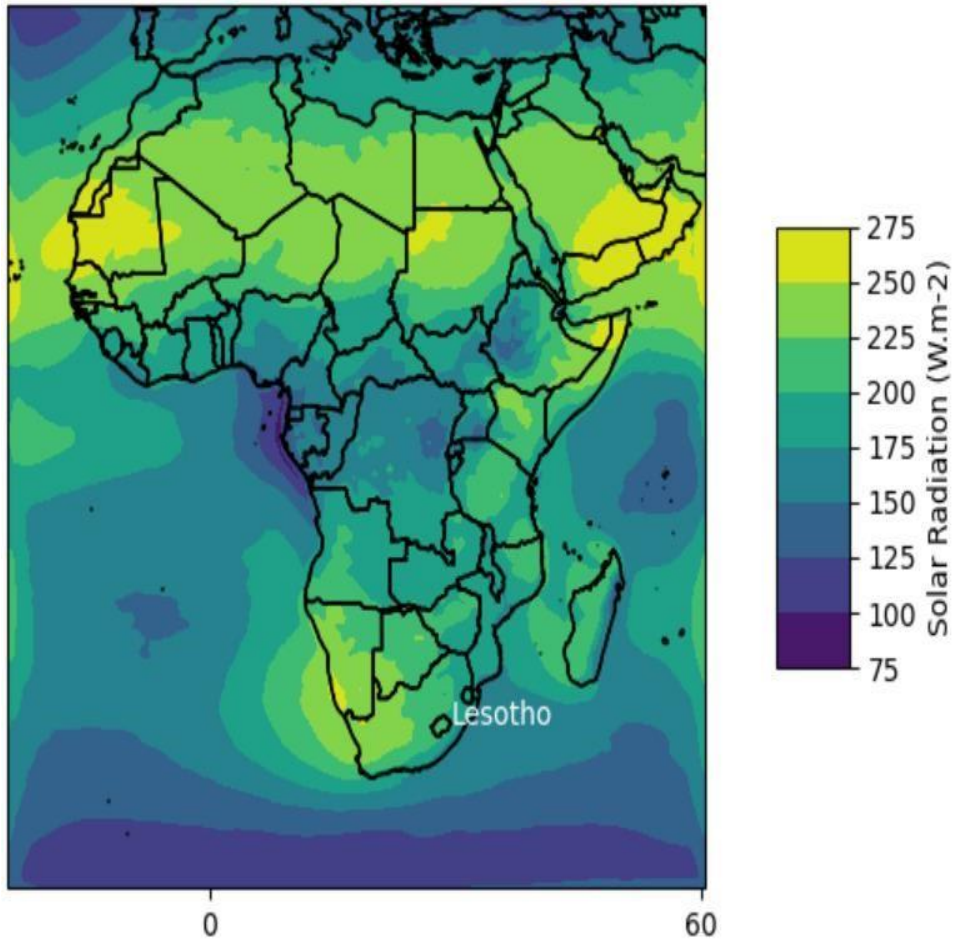

(b) Projected Solar Radiation (2024 - 2045)

Figure 31:Average Solar Radiation in Africa for at 10 m a.g.l

Central Africa had a projected average solar radiation ranging from 150 - 250 W/m^2 which is the lowest on the continent. The observed aerial coverage of the ASR shown in Figure 31 in the region increased from that of the baseline period signifying an increased potential to generate solar energy in the region. Angola showed the best projected ASR of 175 - 225 W/m^2 while DRC was dominated by a relatively lower ASR of 150 - 175 W/m^2 which is the lowest in the terrestrial region. The coastlines of Cameroon, Equatorial Guinea, Gabon and Congo had a projected ASR of 75 - 125 W/m^2 indicating low solar energy along the coastline. In East Africa, the projected ASR ranged from 125 - 275 W/m^2 with Sudan and Somalia having the best ASR of 200 - 275 W/m^2 in the region, the observed variation from the baseline data was the decrease in ASR observed in Sudan while it remained constant in Somalia. Ethiopia and Rwanda had the lowest ASR of 125 - 200 W/m^2 in the region.

The North African countries had the best evenly distributed average solar radiation on the continent under this scenario. The ASR in this region ranged from 175 - 275 W/m^2 which was an increase from 150 - 275 W/m^2 observed from the baseline period. The western Sahara had the best ASR of 225 - 275 W/m^2 on the land. and along the coastline which was similar to the observed ASR from the baseline. South Sudan remained the country with the lowest ASR of 175 - 200 W/m^2 which was an increase from the ASR observed from the baseline data. The observed ASR in Southern Africa was determined to be in the range of 175-275 W/m^2 which is an increase from the observed data from 1950 - 2005. Namibia and South Africa had the best ASR of 200 - 275 W/m^2 in the region. The Namibian coastline had a higher ASR of 250 - 275 W/m^2, and the aerial coverage of this observed variation increased from the baseline observed data signifying an impact brought by the climate change. Zambia remained the country with the lowest ASR of 175 - 200 W/m^2 in the region.

The summarized noticable solar radiation changes on the African continent under RCP4.5 scenario are outlined in Table 2.

Table 2: Notable Solar Radiation Changes in Africa under RCP4.5

Country/Region	**Baseline Solar Radiation (W/m^2)**	**Projected Solar Radiation (W/m^2)**
Central Africa	**125 - 250**	**150 - 250**
Angola	150 - 200	175 - 225

DRC	125 - 175	150 - 175
North Africa	**150 - 275**	**175 - 275**
Western Sahara	225 - 275	225 - 275
South Sudan	150 - 200	175 - 200
Southern Africa	**175 - 275**	**175 - 275**
Namibia and South Africa	200 - 275	200 - 275
Zambia	175 - 200	175 - 225
West Africa	**175 - 275**	**175 - 275**
Mauritania	250 - 275	250 - 275
Sierra Leone, Liberia	150 - 200	150 - 200
East Africa	**125 - 275**	**125 - 275**
Somalia	200 - 275	200 - 275
Ethiopia and Rwanda	125 - 200	125 - 200

The projected average solar radiation in Lesotho from 2024 - 2045 under the RCP4.5 scenario against the observed solar radiation from 1950 - 2045 is shown in Figure 32, during this period, the country projected a dominant display of ASR of 200 - 225 W/m^2 throughout the country and the borders, except in the north-east where Butha-Buthe and Mokhotlong districts are located. The ASR of 175 - 200 W/m^2 was projected in these parts of the country, the aerial coverage was less than that observed in the baseline period indicating an increase in ASR coverage of 200 - 225 W/m^2 in the country, the borderline between Quthing and South Africa also had an increase in aerial coverage. The ASR of 200 - 225 W/m^2 was projected for the rest of the country's borderline with South Africa.

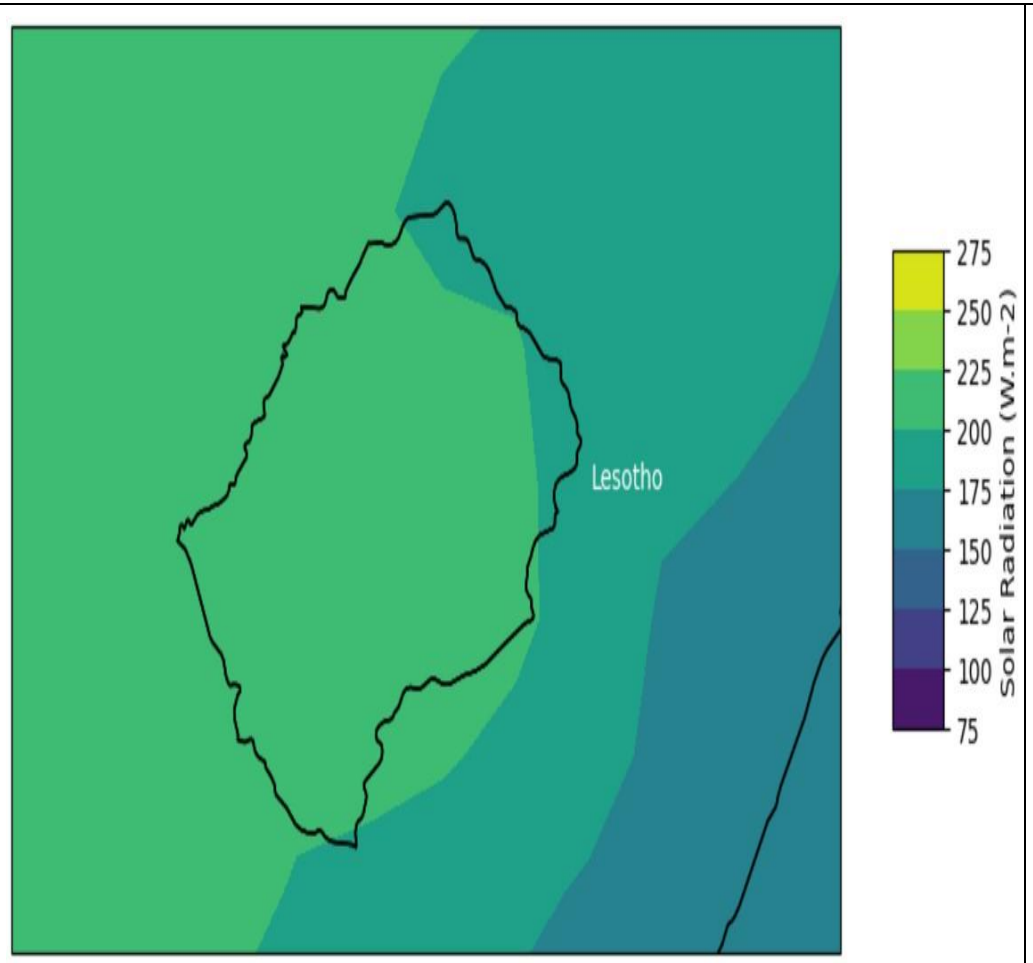

(a) Observed Solar Radiation (1950 - 2005)

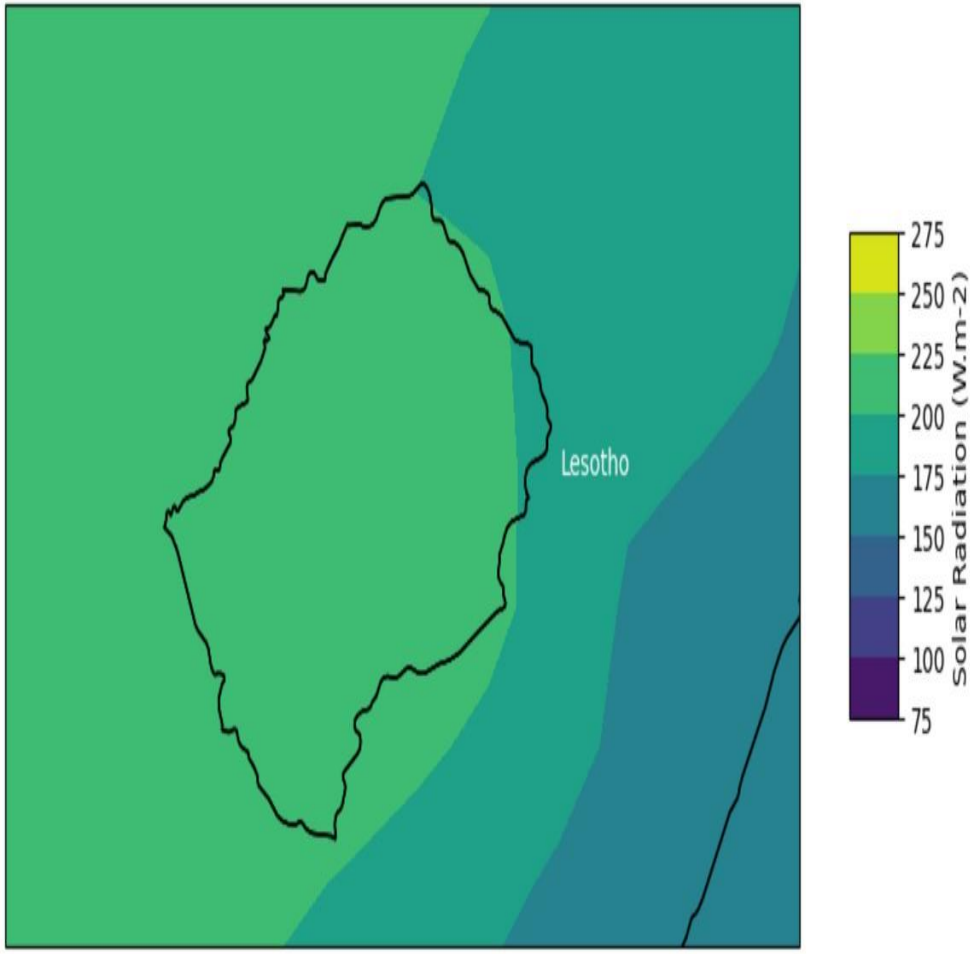

(b) Projected Solar Radiation (2024 - 2045)

Figure 32:Average Solar Radiation in Lesotho from at 10 a.g.l

Projected Solar Radiation Trend in Lesotho

The projected average solar radiation trend simulated against time from 2024 to 2045 under the RCP4.5 is shown in Figure 33. In general, the projected average solar radiation under the RCP4.5 scenario increased from 2024 to 2045 from 140 - 300 W/m^2 range in 1950 to 2005 to 150 - 280 W/m^2. The results showed a minimum average solar radiation of 150 W/m^2 and a maximum average solar radiation of 275 W/m^2 while the literatures states an average solar radiation in the range of 5.5 - 7.2 kWh/m^2. The projected ASR trend remained constant at more than 275 W/m^2 from 2024 to 2029. The projected trend then decreased to ASR below 275 W/m^2 from 2030 to 2034 with the year 2030 having an exception of ASR of about 280 W/m^2. The projected ASR increased significantly from 2035, reaching the values above 300 W/m^2 with 2035, 2039, 2042, and 2043 having ASR of about 340 W/m^2, the projected lowest ASR is in 2034 at 255 W/m^2 and a maximum of 255 W/m^2.

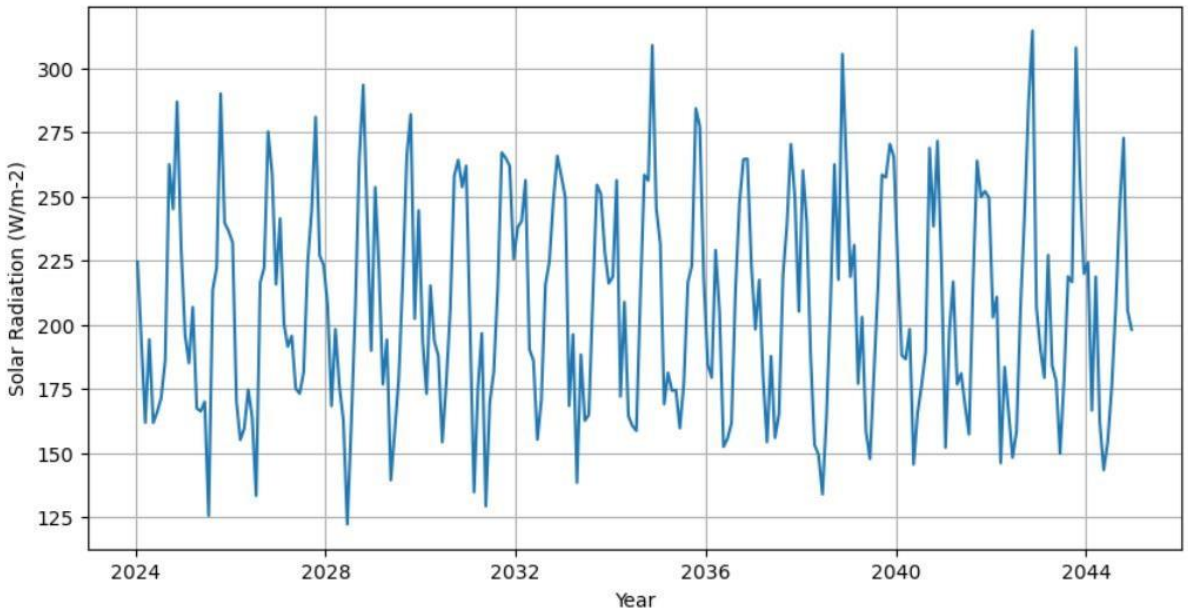

Figure 33: Projected Maximum Solar Radiation Trend in Lesotho at 10 m a.g.l under RCP4.5 Scenario

The impact of climate change on the projected maximum solar radiation under RCP4.5 has the potential to increase or to decrease, depending on the cloud dynamics in certain regions, this scenario assumes moderate atmospheric concentrations hence moderate impact is expected on the energy industry in Lesotho. Over time, the policies aimed at reducing the

presence of aerosols and improving air quality over Lesotho clouds led to increased solar radiation reaching the surface at 10 m above ground level.

4.2.2 Representative Concentration Pathway 8.5 (RCP8.5)

Wind Speed

Shown in Figure 34 is the average wind speed on the African continent between 2024 and 2045 under scenario RCP8.5 against the observed average wind speed from 1950 - 2005 at 10 m a.g.l. The projected AWS data indicates a deviation from the baseline analysis. The AWS along the West African coastline is expected to be between 1.5 and 7.5 m/s. The Mauritania coastline is predicted to have the best AWS is 6.0 to 7.5 m/s while the lowest AWS is 3.0 - 4.5 m/s between the coastlines of Liberia and Sierre Leone. Nigeria, Liberia, and Sierra Leone recorded the worst AWS of 1.5 – 3.0 m/s on land. In central Africa, the AWS was projected to be in the range of 0.0-6.0 m/s which is the lowest among the regions on the continent. Chad was projected to have the best AWS of 1.5 - 6.0 m/s in the area while DRC is dominated by the least AWS of 0.0 - 1.5 m/s.

The AWS in East Africa was in the range of 0.0 - 6.0 m/s, with Somalia having the best AWS in the region at 4.5 to 6.0 m/s and Ethiopia having the lowest AWS at 0.0 to 3.0 m/s. Along the coastline, the regional AWS was between 6.0 and 9.0 m/s, which was higher than the terrestrial average. The AWS in North Africa was found to be between 1.5 and 6.0 m/s on land. Western Sahara had the best AWS of 4.5 to 6.0 m/s, while on the coast, an AWS was recorded to be between 7.5 and 9.0 m/s. South Sudan had the lowest AWS in the region, measuring between 1.5 and 3.0 m/s. From the Mediterranean Sea to the Red Sea, the AWS was between 4.5 and 7.5 m/s. The AWS in Southern Africa was determined to be in the range of 1.5 - 4.5 m/s which was one of the lowest on the continent. South Africa, Botswana, and Namibia had the best AWS of 3.0 - 4.5 m/s while Angola and Zambia had the worst AWS of
1.5 - 3.0 m/s in the region.

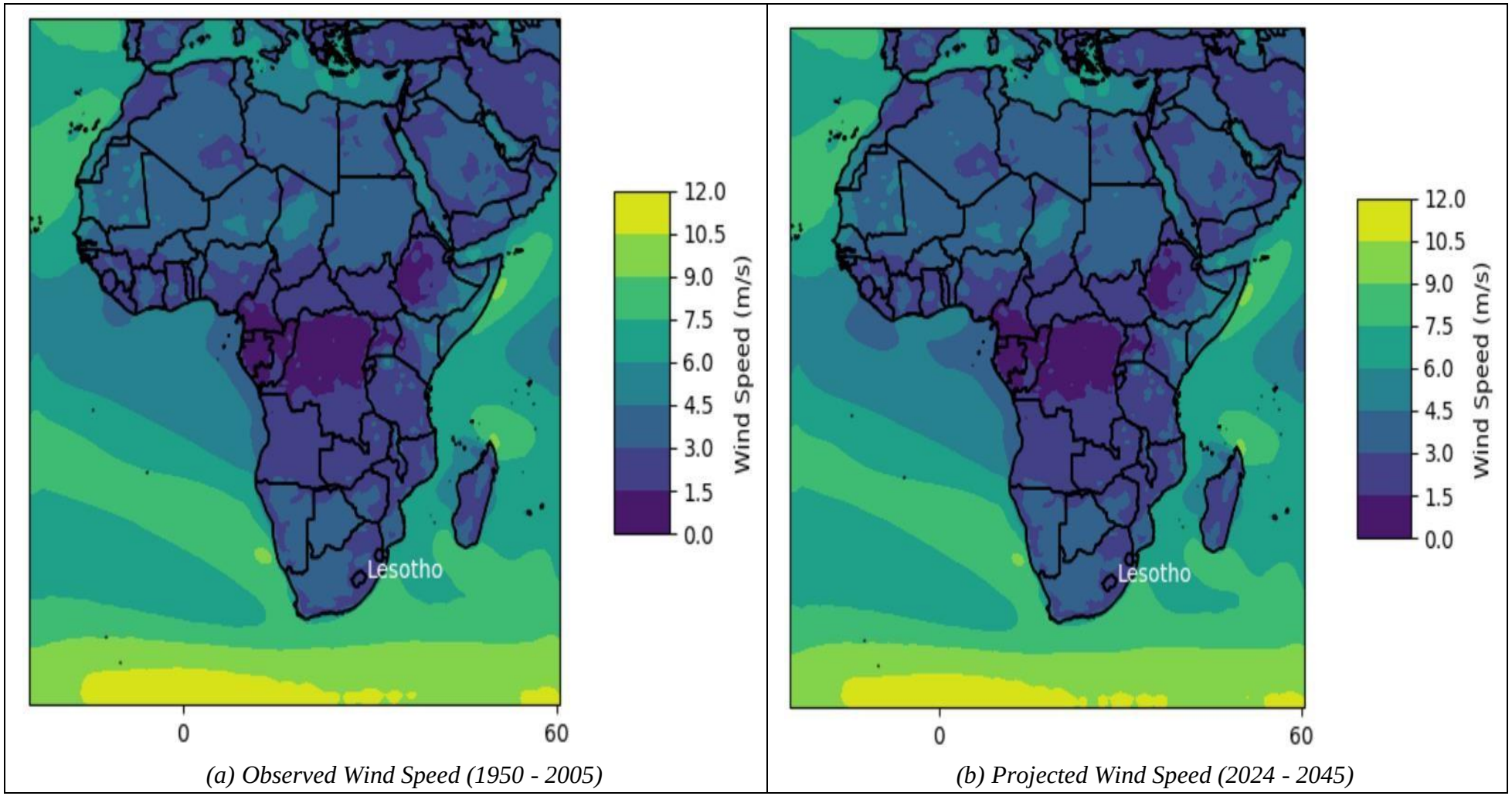

(a) Observed Wind Speed (1950 - 2005)

(b) Projected Wind Speed (2024 - 2045)

Figure 34: Average Wind Speed in Africa for at 10 m a.g.l

The notable wind speed changes on the African continent under the RCP8.5 scenario are summarized in Table 3.

Table 3: Notable Wind Speed Changes in Africa under RCP8.5

Country/Region	**Baseline Wind Speed (m/s)**	**Projected Wind Speed (m/s)**
Central Africa	**0.0 - 3.0**	**0.0 - 6.0**
Chad	1.5 - 6.0	1.5 - 6.0
DRC	0.0 - 3.0	0.0 - 3.0
North Africa	**1.5 - 4.5**	**1.5 - 6.0**
Western Sahara	4.5 - 6.0	4.5 - 6.0
South Sudan	1.5 - 3.0	1.5 - 3.0
Southern Africa	**1.5 - 4.5**	**1.5 - 4.5**
Namibia, Botswana and South Africa	1.5 - 4.5	1.5 - 4.5
Angola, and Zambia	1.5 - 3.0	1.5 - 4.5
West Africa	**1.5 - 6.0**	**1.5 - 6.0**
Mauritania	3.0 - 6.0	3.0 - 6.0
Sierra Leone, Liberia	1.5 - 3.0	1.5 - 3.0
East Africa	**0.0 - 6.0**	**0.0 - 6.0**
Somalia	3.0 - 6.0	4.5 - 6.0
Ethiopia	0.0 - 3.0	0.0 - 3.0

The projected average wind speed in Lesotho under the RCP8.5 scenario from 2024 to 2045 against the observed average wind speed at 10 a.g.l is shown in Figure 35 and it demonstrated an evenly distributed AWS of 1.5 to 3.0 m/s country-wide. The projected AWS was also the same along the country's borders with South Africa indicating the potential to generate wind energy in the country and along the borders. However, other African countries demonstrated a

change under this scenario while Lesotho indicated an anticipated average wind speed being identical to that of the baseline period and the RCP4.5 scenario.

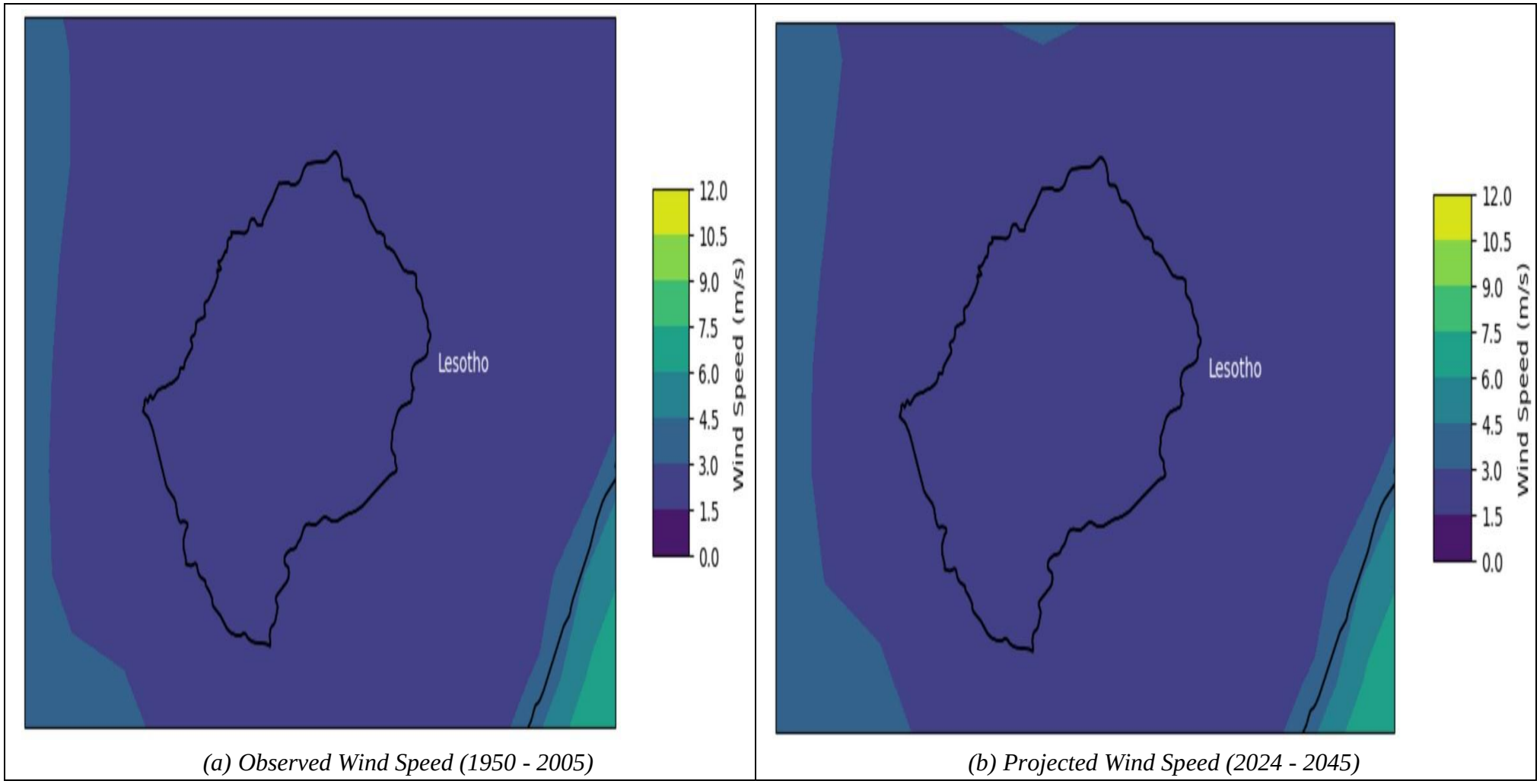

(a) Observed Wind Speed (1950 - 2005)

(b) Projected Wind Speed (2024 - 2045)

Figure 35: Average Wind Speed in Lesotho for at 10 m a.g.l

Projected Wind Speed Trend in Lesotho

The projected average wind speed trend shown in Figure 36 was simulated against time from 2024 to 2045 under the RCP8.5 scenario. The results indicate a minimum average wind speed of 1.50 m/s and a maximum average wind speed of approximately 2.75 - 3.00 m/s at 10 a.g.l. in comparison to the literature of 1.4 m/s - 8 m/s in the westerly region of the country. From 2024 to 2028, the predicted AWS stayed over 2.75 m/s, with 2028 having the highest predicted record of 3.00 m/s. The AWS trend was projected to decrease from 2029 to 2033; in 2029, an AWS of around 2.80 m/s was projected, however, from 2030 to 2033, an AWS of 2.50 - 2.75 m/s was reported. The simulation then showed a consistent AWS exceeding 2.75 m/s from 2034 to 2045 with the maximum record of AWS exceeding 3.00 m/s in 2042 and 2045. The projected AWS trend from 2034 to 2038 showed a decrease of an AWS slightly below 2.75 m/s with 2034 and 2035 indicating an outlier with a projected AWS of more than 2.75 m/s. The lowest projected AWS was in 2042 with a minimum AWS of 1.55 m/s and a maximum AWS of approximately 2.40 m/s.

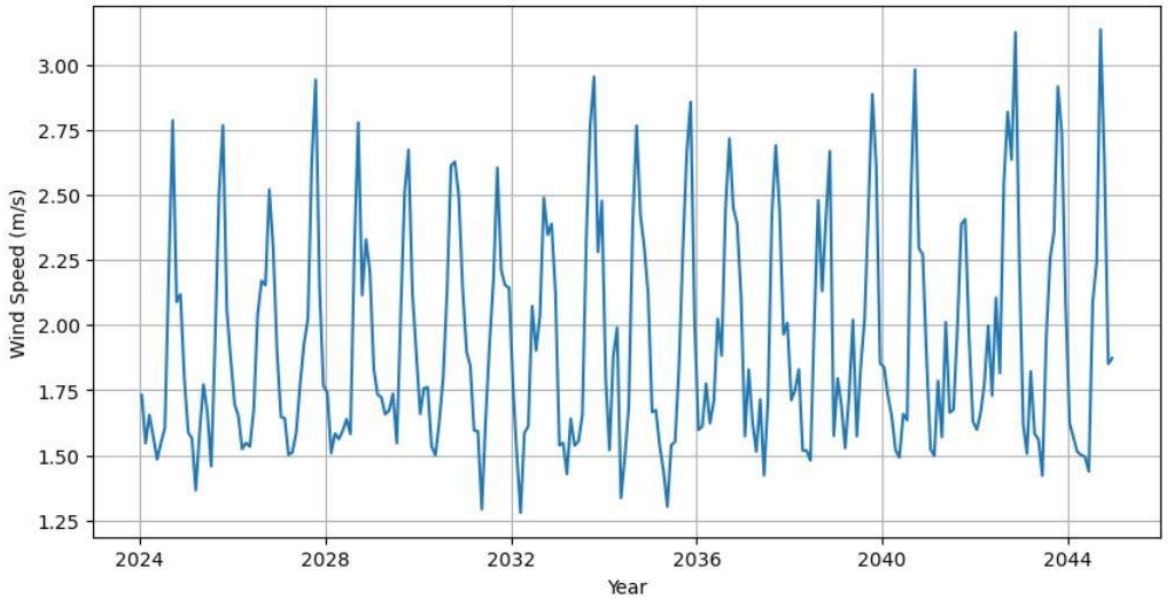

Figure 36: Projected Maximum Wind Speed Trend in Lesotho at 10 m a.g.l under RCP8.5 Scenario

Significant temperature changes and atmospheric pressure variations are expected under the RCP8.5 scenario, hence the projected maximum wind speed variation is expected to be sinusoidal to these changes. Stronger seasonal conditions brought by global warming will result

in extreme wind speed and the changed weather systems can lead to more natural disasters such as cyclones which will affect wind speed patterns in the country.

Solar Radiation

Shown in Figure 37 is the projected average solar radiation (ASR) for the African continent, including the coastlines from 2024 to 2045 against the observed average solar radiation from 1950 - 2005 at 10 m a.g.l. The projected ASR varied greatly from the RCP4.5 scenario shown in Figure 31, suggesting that climate change will have an impact on the ability of the region. ability to generate solar energy, the projected results also showed a slight resemblance to the average solar radiation from baseline data. The highest projected ASR on the continent was expected to be found in West Africa in the range of 175 - 275 W/m^2 with Mauritania having the best projected ASR on the continent in the range of 250 – 275 W/m^2, both on land and along the coastline. In the West Africa region, the projected ASR area coverage was more in line with the ASR observed from the baseline and RCP4.5 scenario. Sierra Leone, Cote D'Ivore, Ghana and Nigeria had the lowest ASR of 150 - 200 W/m^2 while Nigeria had the lowest ASR of 125 - 150 W/m^2 in the region along the coastline.

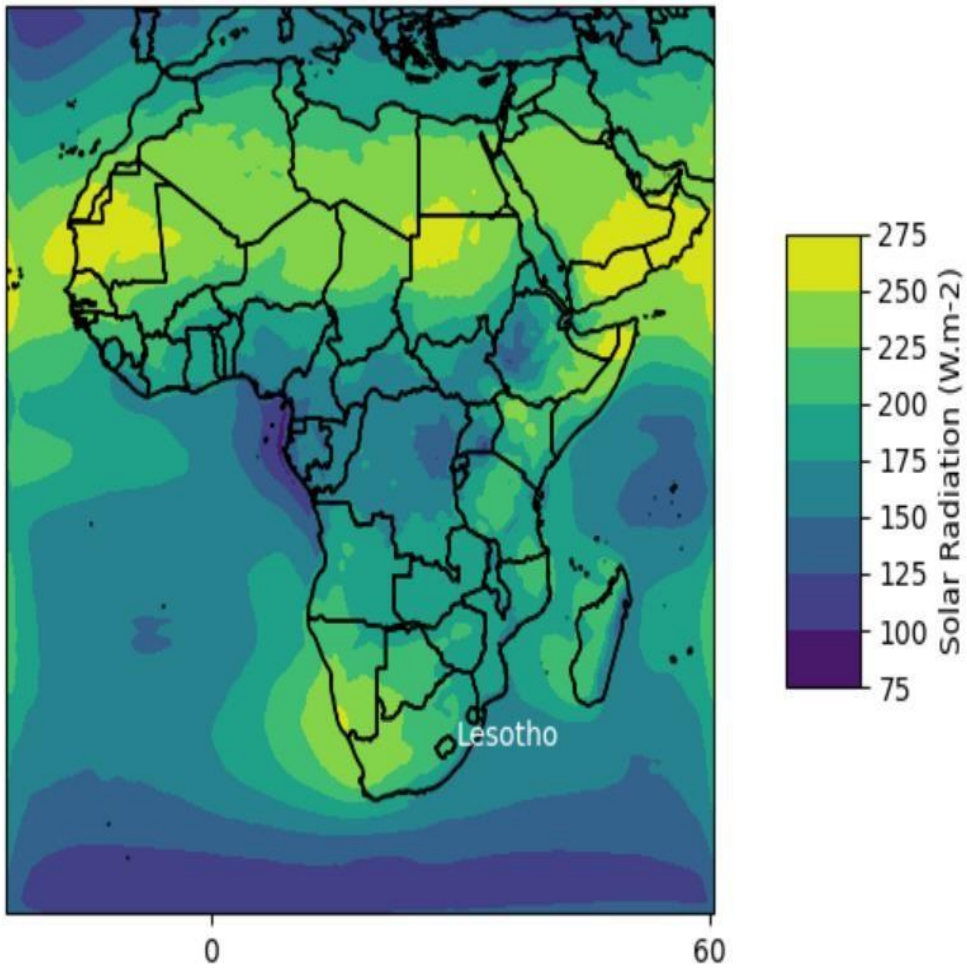

(a) Observed Solar Radiation (1950 - 2005)

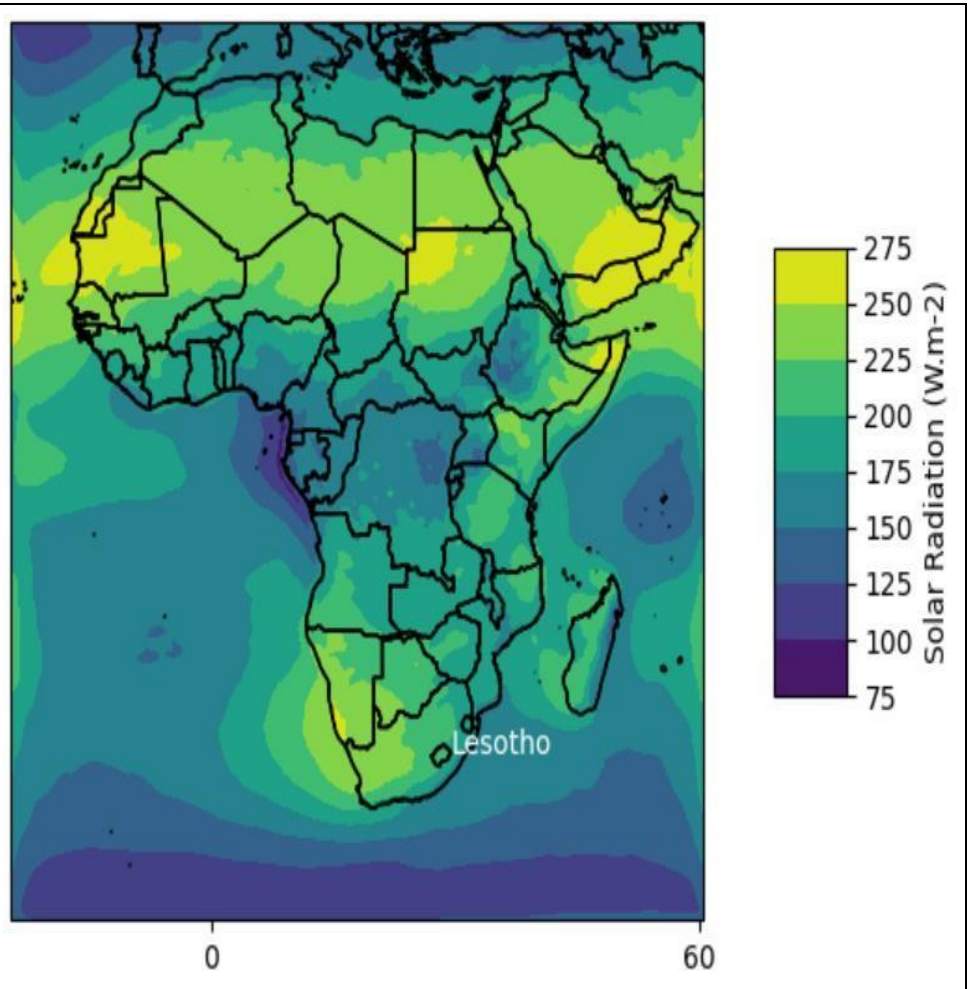

(b) Projected Solar Radiation (2024 - 2045)

Figure 37: Average Solar Radiation in Africa for at 10 m a.g.l

The projected ASR for Central Africa was the lowest on the continent, ranging from 150 to 225 W/m^2. The observed ASR in this region was different from the baseline period and probably similar to the ASR observed in the RCP4.5 scenario as shown Figure 31. Angola outperformed the rest of the terrestrial region with a projected ASR of 175 - 225 W/m^2, while the DRC had the lowest ASR of 150 - 175 W/m^2. The projected ASR along the coastlines of Cameroon, Equatorial Guinea, Gabon and Congo was in the range of 75 - 125 W/m^2, indicating a low potential to generate solar energy along the coastline under this scenario. The projected range of ASR in East Africa was 125 - 275 W/m^2, with Sudan and Somalia having the highest ASR in the region of 200 - 275 W/m^2. The ASR projected in Sudan and Somalia remained constant in the area coverage under this scenario whereas Rwanda and Ethiopia have the lowest ASR in the region, ranging from 125 to 200 W/m^2.

In this scenario, the North African countries exhibited the most evenly distributed ASR across the continent; ASR in this region ranged from 175 - 275 W/m^2, an increase over baseline data observed between 1950 and 2005 of 150 - 275 W/m^2. The western Sahara exhibited the best ASR in the range of 225 – 275 W/m^2 on land and along the shore, matching the baseline recorded ASR. Meanwhile, South Sudan maintained its position as the country with the lowest ASR, at 175 - 200 W/m^2, an increase above the baseline reported ASR of 150 – 200 W/m^2. The observed ASR in Southern Africa was determined to be in the range of 175 - 275 W/m^2 which is an increase from the ASR of 175 - 250 W/m^2 observed from 1950 - 2005 baseline period. The countries with the highest ASRs in the region were Namibia and South Africa, with 200 – 275 W/m^2 .The Namibian coastline had a higher ASR of 250 – 275 W/m^2. The area coverage of this observed variation increased from the baseline data, indicating an impact brought about by climate change. Zambia continued to have the lowest ASR in the region, at 175 - 200 W/m^2. The summarized notable solar radiation changes in the African continent under the RCP8.5 scenario are outlined in Table 4.

Table 4: Notable Solar Radiation Changes in Africa under RCP8.5

Country/Region	**Baseline Solar Radiation (W/m^2)**	**Projected Solar Radiation (W/m^2)**
Central Africa	**125 - 250**	**150 - 225**

Angola	150 - 200	175 - 225
DRC	125 - 175	150 - 175
North Africa	**150 - 275**	**175 - 275**
Western Sahara	225 - 275	225 - 275
South Sudan	150 - 200	175 - 200
Southern Africa	**175 - 275**	**175 - 275**
Namibia and South Africa	200 - 275	200 - 275
Zambia	175 - 200	175 - 200
West Africa	**175 - 275**	**175 - 275**
Mauritania	250 - 275	250 - 275
Sierra Leone, Cote D'Ivore, Ghana, and Nigeria	150 - 200	150 - 200
East Africa	**125 - 275**	**125 - 275**
Somalia	200 - 275	200 - 275
Ethiopia and Rwanda	125 - 200	125 - 200

Projected in Figure 38 is the average solar radiation in Lesotho under the RCP8.5 scenario for the years 2024 – 2045 against observed solar radiation from 1950 - 2005 at 10 m a.g.l. The country predominantly displayed ASR of 200 – 225 W/m^2 across its borders and across the country, with the exception of the eastern region, which is home to the Mokhotlong district. An ASR of 175 - 200 W/m^2 was projected in this part of the country, with the area coverage being less than that observed in the baseline period and the RCP4.5 scenario in Figure 26 and Figure 32 respectively, indicating an increase in ASR coverage of 200 - 225 W/m^2 in the country. The borderline between Quthing and South Africa also had an increase in aerial coverage of 200 - 225 W/m^2. An ASR of 200 - 225 W/m^2 was projected for the rest of the country's borderline with South Africa.

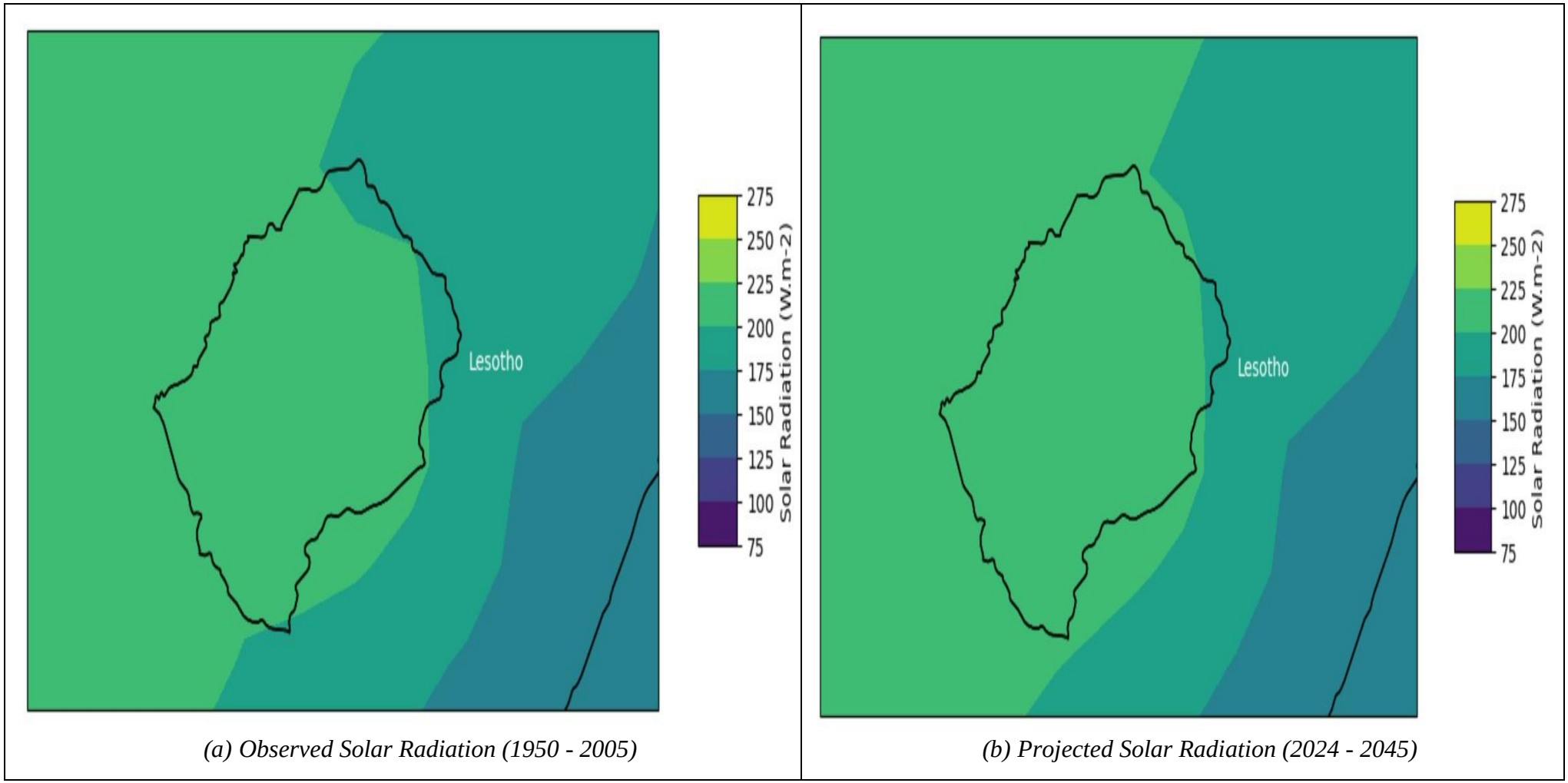

(a) Observed Solar Radiation (1950 - 2005)

(b) Projected Solar Radiation (2024 - 2045)

Figure 38: Average Solar Radiation in Lesotho for at 10 m a.g.l

Projected Solar Radiation Trend in Lesotho

Shown in Figure 39 is the projected average solar radiation trend simulated versus the time from 2024 to 2045 under the RCP8.5. The results indicate a minimum average solar radiation of 150 W/m^2 and a maximum average solar radiation of 275 W/m^2 at 10 m a.g.l. In comparison, the stated literature solar radiation within the country is in the range 5.5 - 7.2 kWh/m^2. The projected ASR trend increased from 2024 to 2030, reaching a value of more than 300 W/m^2 in 2030; the lowest ASR of approximately 240 W/m^2 during this period was recorded in 2027. From 2030 to 2045, the projected trend decreased to ASR below 275 W/m^2, except 2035, 2039, and 2043, when ASR exceeded 300 W/m^2. The projected lowest ASR recorded was in 2035 with a minimum of 150 W/m^2 and a maximum of about 250 W/m^2.

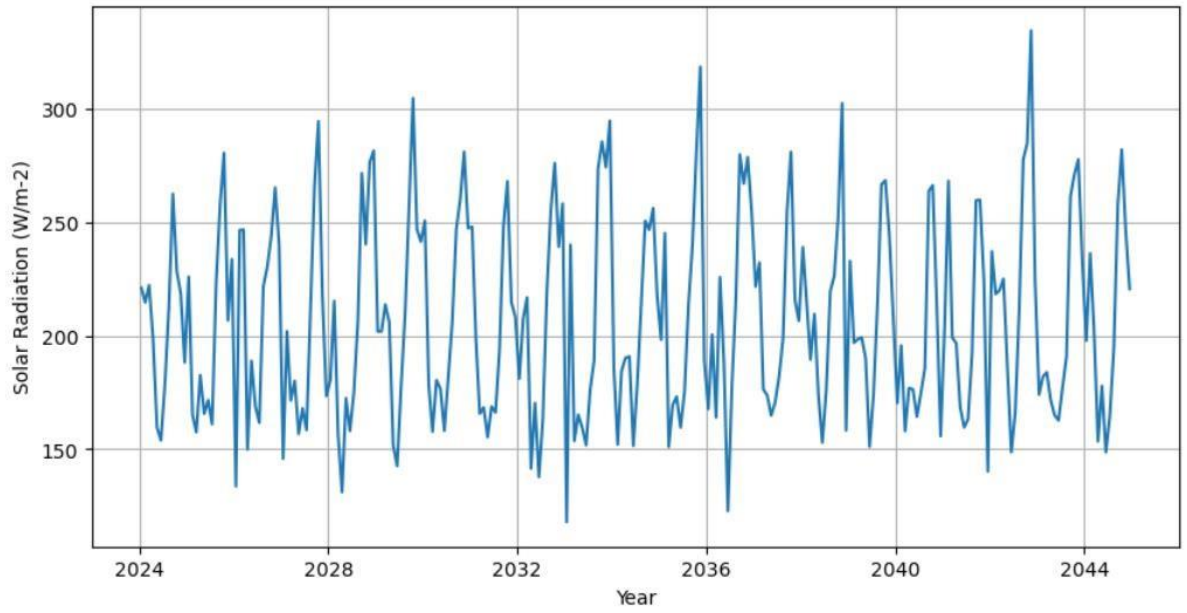

Figure 39: Projected Maximum Solar Radiation Trend in Lesotho at 10 m a.g.l under RCP8.5 Scenario

Under the RCP8.5 scenario, significant solar radiation changes are expected due to the higher greenhouse emissions, leading to a rapid increase in atmospheric concentrations. Over time, without preventative policies limiting the release of pollutants into the atmosphere, aerosols will increase and absorb some solar radiation, reaching the surface over Lesotho and reducing solar radiation. Increased temperatures under this scenario in the country will lead to significant vegetation cover and land use which will affect the absorption of solar radiation.

4.2.3 Discussion

The projected average wind speed in Lesotho from 2024 - 2045 under the RCP4.5 was 2.15 m/s at 10 m a.g.l, ranging from 1.50 – 3.00 m/s while the projected average solar radiation is 200 - 225 W/m^2, except in the north-east where 175 – 200 W/m^2 is projected in the Mokhotlong district. In general, the projected average solar radiation range under the RCP4.5 scenario increased from 2024 to 2045 from 140 – 300 W/m^2 range from 1950 to 2005 to 150-280 W/m^2 while the projected average wind speed trend slightly increased from 1.25 – 3.00 m/s in 1950 - 2005 to 1.30 – 3.00 m/s in 2024 - 2045. Under RCP8.5, the projected average wind speed in the country was 2.15 m/s at a.g.l. with a range of 1.50 – 3.00 m/s. Overall, the average wind speed indicated an increasing trend from 2024 to 2045 under this scenario. The projected average solar radiation was consistent at 200-225 W/m,^{2} with the exception of Mokhotlong district where average solar radiation of 175 - 200 W/m^2 was projected. An increasing trend of the average solar radiation is projected from 2024 to 2045.

The RCP4.5 scenario implies a future where there are mitigations against the impact of climate change and global warming is limited but still exceeds 2℃ above the pre-industrial level, while RCP8.5 assumes a future where global warming exceeds 4℃ above the preindustrial level and no efforts taken to mitigate global warming. RCP4.5 scenario is likely to occur due to the global efforts to mitigate global warming, coupled with the United Nations sustainable development goals and the Paris Agreement aimed at mitigating climate change below 2℃. Lesotho is committed to the global warming mitigation efforts hence the country has presented a Nationally Determined Contribution to strengthen the global efforts of both mitigation and adaptation.

Conclusions and Recommendations

In this study, Jupyter Notebook software was utilized to study the potential impact of climate change on wind speed and solar radiation in Lesotho using a CORDEX-Africa regional climate model to simulate past, present, and future climate conditions under different scenarios at 10 m above ground level. The historical wind speed and solar radiation in Lesotho were simulated with a baseline from 1950 to 2005 established for the two variables, an average wind speed in the range of 1.5 - 3.0 m/s was observed throughout the baseline period while the observed average solar radiation during the same period was at 200 - 225 W/m^2 range except in the north-east part of the country where Butha Buthe and Mokhotlong districts are located where average solar radiation of about 175 - 200 W/m^2 was observed.

Under the RCP4.5, the results showed a minimum average wind speed of 1.50 m/s and a maximum average wind speed of 2.75 m/s with the year 2030 recording a maximum of 3.00 m/s. The projected average wind speed from 2024 to 2045 under this scenario was 2.15 m/s at 10 m a.g.l. The projected solar radiation showed a minimum average solar radiation of 150 W/m^2 and a maximum average solar radiation of 275 W/m^2, with some years recording about 340 W/m^2 average solar radiation. The scenario indicated that Lesotho will not be negatively affected by the renewable energy generation through wind and solar resources.

Under the RCP8.5, the results showed a minimum average wind speed of 1.50 m/s and a maximum average wind speed of 3.00 m/s, however, the years 2042 to 2045 recorded an average wind speeds above 3.00 m/s threshold. The projected solar radiation showed a minimum average solar radiation of 150 W/m^2 and a maximum average solar radiation of 275 W/m^2. Under this scenario, the projected average solar radiation showed an increased trend from 2024 to 2045 with the year 2043 recording the highest maximum average solar radiation of about 370 W/m^2. The scenario also indicates that Lesotho will not be negatively affected by renewable energy generation through wind and solar resources.

The projected stability and increase in wind speed and solar radiation in Lesotho up to 2045 suggest significant opportunities for sustainable energy development, which aligns with both global and national commitments to reduce greenhouse gas emissions and to combat climate change. The increased renewable energy capacity will enhance energy security by reducing Lesotho's reliance on imported fossil fuels and providing a more stable and predictable energy

supply. Investment in these renewable energy infrastructures can drive economic growth by creating jobs, attracting foreign investment, and fostering technological innovation.

The following recommendations should be considered to harness the potential of renewable energy in Lesotho. A significant investment into renewable energy is essential to take advantage of available resources. Wind farms should be developed, and the expansion of solar energy projects in new areas with high solar radiation, such as Butha Buthe, Quthing, and Mokhotlong districts.

References

[1] X. Lyu and A. Shi, “Research on the Renewable Energy Industry Financing Efficiency Assessment and Mode Selection,” *Sustainability*, vol. 10, no. 1, p. 222, Jan. 2018, doi: 10.3390/su10010222.

[2] C. Gutiérrez, A. De La Vara, J. J. González-Alemán, and M. Á. Gaertner, “Impact of Climate Change on Wind and Photovoltaic Energy Resources in the Canary Islands and Adjacent Regions,” *Sustainability*, vol. 13, no. 8, p. 4104, Apr. 2021, doi: 10.3390/su13084104.

[3] REN21, “GSR 2023 Global Overview,” *Renewable Energy 2023 - Global Status Report*, 2023. [Online]. Available: https://www.ren21.net/gsr-2023/modules/global_overview/

[4] C. Arndt, D. Arent, F. Hartley, B. Merven, and A. H. Mondal, “Faster Than You Think: Renewable Energy and Developing Countries,” *Annual Review of Resource Economics*, vol. 11, no. 1, pp. 149–168, 2019, doi: 10.1146/annurev-resource-100518-093759.

[5] IRENA, “Scaling up renewables in landlocked developing countries,” 2022, [Online]. Available: https://www.irena.org/publications/2022/Sep/Scaling-up-renewables-in-landlockeddeveloping-countries

[6] B. M. Taele, K. K. Gopinathan, and L. Mokhuts’oane, “The potential of renewable energy technologies for rural development in Lesotho,” *Renewable Energy*, vol. 32, no. 4, pp. 609–622, Apr. 2007, doi: 10.1016/j.renene.2006.02.014.

[7] “World Bank Open Data,” World Bank Open Data. Accessed: Aug. 26, 2023. [Online]. Available: https://data.worldbank.org

[8] A. Ali, “Techno-economic Feasibility Analysis of an Off-grid Hybrid Renewable Energy System for Rural Electrification,” *Journal of Electrical and Electronic Engineering*, vol. 9, Feb. 2021, doi: 10.11648/j.jeee.20210901.12.

[9] TheReporter, “Electrification of rural areas remains an issue,” The Reporter Lesotho | Fresh News, Daily. Accessed: Oct. 25, 2022. [Online]. Available: https://www.thereporter.co.ls/2022/10/05/electrification-of-rural-areas-remains-an-issue/

[10] LEWA [Lesotho Electricity and Water Authority], “Lesotho Electricity and Water Authority - Annual report 2021/22. LesothoElectricity and Water Authority,” Maseru Lesoth0, 2021.

[11] “Support to the Energy Sector Reform in Lesotho: Skills Audit and Developing Capacity Building Plan for Do.” HCL Consultants, 2020.

[12] kgi-admin, “Power plant profile: Mafeteng Ha Ramarothole Solar PV Park, Lesotho,” Power Technology. Accessed: Aug. 08, 2023. [Online]. Available: https://www.powertechnology.com/marketdata/power-plant-profile-mafeteng-ha-ramarothole-solar-pv-parklesotho/

[13] T. Smith, “Lesotho: financing for 11 new minigrids,” ESI-Africa.com. Accessed: Feb. 12, 2023. [Online]. Available: https://www.esi-africa.com/industry-sectors/finance-and-policy/lesothofinancing-for-11-new-minigrids/

[14] A. D. Bank, “EOI - Lesotho - Auditing Services related AfDB-financed activities for the NEO 1 20 MWac Solar PV power plant,” African Development Bank Group - Making a Difference. Accessed: Aug. 09, 2023. [Online]. Available: https://www.afdb.org/en/documents/eoilesotho-auditing-services-related-afdb-financed-activities-neo-1-20-mwac-solar-pv-powerplant

[15] Leah Shelene, “LHWP Phase 2 to Reach Completion in 2028,” *Engineering News*, Dec. 2022, [Online]. Available: https://www.engineeringnews.co.za/article/lhwp-phase-2-to-reachcompletion-in-2028-2022-12-16

[16] B. M. Taele, L. Mokhutšoane, and I. Hapazari, “An overview of small hydropower development in Lesotho: Challenges and prospects,” *Renewable Energy*, vol. 44, pp. 448–452, Aug. 2012, doi: 10.1016/j.renene.2012.01.086.

[17] M. D'Isidoro *et al.*, "Estimation of solar and wind energy resources over Lesotho and their complementarity by means of WRF yearly simulation at high resolution," *Renewable Energy*, vol. 158, pp. 114–129, Oct. 2020, doi: 10.1016/j.renene.2020.05.106.
[18] M. Mpholo, T. Mathaba, and M. Letuma, "Wind profile assessment at Masitise and Sani in Lesotho for potential off-grid electricity generation," *Energy Conversion and Management*, vol. 53, no. 1, pp. 118–127, Jan. 2012, doi: 10.1016/j.enconman.2011.07.015.
[19] T. Mathaba, M. Mpholo, and M. Letuma, "Velocity and power density analysis of the wind at Letšeng-la-terae in Lesotho," *Renewable Energy*, vol. 46, pp. 210–217, Oct. 2012, doi: 10.1016/j.renene.2012.04.003.
[20] S. Mokeke and L. Z. Thamae, "The impact of intermittent renewable energy generators on Lesotho national electricity grid," *Electric Power Systems Research*, vol. 196, p. 107196, Jul. 2021, doi: 10.1016/j.epsr.2021.107196.
[21] Hirundo Energy, "Projects," Energy.ls. Accessed: Aug. 26, 2023. [Online]. Available: https://www.hirundo.energy/projects-1
[22] P. De Jong *et al.*, "Estimating the impact of climate change on wind and solar energy in Brazil using a South American regional climate model," *Renewable Energy*, vol. 141, pp. 390–401, Oct. 2019, doi: 10.1016/j.renene.2019.03.086.
[23] D. E. H. J. Gernaat, H. S. De Boer, V. Daioglou, S. G. Yalew, C. Müller, and D. P. Van Vuuren, "Climate change impacts on renewable energy supply," *Nat. Clim. Chang.*, vol. 11, no. 2, pp. 119–125, Feb. 2021, doi: 10.1038/s41558-020-00949-9.
[24] T. A. Tsalis, K. E. Malamateniou, D. Koulouriotis, and I. E. Nikolaou, "New challenges for corporate sustainability reporting: United Nations' 2030 Agenda for sustainable development and the sustainable development goals," *Corp Soc Responsib Environ Manag*, vol. 27, no. 4, pp. 1617–1629, Jul. 2020, doi: 10.1002/csr.1910.
[25] T. Bristow and T. H. Ford, *A Cultural History of Climate Change*. Routledge, 2016.
[26] IPCC, "Climate Change 2013: The Physical Science Basis. Contribution of Working Group I to the Fifth Assessment Report of the Intergovernmental Panel on Climate Change," 2013. Accessed: Aug. 18, 2024. [Online]. Available: https://www.ipcc.ch/report/ar5/wg1/
[27] C. Fant, C. Adam Schlosser, and K. Strzepek, "The impact of climate change on wind and solar resources in southern Africa," *Applied Energy*, vol. 161, pp. 556–564, Jan. 2016, doi: 10.1016/j.apenergy.2015.03.042.
[28] "Home," Climate Change: Vital Signs of the Planet. Accessed: Oct. 14, 2023. [Online]. Available: https://climate.nasa.gov/
[29] Ipcc, *Global Warming of 1.5°C: IPCC Special Report on Impacts of Global Warming of 1.5°C above Pre-industrial Levels in Context of Strengthening Response to Climate Change, Sustainable Development, and Efforts to Eradicate Poverty*, 1st ed. Cambridge University Press, 2022. doi: 10.1017/9781009157940.
[30] S. M. Semenov, "Greenhouse Effect and Modern Climate," *Russ. Meteorol. Hydrol.*, vol. 47, no. 10, pp. 725–734, Oct. 2022, doi: 10.3103/S1068373922100016.
[31] K. Calvin *et al.*, "IPCC, 2023: Climate Change 2023: Synthesis Report. Contribution of Working Groups I, II and III to the Sixth Assessment Report of the Intergovernmental Panel on Climate Change [Core Writing Team, H. Lee and J. Romero (eds.)]. IPCC, Geneva, Switzerland.," Intergovernmental Panel on Climate Change (IPCC), Jul. 2023. doi: 10.59327/IPCC/AR69789291691647.
[32] W. K. Darkwah *et al.*, "Greenhouse Effect: Greenhouse Gases and Their Impact on Global Warming," *Journal of Scientific Research and Reports*, vol. 17, pp. 1–9, Feb. 2018, doi: 10.9734/JSRR/2017/39630.
[33] H. Goosse, *Climate System Dynamics and Modeling*. Cambridge University Press, 2015.
[34] R. K. Pachauri, L. Mayer, and Intergovernmental Panel on Climate Change, Eds., *Climate change*

2014: synthesis report. Geneva, Switzerland: Intergovernmental Panel on Climate Change, 2015.
[35] Intergovernmental Panel on Climate Change (IPCC), *Climate Change 2021 – The Physical Science Basis: Working Group I Contribution to the Sixth Assessment Report of the Intergovernmental Panel on Climate Change*. Cambridge: Cambridge University Press, 2023. doi: 10.1017/9781009157896.
[36] S. Fahad *et al.*, Eds., *Environment, Climate, Plant and Vegetation Growth*. Cham: Springer International Publishing, 2020. doi: 10.1007/978-3-030-49732-3.
[37] C. Parmesan, M. D. Morecroft, and Y. Trisurat, "Climate Change 2022:Impacts, Adaptation and Vulnerability," GIEC, Research Report, Feb. 2022. Accessed: Nov. 04, 2023. [Online]. Available: https://hal.science/hal-03774939
[38] J. W. Moore and D. E. Schindler, "Getting ahead of climate change for ecological adaptation and resilience," *Science*, vol. 376, no. 6600, pp. 1421–1426, Jun. 2022, doi: 10.1126/science.abo3608.
[39] Z. Ahmed and S. Ambinakudige, "Does land use change, waterlogging, and salinity impact on sustainability of agriculture and food security? Evidence from southwestern coastal region of Bangladesh," *Environ Monit Assess*, vol. 195, no. 1, p. 74, Jan. 2023, doi: 10.1007/s10661-02210673-w.
[40] "Climate change and food security: risks and responses," *FOOD AND AGRICULTURE ORGANIZATION OF THE UNITED NATIONS*, 2015, [Online]. Available: https://www.fao.org/3/i5188e/I5188E.pdf
[41] K. D. Algur, S. K. Patel, and S. Chauhan, "The impact of drought on the health and livelihoods of women and children in India: A systematic review," *Children and Youth Services Review*, vol. 122, p. 105909, Mar. 2021, doi: 10.1016/j.childyouth.2020.105909.
[42] M. Gebreyes *et al.*, "Local Perceptions of Water-Energy-Food Security: Livelihood Consequences of Dam Construction in Ethiopia," *Sustainability*, vol. 12, no. 6, Art. no. 6, Jan. 2020, doi: 10.3390/su12062161.
[43] R. Warren *et al.*, "Quantifying risks avoided by limiting global warming to 1.5 or 2 °C above preindustrial levels," *Climatic Change*, vol. 172, no. 3–4, p. 39, Jun. 2022, doi: 10.1007/s10584021-03277-9.
[44] Intergovernmental Panel On Climate Change, *Climate Change 2021 – The Physical Science Basis: Working Group I Contribution to the Sixth Assessment Report of the Intergovernmental Panel on Climate Change*, 1st ed. Cambridge University Press, 2023. doi: 10.1017/9781009157896.
[45] L. Gu *et al.*, "Projected increases in magnitude and socioeconomic exposure of global droughts in 1.5 and 2 °C warmer climates," *Hydrology and Earth System Sciences*, vol. 24, no. 1, pp. 451–472, Jan. 2020, doi: 10.5194/hess-24-451-2020.
[46] J. Solé, "Climate and Energy Crises from the Perspective of the Intergovernmental Panel on Climate Change: Trade-Offs between Systemic Transition and Societal Collapse?," *Sustainability*, vol. 15, no. 3, Art. no. 3, Jan. 2023, doi: 10.3390/su15032231.
[47] G. Zhang, G. Zeng, X.-Z. Liang, and C. Huang, "Increasing heat risk in China's urban agglomerations," *Environ. Res. Lett.*, vol. 16, no. 6, p. 064073, Jun. 2021, doi: 10.1088/17489326/ac046e.
[48] D. F. B. Usta, M. Teymouri, and U. Chatterjee, "Assessment of temperature changes over Iran during the twenty-first century using CMIP6 models under SSP1-26, SSP2-4.5, and SSP5-8.5 scenarios," *Arab J Geosci*, vol. 15, no. 5, p. 416, Feb. 2022, doi: 10.1007/s12517-022-09709-9.
[49] J. K. McWhorter, P. R. Halloran, G. Roff, W. J. Skirving, C. T. Perry, and P. J. Mumby, "The importance of 1.5°C warming for the Great Barrier Reef," *Global Change Biology*, vol. 28, no. 4, pp. 1332–1341, 2022, doi: 10.1111/gcb.15994.

[50] V. Popovski, *The Implementation of the Paris Agreement on Climate Change*. Routledge, 2018.
[51] S. Fawzy, A. I. Osman, J. Doran, and D. W. Rooney, "Strategies for mitigation of climate change: a review," *Environ Chem Lett*, vol. 18, no. 6, pp. 2069–2094, Nov. 2020, doi: 10.1007/s10311020-01059-w.
[52] J. Meckling and V. J. Karplus, "Political strategies for climate and environmental solutions," *Nat Sustain*, vol. 6, no. 7, Art. no. 7, Jul. 2023, doi: 10.1038/s41893-023-01109-5.
[53] T. N. Hale *et al.*, "Sub- and non-state climate action: a framework to assess progress, implementation and impact," *Climate Policy*, vol. 21, no. 3, pp. 406–420, Mar. 2021, doi: 10.1080/14693062.2020.1828796.
[54] K. Bäckstrand, J. W. Kuyper, B.-O. Linnér, and E. Lövbrand, "Non-state actors in global climate governance: from Copenhagen to Paris and beyond," *Environmental Politics*, vol. 26, no. 4, pp. 561–579, Jul. 2017, doi: 10.1080/09644016.2017.1327485.
[55] F. Ekardt, B. Jacobs, J. Stubenrauch, and B. Garske, "Peatland Governance: The Problem of Depicting in Sustainability Governance, Regulatory Law, and Economic Instruments," *Land*, vol. 9, no. 3, Art. no. 3, Mar. 2020, doi: 10.3390/land9030083.
[56] J. Burke and A. Gambhir, "Policy incentives for Greenhouse Gas Removal Techniques: the risks of premature inclusion in carbon markets and the need for a multi-pronged policy framework," *Energy and Climate Change*, vol. 3, p. 100074, Dec. 2022, doi: 10.1016/j.egycc.2022.100074.
[57] D. Coady, I. Parry, L. Sears, and B. Shang, "How Large Are Global Fossil Fuel Subsidies?," *World Development*, vol. 91, pp. 11–27, Mar. 2017, doi: 10.1016/j.worlddev.2016.10.004.
[58] F. J. Arze del Granado, D. Coady, and R. Gillingham, "The Unequal Benefits of Fuel Subsidies: A Review of Evidence for Developing Countries," *World Development*, vol. 40, no. 11, pp. 2234–2248, Nov. 2012, doi: 10.1016/j.worlddev.2012.05.005.
[59] I. I. Dorband, M. Jakob, M. Kalkuhl, and J. C. Steckel, "Poverty and distributional effects of carbon pricing in low- and middle-income countries – A global comparative analysis," *World Development*, vol. 115, pp. 246–257, Mar. 2019, doi: 10.1016/j.worlddev.2018.11.015.
[60] K. Handayani, T. Filatova, Y. Krozer, and P. Anugrah, "Seeking for a climate change mitigation and adaptation nexus: Analysis of a long-term power system expansion," *Applied Energy*, vol. 262, p. 114485, Mar. 2020, doi: 10.1016/j.apenergy.2019.114485.
[61] J. Cronin, G. Anandarajah, and O. Dessens, "Climate change impacts on the energy system: a review of trends and gaps," *Climatic Change*, vol. 151, no. 2, pp. 79–93, Nov. 2018, doi: 10.1007/s10584-018-2265-4.
[62] C. Breyer, M. Fasihi, and A. Aghahosseini, "Carbon dioxide direct air capture for effective climate change mitigation based on renewable electricity: a new type of energy system sector coupling," *Mitig Adapt Strateg Glob Change*, vol. 25, no. 1, pp. 43–65, Jan. 2020, doi: 10.1007/s11027-019-9847-y.
[63] K. Calvin *et al.*, "IPCC, 2023: Climate Change 2023: Synthesis Report. Contribution of Working Groups I, II and III to the Sixth Assessment Report of the Intergovernmental Panel on Climate Change [Core Writing Team, H. Lee and J. Romero (eds.)]. IPCC, Geneva, Switzerland.," Intergovernmental Panel on Climate Change (IPCC), Jul. 2023. doi: 10.59327/IPCC/AR69789291691647.
[64] P. Feron *et al.*, "Towards Zero Emissions from Fossil Fuel Power Stations," *International Journal of Greenhouse Gas Control*, vol. 87, pp. 188–202, Aug. 2019, doi: 10.1016/j.ijggc.2019.05.018.
[65] G. Dileep, "A survey on smart grid technologies and applications," *Renewable Energy*, vol. 146, pp. 2589–2625, Feb. 2020, doi: 10.1016/j.renene.2019.08.092.
[66] T. Walker, C. Cucuzzella, S. Goubran, and R. Geith, *The Role of Design, Construction, and Real Estate in Advancing the Sustainable Development Goals*. Springer Nature, 2023.
[67] P. Saha *et al.*, "Grey, blue, and green hydrogen: A comprehensive review of production methods and prospects for zero-emission energy," *International Journal of Green Energy*, vol.

0, no. 0, pp. 1–15, 2023, doi: 10.1080/15435075.2023.2244583.
[68] A. Akinpelu, M. S. Alam, M. Shafiullah, S. M. Rahman, and F. S. Al-Ismail, “Greenhouse Gas Emission Dynamics of Saudi Arabia: Potential of Hydrogen Fuel for Emission Footprint Reduction,” *Sustainability*, vol. 15, no. 7, Art. no. 7, Jan. 2023, doi: 10.3390/su15075639.
[69] G. Gaustad, M. Krystofik, M. Bustamante, and K. Badami, “Circular economy strategies for mitigating critical material supply issues,” *Resources, Conservation and Recycling*, vol. 135, pp. 24–33, Aug. 2018, doi: 10.1016/j.resconrec.2017.08.002.
[70] [P.R. Shukla, E. Calvo Buendia, V. Masson-Delmotte, and H.-O. Pörtner, “Climate Change and Land: an IPCC special report on climate change, desertification, land degradation, sustainable land management, food security, and greenhouse gas fluxes in terrestrial ecosystems,” p. In Press pp., 2019.
[71] D. I. Armstrong McKay *et al.*, “Exceeding 1.5°C global warming could trigger multiple climate tipping points,” *Science*, vol. 377, no. 6611, p. eabn7950, Sep. 2022, doi: 10.1126/science.abn7950.
[72] M. S. Farooq *et al.*, “Uncovering the Research Gaps to Alleviate the Negative Impacts of Climate Change on Food Security: A Review,” *Frontiers in Plant Science*, vol. 13, 2022, Accessed: Nov. 14, 2023. [Online]. Available: https://www.frontiersin.org/articles/10.3389/fpls.2022.927535
[73] R. K. Upadhyay, “Markers for Global Climate Change and Its Impact on Social, Biological and Ecological Systems: A Review,” *American Journal of Climate Change*, vol. 09, no. 03, Art. no. 03, Aug. 2020, doi: 10.4236/ajcc.2020.93012.
[74] G. Ceccherini, S. Russo, I. Ameztoy, A. F. Marchese, and C. Carmona-Moreno, “Heat waves in Africa 1981–2015, observations and reanalysis,” *Natural Hazards and Earth System Sciences*, vol. 17, no. 1, pp. 115–125, Jan. 2017, doi: 10.5194/nhess-17-115-2017.
[75] J. Spinoni *et al.*, “A new global database of meteorological drought events from 1951 to 2016,” *Journal of Hydrology: Regional Studies*, vol. 22, p. 100593, Apr. 2019, doi: 10.1016/j.ejrh.2019.100593.
[76] E. Nyadzi, “Indigenous knowledge and climate change adaptation in Africa: a systematic review,” *CABI Reviews*, 2021, doi: 10.1079/pavsnnr202116029.
[77] E. Nyadzi, S. E. Werners, R. Biesbroek, and F. Ludwig, “Towards weather and climate services that integrate indigenous and scientific forecasts to improve forecast reliability and acceptability in Ghana,” *Environmental Development*, vol. 42, p. 100698, Jun. 2022, doi: 10.1016/j.envdev.2021.100698.
[78] LMS 2017, “Lesotho National climate Change Policy Implementation Strategy NCCPIS,” *Ministry of Energy and Meteorology,Lesotho*.
[79] “CO_2 and Greenhouse Gas Emissions Data Explorer,” Our World in Data. Accessed: Nov. 17, 2023. [Online]. Available: https://ourworldindata.org/explorers/co2
[80] LMS 2017, “Lesotho’s National Climate Change Policy.,” *Ministry of Energy and Meteorology,Lesotho*.
[81] “Lesotho Climate-Smart Agriculture Investment Plan. ‘Opportunities for transitioning to more productive, climate-resilient, and low carbon agriculture,’” *World Bank Group*, 2019.
[82] K. McGuffie and A. Henderson-Sellers, *The Climate Modelling Primer*. John Wiley & Sons, 2014.
[83] R. Colman and S. Soldatenko, “Understanding the links between climate feedbacks, variability and change using a two-layer energy balance model,” *Clim Dyn*, vol. 54, no. 7, pp. 3441–3459, Apr. 2020, doi: 10.1007/s00382-020-05189-3.
[84] K. W. Mayhew, “New Thermodynamics: Rethinking the Science of Climate Change,” *European Journal of Engineering and Technology Research*, vol. 5, no. 5, Art. no. 5, May 2020, doi: 10.24018/ejeng.2020.5.5.1926.
[85] H. B. Bluestein, F. H. Carr, and S. J. Goodman, “Atmospheric Observations of Weather and Climate,” *Atmosphere-Ocean*, vol. 60, no. 3–4, pp. 149–187, Aug. 2022, doi:

10.1080/07055900.2022.2082369.
[86] S. Yang, Y. Gao, K. Torben, N. Keenlyside, and F. Counillon, “The Climate Model: An ARCPATH Tool to Understand and Predict Climate Change,” in *Nordic Perspectives on the Responsible Development of the Arctic: Pathways to Action*, D. C. Nord, Ed., Cham: Springer International Publishing, 2021, pp. 157–180. doi: 10.1007/978-3-030-52324-4_8.
[87] danaallen, “Regional vs Global Models From The Perspective of a Polar Climate Scientist,” Weather and Climate @ Reading. Accessed: Aug. 01, 2024. [Online]. Available: https://blogs.reading.ac.uk/weather-and-climate-at-reading/2021/regional-vs-global-modelsfrom-the-perspective-of-a-polar-climate-scientist/
[88] C. C. Ibebuchi, “On the representation of atmospheric circulation modes in regional climate models over Western Europe,” *International Journal of Climatology*, vol. 43, no. 1, pp. 668–682, 2023, doi: 10.1002/joc.7807.
[89] J. Yuval and P. A. O’Gorman, “Stable machine-learning parameterization of subgrid processes for climate modeling at a range of resolutions,” *Nat Commun*, vol. 11, no. 1, p. 3295, Jul. 2020, doi: 10.1038/s41467-020-17142-3.
[90] R. Vautard *et al.*, “Evaluation of the Large EURO-CORDEX Regional Climate Model Ensemble,” *Journal of Geophysical Research: Atmospheres*, vol. 126, no. 17, p. e2019JD032344, 2021, doi: 10.1029/2019JD032344.
[91] “Downscaling-from-Global-Climate-Models-GCMs-to-Regional-Climate-Models-RCMs-and.png (850×359).” Accessed: Jun. 30, 2024. [Online]. Available: https://www.researchgate.net/profile/Iratxe-Gonzalez-Aparicio/publication/304526712/figure/fig2/AS:377919131144195@1467114350685/Downscaling-from-Global-Climate-Models-GCMs-to-Regional-Climate-Models-RCMs-and.png [92] F. J. Doblas-Reyes *et al.*, “Linking global to regional climate change,” V. Masson-Delmotte, P. Zhai, A. Pirani, S. L. Connors, C. Pean, S. Berger, N. Caud, Y. Chen, L. Goldfarb, M. I. Gomis, M. Huang, K. Leitzell, E. Lonnoy, J. B. R. Matthews, T. K. Maycock, T. Waterfield, O. Yelekci, R. Yu, and B. Zhou, Eds., Cambridge University Press, 2021. Accessed: Apr. 24, 2024. [Online]. Available: https://centaur.reading.ac.uk/99896/
[93] A. F. Prein *et al.*, “Towards Ensemble-Based Kilometer-Scale Climate Simulations over the Third Pole Region,” *Clim Dyn*, vol. 60, no. 11, pp. 4055–4081, Jun. 2023, doi: 10.1007/s00382-02206543-3.
[94] H.-S. Bauer, S. K. Muppa, V. Wulfmeyer, A. Behrendt, K. Warrach-Sagi, and F. Späth, “Multinested WRF simulations for studying planetary boundary layer processes on the turbulencepermitting scale in a realistic mesoscale environment,” *Tellus A: Dynamic Meteorology and Oceanography*, vol. 72, no. 1, pp. 1–28, Jan. 2020, doi: 10.1080/16000870.2020.1761740.
[95] L. Dawkins, D. Bernie, F. Pianosi, J. Lowe, and T. Economou, “Quantifying uncertainty and sensitivity in climate risk assessments: Varying hazard, exposure and vulnerability modelling choices,” *Climate Risk Management*, vol. 40, p. 100511, Apr. 2023, doi: 10.1016/j.crm.2023.100511.
[96] Y. Qian *et al.*, “Uncertainty Quantification in Climate Modeling and Projection,” *Bulletin of the American Meteorological Society*, vol. 97, no. 5, pp. 821–824, May 2016, doi: 10.1175/BAMS-D15-00297.1.
[97] A. Mami, M. Raimonet, D. Yebdri, S. Sauvage, A. Zettam, and J. M. S. Perez, “Future climatic and hydrologic changes estimated by bias-adjusted regional climate model outputs of the Cordex-Africa project: case of the Tafna basin (North-Western Africa),” *International Journal of Global Warming*, vol. 23, no. 1, pp. 58–90, Jan. 2021, doi: 10.1504/IJGW.2021.112489.

[98] C. Teichmann *et al.*, “Assessing mean climate change signals in the global CORDEX-CORE ensemble,” *Clim Dyn*, vol. 57, no. 5, pp. 1269–1292, Sep. 2021, doi: 10.1007/s00382-02005494-x.
[99] T. D. Geleta, D. K. Dadi, C. Funk, W. Garedew, D. Eyelade, and A. Worku, “Downscaled Climate Change Projections in Urban Centers of Southwest Ethiopia Using CORDEX Africa Simulations,” *Climate*, vol. 10, no. 10, Art. no. 10, Oct. 2022, doi: 10.3390/cli10100158.
[100] W. Abbas, A. Hassan, and H. Ismael, “Climate Change Impact On Renewable Energy Resources In The Arab World Based On Jacobson’s Roadmap Of Renewable Wind, Water, And Sunlight (Wws) 2050,” *GES*, vol. 14, no. 2, pp. 92–104, Jul. 2021, doi: 10.24057/2071-9388-2020-133.
[101] M. A. Russo, D. Carvalho, N. Martins, and A. Monteiro, “Forecasting the inevitable: A review on the impacts of climate change on renewable energy resources,” *Sustainable Energy Technologies and Assessments*, vol. 52, p. 102283, Aug. 2022, doi: 10.1016/j.seta.2022.102283.
[102] P. Su, A. Zhang, R. Wang, J. Wang, Y. Gao, and F. Liu, “Prediction of Future Natural Suitable Areas for Rice under Representative Concentration Pathways (RCPs),” *Sustainability*, vol. 13, no. 3, Art. no. 3, Jan. 2021, doi: 10.3390/su13031580.
[103] REN21, “Renewables 2023 Global Status Report Collection, Renewables in Energy Supply,” 2023, Accessed: Nov. 20, 2023. [Online]. Available: https://www.ren21.net/gsr-2023/ [104]
“World Energy Transitions Outlook 2023: 1.5°C Pathway”.
[105] S. Y. In, B. Manav, C. M. A. Venereau, L. E. Cruz R., and J. P. Weyant, “Climate-related financial risk assessment on energy infrastructure investments,” *Renewable and Sustainable Energy Reviews*, vol. 167, p. 112689, Oct. 2022, doi: 10.1016/j.rser.2022.112689.
[106] Yuting Sun, “INVESTMENT DECISION MAKING UNDER DEEP UNCERTAINTY IN THE CONTEXT OF OFFSHORE WIND FINANCING,” Dec. 2021, Accessed: Jul. 15, 2024. [Online]. Available: https://www.firm.fm/wp-content/uploads/2022/02/Paper-2-DeepUncert_WindoffShore_Report.pdf
[107] H. Chen, J. Sun, W. Lin, and H. Xu, “Comparison of CMIP6 and CMIP5 models in simulating climate extremes,” *Science Bulletin*, vol. 65, May 2020, doi: 10.1016/j.scib.2020.05.015.
[108] H.-J. Panitz, M. Schubert-Frisius, and A. Dosio, “CORDEX simulations (evaluation, historical, rcp85, and rcp45) on a ca. 50 km grid over Africa based on CCLM4-8-17 forced by MPI-ESM-LR, EC-EARTH, CNRM-CM5 and HadGEM2-ES.” World Data Center for Climate (WDCC) at DKRZ, Mar. 03, 2015. doi: 10.1594/WDCC/CXAF44CLCL.
[109] B. K. Pandey, D. Khare, A. Kawasaki, and P. K. Mishra, “Climate Change Impact Assessment on Blue and Green Water by Coupling of Representative CMIP5 Climate Models with Physical Based Hydrological Model,” *Water Resour Manage*, vol. 33, no. 1, pp. 141–158, Jan. 2019, doi: 10.1007/s11269-018-2093-3.
[110] J. Wang, L. Li, and A. Zeller, “Better code, better sharing: on the need of analyzing jupyter notebooks,” in *Proceedings of the ACM/IEEE 42nd International Conference on Software Engineering: New Ideas and Emerging Results*, Seoul South Korea: ACM, Jun. 2020, pp. 53–56. doi: 10.1145/3377816.3381724.
[111] J. F. Pimentel, L. Murta, V. Braganholo, and J. Freire, “Understanding and improving the quality and reproducibility of Jupyter notebooks,” *Empir Software Eng*, vol. 26, no. 4, p. 65, May 2021, doi: 10.1007/s10664-021-09961-9.
[112] A. Cardoso, J. Leitão, and C. Teixeira, “Using the Jupyter Notebook as a Tool to Support the Teaching and Learning Processes in Engineering Courses,” in *The Challenges of the Digital Transformation in Education*, vol. 917, M. E. Auer and T. Tsiatsos, Eds., in Advances in Intelligent Systems and Computing, vol. 917. , Cham: Springer International Publishing, 2019, pp. 227–236. doi: 10.1007/978-3-030-11935-5_22.
[113] A. Dosio *et al.*, “Projected future daily characteristics of African precipitation based on global (CMIP5, CMIP6) and regional (CORDEX, CORDEX-CORE) climate models,” *Clim Dyn*, vol. 57, no.

11, pp. 3135–3158, Dec. 2021, doi: 10.1007/s00382-021-05859-w.
[114] O. W. Ilori and I. A. Balogun, “Evaluating the performance of new CORDEX-Africa regional climate models in simulating West African rainfall,” *Model. Earth Syst. Environ.*, vol. 8, no. 1, pp. 665–688, Mar. 2022, doi: 10.1007/s40808-021-01084-w.
[115] A. B. Sarr, M. Camara, and I. Diba, “Spatial Distribution of Cordex Regional Climate Models Biases over West Africa,” *International Journal of Geosciences*, vol. 6, no. 9, Art. no. 9, Sep. 2015, doi: 10.4236/ijg.2015.69081.
[116] M. Yengane, S. Mokeke, and M. Mpholo, “Design and Economic Analysis of a Solar Thermal Pre-Cooling System for Agro-Cold Chain in Lesotho,” *International Sustainable Energy Conference - Proceedings*, vol. 1, Apr. 2024, doi: 10.52825/isec.v1i.1168.
[117] LMS, “The Kingdom of Lesotho’s Third National Communication on Climate Change.” Lesotho Metereological Services, 2021. Accessed: Aug. 08, 2024. [Online]. Available: https://unfccc.int/sites/default/files/resource/NAI_NC3.pdf
[118] S. Watson, “Quantifying the variability of wind energy,” *WIREs Energy & Environment*, vol. 3, no. 4, pp. 330–342, Jul. 2014, doi: 10.1002/wene.95.